METABOLITE PROFILING OF HARD RED SPRING WHEAT (TRITICUM AESTIVUM) INOCULATED WITH FUSARIUM GRAMINEARUM UTLIZING ULTRA HIGH PRESSURE LIQUID CHROMATOGRAPHY- QUADRUPOLE TIME OF FLIGHT/MASS SPECTROMETRY

A Dissertation
Submitted to the Graduate Faculty
of the
North Dakota State University
of Agriculture and Applied Science

By

Gerardo Gracia Gonzalez

In Partial Fulfillment of the Requirements
for the Degree of
DOCTOR OF PHILOSOPHY

Major Program:
Cereal Science

April 2015

Fargo, North Dakota

North Dakota State University
Graduate School

Title

METABOLITE PROFILING OF HARD RED SPRING WHEAT (TRITICUM AESTIVUM) INOCULATED WITH FUSARIUM GRAMINEARUM UTILIZING ULTRA HIGH PRESSURE LIQUID CHROMATOGRAPHY-QUADRUPOLE TIME OF FLIGHT/MASS SPECTROMETRY

By

Gerardo Gracia Gonzalez

The Supervisory Committee certifies that this ***disquisition*** complies with North Dakota State University's regulations and meets the accepted standards for the degree of

DOCTOR OF PHYLOSOPHY

SUPERVISORY COMMITTEE:

Dr. Senay Simsek
Chair

Dr. Paul Schwarz

Dr. Mohammed Mergoum

Dr. Steven Meinhardt

Approved:

4-16-2015
Date

Dr. Frank Manthey
Department Chair

ABSTRACT

Fusarium Head Blight (FHB) of wheat is a fungal disease caused mainly by *Fusarium graminearum*. It has been a persistent worldwide problem for years causing substantial economic losses. Efforts to breed resistance in wheat cultivars represent a practical way to manage this disease. However, there is still much to contribute on how the infection develops and what events make a cultivar resistant to the infection at a molecular level. A metabolite profiling time course strategy was applied to a wheat near isogenic lines (NIL), with contrasting resistant alleles, and three hard red spring wheat cultivars with various degrees of resistance. The analytical time window where no significant difference occurs from sample extraction to sample analysis was also determined adding robustness to this study. Results indicate a maximum analytical window time of 7:45 hours for a wheat extraction queued in an UHPLC auto-sampler at 25 °C. Combining UHPLC-QTOF/MS technology with statistical analyses resulted in 61 significant metabolites ($p < 0.05$; fold change ≥ 2). The NIL and wheat cultivars had profiles with common and unique molecules. Tentative identification was performed by using accurate mass search, tandem MS fragmentation data with internal and online databases. Taking into account the restriction of database identifications, results confirm the presence of hydroxycinnamic acid amides (HCAA) which have been shown to induce thickening of cell walls. These compounds were seen in the resistant and susceptible genotypes with no difference in their intensities but can appear as early or late occurring between 0 and 48 hours after inoculation. Compounds classified as resistant related induced and resistant related constitutive were found in the NIL resistant pair at 48hrs. “Susceptibility indicator” molecules were also observed in the susceptible NIL pair. This suggest that for the NIL pair, HCAA were a normal part of host reaction, while potentially important metabolites for the host resistance may develop

later than 48 hours after inoculation. It was possible to establish an analytical and data mining methodology to perform metabolite profiling in wheat florets utilizing a UPLC-QTOF/MS.

ACKNOWLEDGEMENTS

I give thanks to God the almighty for all the blessings that He continues to give me throughout life. To my parents Abdías and Elvia, my upmost gratitude for their unconditional support and love. To my brother that has always been there for me.

I want to express my sincere gratitude to Dr. Senay Simsek, who gave me the opportunity to be her student and entrusted me to work in this research. My gratitude extends to Dr. Steven Meinhardt, for his valuable mentoring and continual support throughout my research. I also thank the rest of the graduate committee members: Dr. Paul Schwarz, who always gave me the opportunity to learn more about malting and brewing in his lab and Dr. Mohamed Mergoum who gave key input for the completion of this work.

My recognition to Dr. Karl Dria from the Department of Chemistry & Chemical Biology in Indiana University Purdue University Indianapolis and Dr. Rick Reisdorph Assistant Professor at National Jewish Health for their kind assistance in clarifying technical queries. I also want to thank Kristin Whitney and James Gillespie for their time and technical skills that made a positive impact on this research. I want to acknowledge the Faculty professors and support staff at Plant Sciences and Cereal Science graduate program for their assistance with my studies.

Also, my appreciation to all the friends, class mates and people that I had the fortune to meet during my time at NDSU.

Lastly, The North Dakota Wheat Council is acknowledged for the funding of this project.

TABLE OF CONTENTS

LIST OF TABLES

LIST OF FIGURES

LIST OF ABBREVIATIONS

°C .....Celsius

CAS.....Chemical Abstracts Service

CE .....Collision energy

Da.....Daltons

dai.....Days after inoculation

DON.....Deoxynivalenol

EIC .....Extracted ion chromatogram

ESI.....Electro spray ionization

Fhb1 .....*Fusarium* head blight 1 locus

GC-MS.....Gas chromatography mass spectrometer

GHz.....Giga Hertz

hai.....Hours after inoculation

HMDB.....Human metabolome database

KEGG .....Kyoto Encyclopedia of Genes and Genomes

LC-MS .....Liquid chromatography mass spectrometry

LMP .....Lipid maps

MFE .....Molecular feature extractor

MH Qual .....Mass hunter qualitative

µm .....Micro meter

µM.....Micro molar

MPP.....Mass profiler professional

MS-TOF.....Mass spectrometer time of flight

NIL.....Near isogenic line

NIL-R.....Near isogenic line resistant allele

NIL-S .....Near isogenic line susceptible allele

PCA.....Principal component analysis

ppm .....Parts per million

PRr .....Pathogenesis related resistant

PRs .....Pathogenesis related susceptible

PTFE .....Polytetrafluoroethylene

QC.....Quality control

QTL.....Quantitative trait locus

QTOF .....Quadrupole time of flight

RI.....Resistant pathogen inoculated

RM .....Resistant mock inoculated

RRc .....Resistant related constitutive

RRi .....Resistant related induced

RT .....Retention time

SI.....Susceptible pathogen inoculated

SM.....Susceptible mock inoculated

TIC .....Total ion current

UHPLC .....Ultra high pressure liquid chromatographer

LIST OF APPENDIX FIGURES

GENERAL INTRODUCTION

Fusarium Head Blight (FHB), also named “scab”, has been a persistent worldwide problem in small grains for many years. The first well documented case dates back to 1884 in England, were the disease was named “wheat scab”(1). Since then, there have been other outbreaks worldwide. A FHB epidemic during the 1990s in the United States brought estimated economic losses of 3 billion USD (2). In the Great Planes regions, an estimated loss of 2.49 billion USD were calculated between 1993 and 2001(3).

A vast amount of research has been conducted in order to determine solutions to this problem. Effective practices to manage FHB include variety resistance, fungicides and crop rotation (4). Although the pathology of the disease is not well understood at the molecular level (5), new analytical tools can be used to aid in the deciphering of the disease. Recent advancement in technology has given rise to the study of the metabolome in an attempt to detect the totality of biomolecules and their involvement in host-pathogen interactions (6).

To further understand the scope of these metabolic interactions, new hyphenated technologies such as Ultra High Performance Liquid Chromatography Quadrupole Time of Flight Mass Spectroscopy (UHPLC-QTOF/ MS), has provided a very powerful tool in the field of metabolomics (7). The use of this technology with powerful statistical software, can effectively contribute in the detection and understanding of metabolites that are the ultimate expression of genes (8,9).

The present work focuses on two aspects of metabolic profile analysis: stability of the samples to be analyzed and the metabolite profiling of hard red spring wheat (HRSW) infected by *F.graminearum*, utilizing a UHPLC-QTOF/MS analytical approach. Furthermore, the common metabolites between a HRSW near isogenic line (NIL) with contrasting *Fhb1* alleles

and three wheat cultivars are compared in a time course fashion. Finally, the tentative identification of metabolites and the potential implications to FHB resistance are discussed.

Objectives

Determine the metabolites in wheat as a response to *Fusarium graminearum* inoculation utilizing UHPLC-QTOF/MS technology.

Particular Objectives

- Develop an analytical and data mining methodology to perform metabolite profiling in wheat florets utilizing a UHPLC - QTOF/MS.
- Determine the stability of metabolites in extracted wheat samples during the analysis.
- Detect and distinguish the metabolites as the result of *F. graminearum.* inoculation/incubation time treatments using wheat varieties and NIL with contrasting *Fhb1*alleles.
- Putatively identify the metabolites detected using exact mass and MS/MS fragmentation patterns using online databases.

LITERATURE REVIEW

Fusarium Head Blight

Wheat (*Triticum aestivum*) is an important food grain throughout the world. High levels of relative humidity during wheat cultivation, maturation and inadequate drying during grain harvesting and storage can result in fungal growth and mycotoxin production. This strongly reduces its value as food (10,11).

Many species of the genus *Fusarium* are considered important pathogens of wheat. FHB is mainly caused by *Fusarium graminearum* Schawabe (telemorph: *Gibberella zeae* (Schweinitz) Petch) and *Fusarium culmorum* (W.G. Smith) Saccardo (12). The genus *Fusarium* is a large and common group of fungi that produce large spores and can develop on many substrates. The genus was named in 1809 by the German mycologist Link. In 1838, Schwabe described *Fusarium graminearum*. In the 1870's the Italian mycologist P.A. Saccardo, sorted the many names that existed at the time, and compiled all of them into the genus *Fusarium*, giving the combinations that are recognized today such (1,13).

The fungal species mentioned previously infect floral tissues, seedlings, stem bases and roots causing Fusarium head blight (FHB), seedling blight, crown rot and root rot respectively (14). From the diseases mentioned above, FHB is the one with the greatest significance worldwide due to its negative economic and health impact (12). The disease manifests as premature bleaching of the wheat heads. Effects of low yield and low quality has an estimated losses in the millions of dollars per year in the USA (3).

In the East and Midwest of the United States, FHB has become an important problem. Overtime, epidemics have made an impact on yield and quality, with an additional penalties due to Fusaium-damage in kernels, associated mainly with deoxynivalenol (DON) (2,15). In the

upper Midwest, the most common pathogen related to FHB is *Fusarium graminearum* teleomorph *Gibberella zeae* (16). However, other fungi connected to FHB include *F. avenaceum, F. culmorum, F. poae,* and *Microdochium nivale* (16,17), which produce a mixed infection in nature. There is known variation for resistance to FHB, but no complete immunity exists for wheat or barley (18).

Toxic Effects

In addition to the effects on yield loss, FHB is of primary concern due to the synthesis of toxic secondary metabolites produced within the infected grain that affect humans and animals. The most common *Fusarium* mycotoxins in wheat are trichothecenes such as DON and nivalenol (NIV) (19). Trichothecenes are a diverse family of sesquiterpenoid mycotoxins produced by *Fusarium sp.* and other fungi. They are paracyclic ring structure, a double bond at C-9, 10 and an epoxide at C-13 (20).

DON is a potent inhibitor of protein biosynthesis. Consumption of grain contaminated by trichothecenes can cause anemia, immunosuppression, hemorrhage, nausea, diarrhea and emesis (21). Cellular effects such as inhibition of mitochondrial enzymes and electrolyte loss have also been reported (22). The enhanced detrimental effects observed in the consumption of *Fusarium* contaminated feed may be due to the presence of diverse mycotoxins (19).

The phytotoxic effects of DON in wheat can manifest as chlorosis, necrosis and wilting, which can culminate in the bleaching of the whole head above the inoculation point (20). DON induces hydrogen peroxide production in wheat and promotes cell death (23). Experiments using *F. graminearum* mutants unable to produce DON showed that this mycotoxin functions as a virulence factor in wheat, enhancing spread of the disease within the spike (20).

Pathology Description

In wheat, FHB appears in the heads and peduncles turning them brown or tan with premature senescence. The fungal growth is sometimes visible on the head and may include purple-black perithecia and/or pink sporodochia especially on glumes. FHB infected seed usually have a characteristic shrunken bleached appearance (2,24).

F. graminearum is able to survive across crop cycles as a saprophyte in the debris of infected cereals and grasses with ascospores and macroconidia produced on these residues (25,26). These in turn may infect wheat spikelets under warm and moist conditions during wheat anthesis to kernel soft dough stage (27). The fungus initially invades individual florets and then spreads systemically throughout the vascular bundles in the rachilla and rachis (28). On the field, signs of FHB start between 5 days to 3 weeks after infection with clear signs of bleaching of infected spikelets or portions of spikes and by pink colored masses of spores in humid conditions (29). As disease progresses, wheat kernels become infective to other spikes.

Resistance

Host resistance and reaction of resistant wheat cultivars to FHB infection is quite complex and has been classified as passive or active. Passive mechanisms could include phenological and morphological traits such as plant height, the presence of awns, spikelet density, and time to flower (30). Active mechanisms of FHB resistance have been proposed to involve a number of types: resistance to invasion or type I; resistance to spreading or type II; resistance to mycotoxin accumulation or type III; resistance to kernel infection or type IV and tolerance or type V(31). Many of the resistance mechanisms that are studied separately in wheat may be overlapping mechanisms in nature (32).

For wheat, it is considered that type II resistance is the most used (33). Aside from type II resistance seen on cultivar sources like Sumai3 and Niang the genetics of the other types of resistance remain to be fully understood (34,35).

Plant defense response genes are known to be activated as a respond to *F. graminearum*. Pritsch, (2000) using a susceptible (Wheaton) and a resistant variety (Sumai3) showed the activation of genes such as peroxidase, PR1, PR2 (β-1, 3-glucanase), PR3 (chitinase), PR4 and PR5 (thaumatin-like protein) accumulated 6 to 12 hours after inoculation (hai). Transcripts accumulation was the same but the time of appearance in PR4 and PR5 was earlier, meaning that the time of appearance may be a factor in resistance (36). Steiner *et al*. (2009) demonstrated the expression of plant defense transcripts against *F. graminearum*. After inoculating spring wheat genotypes with contrasting FHB resistance and measuring at 6 time points after inoculation (0-72 hai), found that the amount of transcripts highest between 48 and 72 hai (11).

Wheat resistance to FHB appears to be quantitative and controlled by multiple genes (35). Resistance to initial infection (type I) as quantitative trait loci (QTL) has been reported on chromosomes 2DS, 3AS, 3BS, 3BC, 4DL, 5AS, and 6BS of Sumai3 (32) and 2DL for Nyubai (37). Resistance to spread or type II resistance QTLs have been reported on several chromosomes 2DL, 2DS, 3AS, 3BC, 3BS, 4B, 4DL, 5AS, 6BS, and 7BL (32). Some of these QTL are found in common with both types of resistance.

Sumai3, a Chinese spring wheat cultivar, is one of the most widely used breeding sources. The QTL on chromosome 3BS or *Fhb1* has been identified to have a high type II resistance in the range of 15-60% of phenotypic variation (32). The identification of this QTL by the use of markers is used by breeders in the selection of new wheat lines. However, marker assisted selection might fail in some cases to transfer the expected level of traits (38). Past

studies have linked specific metabolites to particular genomic regions, thus a set of genes regulating metabolic pathways through enzymatic reactions gives way to the production of metabolites constituting a unique phenotype (6,8). In summary, the metabolome is the ultimate expression of genes (9). In order to study the metabolome, the development and use of metabolomics techniques has as objective to identify and quantify the totality of metabolites in a biological system (6). As part of metabolomics, the use of metabolite profiling appears to be a good strategy to increase the knowledge of host-pathogen interactions.

Metabolite Profiling

Metabolite profiling is a strategy for screening the wide array of small molecules that can appear in a plant as response to a stimulus (39)Metabolites have roles in energy, redox control, defense, structural integrity and signaling. Therefore the study of the metabolome can yield direct insight into many biological processes (40).

The objective of metabolite profiling is to understand and predict the molecular behavior of living models. The information collected can then be explored utilizing data mining tools for modeling and simulation (41). Plants represent an extended natural compound library (40) that in spite of everyday discoveries of new metabolites, has a vast universe of natural compounds which has yet to be identified and classified. Many common plant metabolites such as: monoterpenoid volatiles, polar amino acids, or hydrophobic lipids can result in a very complex analytical experiment (39). These discoveries not only contribute to the understanding of the metabolome but also have shown to be of phenotypic and physiological importance, as in the case of protective properties in disease or stress (42), antioxidant, and other characteristics (43).

Metabolite Profiling Technology

Although metabolomic plant analyses aims, at the simultaneous detection of the totality of the metabolites in plant tissues, is not currently possible to use a single extraction/separation/detection methodology to accomplish that (39). With an estimated range between 100 000 to 200 000 metabolites, plants represent a challenge but also aa great discovery potential (44).

Various analytical approaches have been taken in an attempt to detect and quantify the diversity of compounds: separation techniques like liquid chromatography (LC), gas chromatography (GC), capillary electrophoresis (CE) (45-47) and detection technologies like nuclear magnetic resonance (NMR) and mass spectrometry (MS) (9), have been used in various combinations.

GC-MS has been widely utilized over time with proven reliability to detect volatile organic compounds (9). GC-MS is mainly used for detection of amino acids, fatty acids, carbohydrates and organic acids, all primary metabolism chemical groups (48). For this technique, it is often necessary to derivatize the sample by including trimethylsilyl (TMS) groups through the addition of N-methyl-N-trifluoroacetamide (MSTFA) (49).

LC–MS is more suitable for detecting the overall biochemical diversity of plants. It does not require previous derivatzation of samples to make metabolite groups of interest available for detection. It has been shown to be appropriate for the detection of a wide range of metabolite classes (9,50) that covers the large (semi-polar) group of plant secondary metabolites such as alkaloids, saponins, phenolic acids, phenylpropanoids, flavonoids, glucosinolates, polyamines and derivatives. In addition, LC-MS can also detect some primary metabolites depending on the type of stationary phase being used (50). Something to consider is that, although the number of

peaks that may appear could be excessive, they remain as ‘‘unknown’’ compounds until they are positively confirmed using authentic standards (40).

Liquid Chromatography-Quadrupole Time of Flight/Mass Spectrometry

LC QTOF/MS technique is the preferred method for metabolic profiling of semi-polar secondary metabolites. These compounds can be effectively extracted with aqueous alcohol solutions and analyze directly. Ionization in these instruments typically involves soft ionization techniques, such as electrospray ionization (ESI) or atmospheric pressure chemical ionization (APCI), resulting in a protonated (in positive mode) or deprotonated (in negative mode) molecular ions. Modern resolution instruments with exact mass detection such as TOF/MS enable the profiling of hundreds to thousands of compounds in crude extracts, combined with elemental formula calculations of the detected masses (9,39). A particular version of Liquid chromatography is the UHPLC (Ultra high pressure liquid chromatography) coupled with QTOF/MS operate at a higher pressure (15 000 000 psi. compared to 6000 psi in HPLC). Their columns are packed with smaller beads (< 2 µm) which increases the resolution of the chromatogram (51). This is important in untargeted metabolomics, since it is possible to separate complex biological mixtures, such as crude extracts.

A very common separation column used in this platform is a C-18 in reversed phase. It permits the separation of a large variety of semi polar compounds from crude plant extracts (50,52). However a variety of columns are available to separate and detect primary metabolites like polar organic acids and amino acids (53)

The analysis of samples in negative and positive modes would certainly detect more compounds than only a single mode, since semi polar metabolites like glucosinolates, polyphenols and other glycosylated compounds are detectable by ESI negative mode while

polyamines, alkaloids and anthocyanins ionize easily in positive mode (52). This being said, single ionization profiles can be performed depending on the compound classes of interest (39).

After the LC-MS analysis, untargeted data pre-processing is usually achieved by using specialized software that perform corrections like base line, time and mass alignment for hundreds of samples, resulting in a matrix of mass signal intensities (54).

Quality control samples (sample mixtures) can be used to check for consistent peak picking and alignment. A 70 to 80% of all peaks should be present in all QC samples with an overall variation of less than 20% and a mass deviation of less than 3 ppm (39). Alternatively, standards can be spiked in or run alongside the rest of the samples (55). This option will depend on the nature of the samples and the focus of the study. Later on, with the help of the processing software, all similar mass signals from the same metabolite are grouped according their mass, retention time and intensities across samples to reconstruct a spectrum with a single representative metabolite signal (56). Finally, identification of metabolites can be performed by matching the exact mass of the observed molecular ion with available online plant mass databases. As an option, tandem MS experiments may be performed to further identify the significant secondary metabolites (39,50).

Metabolic Profiling of FHB in Wheat

Metabolite profiling studies that identify potential resistance metabolites as biomarkers in FHB resistant wheat lines has been performed. These studies relied on GC-MS for processing the samples and encountered compounds such as: fatty acids, aromatic compounds, *p*- and *m*-coumaric acids, myo-inositol, malonic acid, amino acids, fatty acids, and aromatics as unique to the plant-pathogen interaction. This technology usually detects only relatively low molecular weight compounds (53,57-59). Another study uses GC-EI-TOF/MS (Gas Chromatography

coupled to Electron Ionization-Time-of-flight mass spectrometry) aimed mainly to detect polar compounds. They identified several resistance related metabolites detected in cultivars which had several FHB resistance QTLs (60). More recently, non-targeted metabolo-proteomics approaches have used 2D gel electrophoresis combined with LC-MS/MS strategies in order to elucidate wheat defense systems in a FHB infection(61). By applying a time course of the FHB infection and UHPLC-QTOF/MS technology for the detection of metabolites in wheat, it may be possible to contribute to the knowledge of FHB wheat infection.

References

1. Stack, R. W. (2003) History of fusarium head blight with emphasis on North America. in *Fusarium Head Blight fo Wheat and Barley* (Leonard K. J., B. W. R. ed.), APS, St. Paul, MN. pp 1-34

2. McMullen, M., Jones, R., and Gallenberg, D. (1997) Scab of Wheat and Barley: A Re-emerging Disease of Devastating Impact. *Plant Disease* **81**, 1340-1348

3. Nganje, W. E., Bangsund, D. A., Leistritz, F. L., Wilson, W. W., and Tiapo, N. M. (2004) Regional Economic Impacts of Fusarium Head Blight in Wheat and Barley. *Applied Economic Perspectives and Policy* **26**, 332-347

4. McMullen, M., Halley, S., Schatz, B., Meyer, S., Jordahl, J., and Ransom, J. (2008) Integrated strategies for Fusarium head blight management in the United States. *Cereal Research Communications* **36**, 563-568

5. Bai, G., and Shaner, G. (2004) Management and resistance in wheat and barley to fusarium head blight. *Annu Rev Phytopathol* **42**, 135-161

6. Schauer, N., and Fernie, A. R. (2006) Plant metabolomics: towards biological function and mechanism. *Trends in plant science* **11**, 508-516

7. Theodoridis, G. A., Gika, H. G., Want, E. J., and Wilson, I. D. (2012) Liquid chromatography-mass spectrometry based global metabolite profiling: a review. *Analytica chimica acta* **711**, 7-16

8. Keurentjes, J. J. B., Fu, J., de Vos, C. H. R., Lommen, A., Hall, R. D., Bino, R. J., van der Plas, L. H. W., Jansen, R. C., Vreugdenhil, D., and Koornneef, M. (2006) The genetics of plant metabolism. *Nat Genet* **38**, 842-849

9. Allwood, J. W., and Goodacre, R. (2010) An introduction to liquid chromatography–mass spectrometry instrumentation applied in plant metabolomic analyses. *Phytochemical Analysis* **21**, 33-47

10. Steffenson, B. J. (2003) Fusarium head blight of barley: impact, epidemics, management, and strategies for identifying and utilizing genetic resistance. in *Fusarium Head Blight of Wheat and Barley* (Leonard K. J., B. W. R. ed.), APS press, St. Paul, MN. pp 241-295

11. Steiner, B., Kurz, H., Lemmens, M., and Buerstmayr, H. (2009) Differential gene expression of related wheat lines with contrasting levels of head blight resistance after Fusarium graminearum inoculation. *TAG. Theoretical and applied genetics. Theoretische und angewandte Genetik* **118**, 753-764

12. Parry, D. W., Jenkinson, P., and McLeod, L. (1995) Fusarium ear blight (scab) in small grain cereals—a review. *Plant Pathology* **44**, 207-238

13. Booth, C. (1971) *The Genus Fusarium*, Commonwealth Agricultural Bureaux [for the] Commonwealth Mycological Institute

14. McMullen, M., Bergstrom, G., De Wolf, E., Dill-Macky, R., Hershman, D., Shaner, G., and Van Sanford, D. (2012) A Unified Effort to Fight an Enemy of Wheat and Barley: Fusarium Head Blight. *Plant Disease* **96**, 1712-1728

15. Clear, R., and Abramson, D. (1986) Occurrence of Fusarium head blight and deoxynivalenol(vomitoxin) in two samples of Manitoba wheat in 1984. *Canadian Plant Disease Survey* **66**, 9-11

16. Wilcoxson, R., Kommedahl, T., Ozmon, E., and Windels, C. (1988) Occurrence of Fusarium species in scabby wheat from Minnesota and their pathogenicity to wheat. *Phytopathology* **78**, 586-589

17. Sutton, J. C. (1982) Epidemiology of wheat head blight and maize ear rot caused by Fusarium graminearum. *Canadian Journal of Plant Pathology* **4**, 195-209

18. Rudd, J. C., Horsley, R. D., McKendry, A. L., and Elias, E. M. (2001) Host Plant Resistance Genes for Fusarium Head Blight. *Crop Sci.* **41**, 620-627

19. Placinta, C. M., D'Mello, J. P. F., and Macdonald, A. M. C. (1999) A review of worldwide contamination of cereal grains and animal feed with Fusarium mycotoxins. *Animal Feed Science and Technology* **78**, 21-37

20. McCormick, S. (2003) The role of DON in pathogenicity. in *Fusarium head blight of wheat and barley* (Leonard K. J., B. W. R. ed.), The American Phytopathological Society, St. Paul, MN. pp 165-183

21. Desjardins, A. E., Manandhar, G., Plattner, R. D., Maragos, C. M., Shrestha, K., and McCormick, S. P. (2000) Occurrence of Fusarium Species and Mycotoxins in Nepalese Maize and Wheat and the Effect of Traditional Processing Methods on Mycotoxin Levels. *Journal of agricultural and food chemistry* **48**, 1377-1383

22. Cossette, F., and Miller, J. D. (1995) Phytotoxic effect of deoxynivalenol and gibberella ear rot resistance of com. *Natural toxins* **3**, 383-388

23. Desmond, O. J., Manners, J. M., Stephens, A. E., Maclean, D. J., Schenk, P. M., Gardiner, D. M., Munn, A. L., and Kazan, K. (2008) The Fusarium mycotoxin deoxynivalenol elicits hydrogen peroxide production, programmed cell death and defence responses in wheat. *Molecular plant pathology* **9**, 435-445

24. Goswami, R. S., and Kistler, H. C. (2004) Heading for disaster: Fusarium graminearum on cereal crops. *Molecular plant pathology* **5**, 515-525

25. Dill-Macky, R., and Jones, R. (2000) The effect of previous crop residues and tillage on Fusarium head blight of wheat. *Plant disease* **84**, 71-76

26. Khonga, E., and Sutton, J. (1988) Inoculum production and survival of Gibberella zeae in maize and wheat residues. *Canadian Journal of Plant Pathology* **10**, 232-239

27. Paulitz, T. C. (1999) Fusarium head blight: a re-emerging disease. *Phytoprotection* **80**, 127-133

28. Ribichich, K. F., Lopez, S. E., and Vegetti, A. C. (2000) Histopathological Spikelet Changes Produced by Fusarium graminearum in Susceptible and Resistant Wheat Cultivars. *Plant Disease* **84**, 794-802

29. Del Ponte, E. M., Shah, D. A., and BERGSTROM, G. (2003) Spatial patterns of Fusarium head blight in New York wheat fields suggest role of airborne inoculum. *Plant Health Progress doi* **10**

30. Mesterházy, A. (1995) Types and components of resistance to Fusarium head blight of wheat. *Plant Breeding* **114**, 377-386

31. Mesterházy, Á., Bartók, T., Mirocha, C. G., and Komoróczy, R. (1999) Nature of wheat resistance to Fusarium head blight and the role of deoxynivalenol for breeding. *Plant Breeding* **118**, 97-110

32. Yang, Z., Gilbert, J., Fedak, G., and Somers, D. J. (2005) Genetic characterization of QTL associated with resistance to Fusarium head blight in a doubled-haploid spring wheat population. *Genome* **48**, 187-196

33. Bushnell, W. R. (2003) Hitstology and physiology of Fusarium head blight. in *Fusarium Head Bligth of Wheat and Barley* (Leonard K. J., B. W. R. ed.), American Phytopathological Society, St. Paul, MN. pp 44-83

34. Anderson, J. A., Stack, R. W., Liu, S., Waldron, B. L., Fjeld, A. D., Coyne, C., Moreno-Sevilla, B., Fetch, J. M., Song, Q. J., Cregan, P. B., and Frohberg, R. C. (2001) DNA markers for Fusarium head blight resistance QTLs in two wheat populations. *Theoretical and Applied Genetics* **102**, 1164-1168

35. Bai, G. H., Chen, L. F., and Shaner, G. (2003) Breeding for Fusarium Head Blight of Wheat in China. in *Fusarium Head Bligth of Wheat and Barley* (Leonard K. J., B. W. R. ed.), American Phytopathological Society, St. Paul, MN. pp 296-317

36. Pritsch, C., Muehlbauer, G. J., Bushnell, W. R., Somers, D. A., and Vance, C. P. (2000) Fungal Development and Induction of Defense Response Genes During Early Infection of Wheat Spikes by Fusarium graminearum. *Molecular Plant-Microbe Interactions* **13**, 159-169

37. Somers, D. J., Thomas, J., DePauw, R., Fox, S., Humphreys, G., and Fedak, G. (2005) Assembling complex genotypes to resist Fusarium in wheat (Triticum aestivum L.). *Theoretical and Applied Genetics* **111**, 1623-1631

38. Collard, B. C. Y., Jahufer, M. Z. Z., Brouwer, J. B., and Pang, E. C. K. (2005) An introduction to markers, quantitative trait loci (QTL) mapping and marker-assisted selection for crop improvement: The basic concepts. *Euphytica* **142**, 169-196

39. Allwood, J. W., De Vos, R. C. H., Moing, A., Deborde, C., Erban, A., Kopka, J., Goodacre, R., and Hall, R. D. (2011) Plant Metabolomics and Its Potential for Systems Biology Research: Background Concepts, Technology, and Methodology. in *Methods in Enzymology* (Daniel Jameson, M. V., and Hans, V. W. eds.), Academic Press. pp 299-336

40. Fernie, A. R. (2007) The future of metabolic phytochemistry: larger numbers of metabolites, higher resolution, greater understanding. *Phytochemistry* **68**, 2861-2880

41. Fiehn, O. (2002) Metabolomics – the link between genotypes and phenotypes. *Plant Mol Biol* **48**, 155-171

42. Dixon, R. A., Gang, D. R., Charlton, A. J., Fiehn, O., Kuiper, H. A., Reynolds, T. L., Tjeerdema, R. S., Jeffery, E. H., German, J. B., Ridley, W. P., and Seiber, J. N. (2006) Applications of Metabolomics in Agriculture. *Journal of agricultural and food chemistry* **54**, 8984-8994

43. Allwood, J. W., Ellis, D. I., and Goodacre, R. (2008) Metabolomic technologies and their application to the study of plants and plant-host interactions. *Physiologia plantarum* **132**, 117-135

44. Oksman-Caldentey, K. M., and Saito, K. (2005) Integrating genomics and metabolomics for engineering plant metabolic pathways. *Current opinion in biotechnology* **16**, 174-179

45. Sumner, L. W., Mendes, P., and Dixon, R. A. (2003) Plant metabolomics: large-scale phytochemistry in the functional genomics era. *Phytochemistry* **62**, 817-836

46. Timischl, B., Dettmer, K., Kaspar, H., Thieme, M., and Oefner, P. J. (2008) Development of a quantitative, validated capillary electrophoresis-time of flight-mass spectrometry method with integrated high-confidence analyte identification for metabolomics. *Electrophoresis* **29**, 2203-2214

47. Roessner, U., Willmitzer, L., and Fernie, A. (2002) Metabolic profiling and biochemical phenotyping of plant systems. *Plant Cell Rep* **21**, 189-196

48. Fiehn, O., Kopka, J., Dormann, P., Altmann, T., Trethewey, R. N., and Willmitzer, L. (2000) Metabolite profiling for plant functional genomics. *Nat Biotech* **18**, 1157-1161

49. Gullberg, J., Jonsson, P., Nordström, A., Sjöström, M., and Moritz, T. (2004) Design of experiments: an efficient strategy to identify factors influencing extraction and derivatization of Arabidopsis thaliana samples in metabolomic studies with gas chromatography/mass spectrometry. *Analytical biochemistry* **331**, 283-295

50. De Vos, R. C., Moco, S., Lommen, A., Keurentjes, J. J., Bino, R. J., and Hall, R. D. (2007) Untargeted large-scale plant metabolomics using liquid chromatography coupled to mass spectrometry. *Nature protocols* **2**, 778-791

51. Bedair, M., and Sumner, L. W. (2008) Current and emerging mass-spectrometry technologies for metabolomics. *TrAC Trends in Analytical Chemistry* **27**, 238-250

52. Hanhineva, K., Rogachev, I., Kokko, H., Mintz-Oron, S., Venger, I., Karenlampi, S., and Aharoni, A. (2008) Non-targeted analysis of spatial metabolite composition in strawberry (Fragariaxananassa) flowers. *Phytochemistry* **69**, 2463-2481

53. Hamzehzarghani, H., Paranidharan, V., Abu-Nada, Y., Kushalappa, A. C., Dion, Y., Rioux, S., Comeau, A., Yaylayan, V., and Marshall, W. D. (2008) Metabolite profiling coupled with statistical analyses for potential high-throughput screening of quantitative resistance to fusarium head blight in wheat. *Canadian Journal of Plant Pathology* **30**, 24-36

54. Lommen, A. (2009) MetAlign: Interface-Driven, Versatile Metabolomics Tool for Hyphenated Full-Scan Mass Spectrometry Data Preprocessing. *Analytical Chemistry* **81**, 3079-3086

55. Theodoridis, G., Gika, H. G., and Wilson, I. D. (2008) LC-MS-based methodology for global metabolite profiling in metabonomics/metabolomics. *TrAC Trends in Analytical Chemistry* **27**, 251-260

56. Tikunov, Y., Lommen, A., de Vos, C. H., Verhoeven, H. A., Bino, R. J., Hall, R. D., and Bovy, A. G. (2005) A novel approach for nontargeted data analysis for metabolomics. Large-scale profiling of tomato fruit volatiles. *Plant physiology* **139**, 1125-1137

57. Hamzehzarghani, H., Paranidharan, V., Abu-Nada, Y., Kushalappa, A. C., Mamer, O., and Somers, D. (2008) Metabolic profiling to discriminate wheat near isogenic lines, with quantitative trait loci at chromosome 2DL, varying in resistance to fusarium head blight. *Canadian Journal of Plant Science* **88**, 789-797

58. Hamzehzarghani, H., Kushalappa, A. C., Dion, Y., Rioux, S., Comeau, A., Yaylayan, V., Marshall, W. D., and Mather, D. E. (2005) Metabolic profiling and factor analysis to discriminate quantitative resistance in wheat cultivars against fusarium head blight. *Physiological and Molecular Plant Pathology* **66**, 119-133

59. Shen, X., Zhou, M., Lu, W., and Ohm, H. (2003) Detection of Fusarium head blight resistance QTL in a wheat population using bulked segregant analysis. *Theoretical and Applied Genetics* **106**, 1041-1047

60. Paranidharan, V., Abu-Nada, Y., Hamzehzarghani, H., Kushalappa, A. C., Mamer, O., Dion, Y., Rioux, S., Comeau, A., and Choiniere, L. (2008) Resistance-related metabolites in wheat againstFusarium graminearumand the virulence factor deoxynivalenol (DON). *Botany* **86**, 1168-1179

61. Gunnaiah, R., Kushalappa, A. C., Duggavathi, R., Fox, S., and Somers, D. J. (2012) Integrated metabolo-proteomic approach to decipher the mechanisms by which wheat QTL (Fhb1) contributes to resistance against Fusarium graminearum. *PloS one* **7**, e40695

PAPER 1. SHORT-TERM SAMPLE STABILITY OF WHEAT FLORET METABOLITE PROFILES USING ULTRA HIGH PERFORMANCE LIQUID CHROMATOGRAPHY COUPLED WITH QUADRUPOLE TIME OF FLIGHT MASS SPECTROMETRY

Abstract

A typical metabolomic analysis consists of a multi-step procedure. Variation can be introduced in any segment of the analysis if proper care in quality assurance is not taken, thus compromising the final results. Sample stability is one of those factors. Although sophisticated studies addressing sample decay over time have been performed in the medical field, they are just emerging in plant metabolomics. Here we focus on the stability of wheat floret extracts on queue inside an auto-injector held at 25 °C. The objective was to locate an analytical time window from extraction to injection with no significant difference occurring in the sample. Total ion current chromatogram, principal component analysis and volcano plots were used to measure changes in the samples. Results indicate a maximum work window time of 7:45 hours for Steele-ND wheat methanolic extractions in an auto-sampler at 25 °C. Comparisons showed a gradual significant increase in the number and intensity of compounds observed that may be caused by degradation of other molecules in the sample extract. The approach can be applied as preliminary work in a metabolite profiling study helping to set the appropriate workload with the aim of producing confident results.

Introduction

Metabolite profiling refers to the identification and quantitation of low molecular weight molecules that may be found in a particular metabolic pathway using a hyphenated analytical technology such as LC-MS/MS (1). A typical metabolomic analysis consists of sample

preparation, extraction, chemical analysis, data collection, data pre-treatment, data analysis and interpretation. Variation can be introduced in any segment of this multi-step process, thus it is important to give the same weight to each of its parts, otherwise conclusions could be misleading (2).

One of the many analytical technologies used for the study of metabolites is liquid chromatography coupled to mass spectrometry or LC-MS. This analytical technology has been widely used for its capacity to separate and detect a diverse set of molecules with high sensitivity(3). An example of a comprehensive untargeted protocol using an Ultra-high performance LC-MS by De Vos et al. (2007) resulted in the detection of several hundred metabolites from the analysis of *Arabidopsis* seedlings. In addition, this work shows quality assurance results that ensure the stability of the masses detected for 240 hours (4).

Application of metabolomics in cereal science has been substantial in maize, rice, wheat, barley, oat and rye (2). Wheat has been investigated using metabolomics for a variety of phenomena. For example, GC-MS was used to investigate the metabolic response to *Fusarium graminearum* infection (5); to compare GMO wheat lines and their parental lines(6); to evaluate the environmental effects on genotype, free amino acids of released wheat varieties and experimental lines (7) and to compare conventional and organic farming systems over time using durum lines (8). In another study, wheat metabolomics was applied for mapping the variation of European wheat cultivar profiles using NMR technology (9). An ultra-performance liquid chromatography coupled with time-of-flight mass spectrometry approach (UHPLC-TOF) was utilized in comparison of diverse wheat representing durum, soft wheat and hard bread wheat to detect desirable agronomic and human health traits (10).

Due to the diverse nature of metabolites, their complete recovery in a given sample has proven to be difficult. Moreover, it should also be considered how many of the metabolites are prone to decay due to events such as oxidation and hydrolysis during sample preparation (11). An important consideration is that the goal of an extraction method should be to minimally alter the sample to avoid the increase or degradation of metabolites (3). A practical and common way to do this involves submerging the specimen in liquid nitrogen (4,12,13). The rationale for this technique is to stop all enzymatic reactions and reduce the rate of chemical reactions in order to get a snapshot of the metabolites at the time of collection (14,15).

Shock freezing at -80 °C and freeze drying are two recommendations that exist in sample preservation after the collection of tissue (15,16). A few studies deal with the effects of storing the sample after extraction and before its injection into the analytical equipment (17,18). Sophisticated studies in sample decay over time have been researched in biofluids such urine (19,20) and blood (20-22); also in human cell lines and mouse liver tissue (23). These investigators studied the changes that occurred from short or long term cryo-preservations and from freezing and thawing the samples, providing the conditions and time best suited for sample preservation in medical metabolomics. They illustrate the importance of having quality assurance procedures integrated into the total design of an experiment.

As mentioned before, the cited studies are representative of medical research. In contrast, this approach is not often seen in plant metabolite profiling studies (24-26), specifically in wheat developing tissues analyzed in a UPLC-MS environment. Our interest in this study was not to identify the metabolites in the samples, but rather to establish an analysis time window before significant changes occur during an analytical cycle.

Materials and Methods

Wheat Planting, Inoculation and Sampling

Seeds of the hard red spring wheat (HRSW) Steele-ND (27) were obtained from Dr. Senay Simsek , Department of Plant Sciences of the North Dakota State University (NDSU). Samples were selected based on resistance to Fusarium Head blight (28). Steele-ND's pedigree consists of: 'Parshall' (PI 613587)/5/ 'Grandin' (PI 531005)/3/IAS[20.sup.*]4/H567.71//'Amidon' (PI 527682)/ 4/[Grandin.sup.*]2/'Glupro' (PI 592759) (27).

Wheat was sown in 3.8 cm Ray Leach Cone-Tainers (RL cones), planting 1 seed in each cone. Sunshine Mix #1/LC1 soil was used for planting. The plant number was set at 70 cones per rack. After emergence, 8 beads of Multicoat 4 fertilizer (Haifa group, Israel) were applied to the top soil of each cone. The racks containing the cones were kept in trays full of reverse osmosis water. Greenhouse temperature was set at 25 ± 2 °C with a 16:8 hour photoperiod until booting stage.

A *Fusarium graminearum* strain isolated at Foster, North Dakota in 2008 named Fg08-001, was provided by Dr. Shaobin Zhong of the Plant Pathology Department at NDSU. It is regarded as a strain with a 3-Acetyl-DON chemotype (29). The strain was cultured in Mung Bean Agar (40g of mung beans per liter [wt/vol] in milliQ water, boiled for 23 min, and filtered through four layers of cheesecloth; 1.5% agar [wt/vol]) and was incubated at room temperature with 12 hour fluorescent light cycles. After 7 days, the cultures were inundated with sterile water and the spores/mycelia were dislodged with a sterile loop. The resulting suspension was filtered through two layers of cheesecloth. A quantified spore suspension was prepared by counting macroconidia using a hemocytometer. Appropriate adjustments were performed using an aqueous solution of 0.02% Tween 80 to reach a concentration of 10^5 macroconidia/ml (29).

Aliquots of this suspension were stored at -20 °C for later use. Prior to usage, the frozen macroconidial suspension was thawed for approximately 8 hours at 4 °C. The suspension was utilized for the next three days and stored at 4 °C.

When the first awns were visible (GS= 47-49, Zadoks scale(30)), wheat plants were incubated in a growth room with conditions similar to the greenhouse, with the exception that the light intensity was ≈15000 lm/m^2. The purpose of this was to stabilize the plants by having a constant light intensity while avoiding temperature changes. At anthesis (GS=60-69 Zadoks scale (30), wheat florets were inoculated with *F. graminearum* spores using 10 µl of the macroconidial suspension (100 conidia per µl) injected between the palea and lemma of four central spikelets within a spike. A total of four spikes were inoculated. Inoculated spikelets were marked by cutting their respective awns. All treated plants were incubated in a mist chamber for 24 hours. Mist chamber conditions were maintained at 28.5 +/- 0.5 °C, with a spaying rate of 20 seconds at 15 minutes intervals to ensure 90 to 95% RH for fungal colonization.

After incubation, inoculated florets in each wheat spike were collected by cutting the rachilla at the base of each spikelet. A composite sample was composed of 16 pooled florets originating from four spikes. Four florets were inoculated in each spike (31).

Florets were collected in labeled #1 Kraft paper coin envelopes (2-1/4 x 3-1/2). The envelopes were stapled and submerged immediately in liquid nitrogen. Frozen tissue was stored in an ultra-freezer at -80 ± 1 °C until use.

Sample Extraction

Mortar and pestles were washed with 2% phosphate-free detergent followed by a two day distilled water soaking/rinse-cycles. After drying, the ceramic was baked at 590 °C for 4 hours. The frozen tissue was crushed into powder utilizing a clean ceramic pestle and mortars sitting on

dry ice. Tissue thawing was avoided by carefully pouring a small volume of liquid nitrogen onto the sample during crushing.

Six composite samples were ground together and the powder was collected into a single plastic conical tube. The tube was kept at -80 °C. Two portions of the ground tissue were weighed (marked A and B) and extracted each day of analysis, repeating the procedure for a total of 3 consecutive days.

Samples prepared for small molecules analysis were extracted based on the methods developed by De Vos et al. (2007) (4) and t'Kindt et al. (2009) (25) with modifications. Tissue extracts were prepared freshly at the beginning of each day of analysis. Extraction time was recorded as the start time and counted as part of the total analytical run. The ground, 300 mg ±5%, was transferred into a pre-frozen 1.5 ml micro tube. Cryogenic conditions were kept by submerging the tube and spatula into liquid nitrogen. Sample extraction solution (80:20 methanol/water HPLC grade) stored at -80 °C was added in a 3:1 volume/fresh weight ratio.

Tubes were stirred in 2 second pulses using a vortex shaker for a total of 10 seconds. Next, to facilitate extraction, each sample was submerged in a Branson 2510 bath sonicator (Branson ultrasonics corp.) at 25 °C for 15 minutes set on maximum frequency (40 kHz). This was followed by two sequential centrifuge cycles of 10 min each at 3,000g at 6 ± 1 °C. The supernatant of each sample was filtered through a 0.2 μm PTFE membrane (VWR International) by using 1 ml disposable syringes into new 1.8 ml amber glass vials with Teflon caps. Ambar vials labeled used as blank were prepared in the same way as the samples, except they only contained extraction solution.

Sample Analysis

Metabolite data was obtained using a 6540 series UHPLC-ESI-QTOF/MS (Agilent Technologies, Inc.) utilizing the Mass Hunter Workstation software-LC/MS Acquisition for 6200 series TOF/6500 QTOF version B.05.00 /build 5.05.042.0.

The Infinity 1290 UHPLC section (Agilent Technologies, Inc.) was composed of a G44227A flex cube, G4220A binary pump, G1210B Iso pump, G1316C TCL and a G4226A sampler unit. A Zorba X Eclipse plus C-18 column (1.8 μm; 2.1 x 100mm) was utilized. Reverse phase conditions were maintained at 40 °C with a flow rate of 0.4ml/min. The mobile phase consisted of Water with 0.1% of formic acid (solvent A) and acetonitrile with 0.1% of formic acid (solvent B).

For the analysis of Steele-ND, a step gradient elution profile was used starting with 5% B for 0.75 min; increasing from 5% to 35% B between 0.75 to 15 min; from 35 to 100% B between 15 to 30 min; back from 100% to 5% B until minute 34.01 min. Post-run time was set at 2 minutes to clean the column. The injection volume was 2 μl. A blank sample was run two times before the beginning of a series of injections and at the end of the run. A needle wash of 3 seconds with needle seat black flush was included.

The UHD Accurate-Mass MS general acquisition settings and MS-TOF settings were left as default except for the parameters described in the supplemental material (TOF/Q-TOF Mass Spectrometer section). Reference mass solution was prepared using an API-TOF Reference Mass Solution Kit (Supelco/Agilent Part No. G1969-85001). It consisted of 1.0 ml Ammonium Trifluoroacetate (100 μM); 2.0 ml purine (10 μM); 0.8ml (2.5 μM) Hexakis (1H, 1H, 3H-tetrafluoropropoxy) phosphazine; dissolved in 500 ml of 95% acetonitrile : 5% water. Reference masses were 121.050873 and 922.009798.

Sample vials that contained either a blank or inoculated floret extracts, were held in the Infinity 1290 UHPLC auto-injector at 25 °C for the duration of the analysis run (more than 24 hr.). The process was as follows: The ground Steele-ND sample was divided and extracted in two vials (A and B). Time count started at the moment the solvent was added to the ground florets. After extraction, 7 consecutive time points were analyzed: 5:14, 6:30, 7:46, 9:02, 10:18, 11:34 and 12:50 hours. After a pause, the last time point was collected at 26:29 hours (Table 1). The process was repeated 3 consecutive days; each one began with a fresh sample extraction. The results files of the analysis had a *.d extension.

Data Pre-Processing

Raw *.d files from the Mass Hunter acquisition software were processed using Mass Hunter Workstation Qualitative (MH Qual) analysis ver. B.5.00 Build 5.0.519.0 (Agilent Technologies, Inc.). Within this software, the Molecular Feature Extraction (MFE) algorithm provided a *naïve* finder that was effective as a first way to scrutinize UHPLC QTOF/MS raw data. The algorithm was set accordingly for small molecules discovery. The adjusted parameters can be found in supplemental material (Find by Molecular Feature). Pre-processing was assisted by the DA reprocessor software ver. B.05.00 (Agilent Technologies, Inc.) which converted *d files to *cef files.

Mass and time alignments

The retention time (RT) window was estimated on the MH Qual software. By overlaying the raw peaks or the total ion current (TIC) scan within each day and clicking the apex of the left-most peak of a zoomed –in plot. This time was recorded and subtracted to the right-most peak of another TIC. Comparative sample plots were assembled at this stage.

The output ".cef" files were aligned for time and mass using Mass Profile Professional (MPP) ver. 12.1 Build 170166 (Agilent Technologies, Inc). The compound alignment option was modified as to set a retention time window of 0.15 minutes. A filter by flags option was selected at 10% of the total samples in order to discard some of the artifacts generated by the previous processes. Flags are attributes that denote feature quality. Selected options can be: "present" (mass was detected), "absent" (no mass detected) and "marginal" (signal saturated). The filter finds masses based on the quality of these flags in the sample files. A recommended setting involves detecting the present and marginal features found in at least 2 out of 20 or less sample files. The features that pass the filter will be collected in a new list for further processes. The masses that were only found once in the entire data file are likely to be artifacts and will be discarded. Due to the number of files (more than 20) a 10% of the total sample files seemed to work well according to the manufacturer (32).The resulting aligned data was exported for recursion analysis using a single *.cef file.

Recursion analysis

This step was performed in the MH Qual program after completing the MFE run, mass and time alignment. Utilizing this approach significantly reduced the false positive features generated by the MFE. The algorithm "find by formula" included: options, chromatograms and mass spectra. The unique *.cef file generated by the alignment process was used as template to start the recursion analysis. The specific settings can be found in the supplementary material (Find Compounds by Formula section). The MH Qual software was again assisted by the DA re-processor program and was used in the same fashion as mentioned before. After the recursion analysis, the new output sample *.cef files were loaded to the MPP software for statistical analyses. The MH Qual software was again assisted by the DA re-processor program. After the

recursion analysis, the new output sample *.cef files were loaded to the MPP software for statistical analyses.

Statistical Analyses

Blank subtraction & Venn diagrams

These operations were necessary to effectively subtract the features (also called entities, unidentified compounds with a mass and retention time) found in the blanks from the actual samples. It was performed using MPP software. As recommended by the manufacturer, data was log2 transformed and then filtered by flags at 10% before performing a Venn diagram to separate and save the features unique to the experimental samples. After collecting a blanked data set, another Venn diagram was prepared to obtain a common set of features between days and samples These blanked common feature set was saved as an entity list to be used in unsupervised PCA plots to verify general tendencies, and Volcano plots (*t*-test) to identify statistical significance and magnitude changes throughout injection times.

Interpretations

The use of MPP software needs to create "interpretations" to answer a particular question. In this study a "Day" interpretation was created to visualize the relation for the 3 days. As the interest was to assess a total universe of compounds and a maximum analytical time window, we created the "injection" interpretation which focused on time point considering day and replicate. Other interpretations were created in this fashion to perform blanking or do other preliminary comparisons.

Principal component Analysis

All plots on experimental conditions were displayed as 3D PCA score plots on the MPP platform. The Day and Injection interpretations were used. The samples were analyzed as injection number. The PCA was made after filtering by flags 10%.

Volcano plots

Since our ultimate goal was to have a practical window time for analysis, data was compiled into volcano plots comparison. This statistical test was very useful for visualizing differences between the first and any other sample time point. It was performed using the MPP software. This arrangement allows distinguishing masses with a fold-change (magnitude of change) as a biological significance; and also statistical significance (takes both magnitude of change and variability into consideration). A two fold change in magnitude represented a relevant biological change and was equal to the absolute ratio between the normalized average intensities of condition 1/condition 2.

The paired *t*-test option was selected to compare the initial time point against the rest. Benjamini-Hochberg FDR multiple testing correction was added for *p*-value correction. The *p*-value cut off was set to 0.05. The fold change cut-off was set at 2. The abundance difference (raw, abs) cut-off was set to lower the number of false positive features originated by the process. A value of 500 was enough to eliminate meaningless fold change differences (32).

Results and Discussion

In this study we investigated the stability of samples as part of the initial steps in designing an untargeted metabolite profiling study. It has been recommended that samples should be analyzed as soon as extracted to prevent the decay of metabolites (33). Often this is not possible and measures to preserve the integrity of the extracted sample such as: reduced

temperatures, darkness, enzyme addition, inert gases, etc., are commonly employed (4,33,34). The number of samples or replicates in a single analytical run and the time for analysis needs to be considered to prevent a potential change within an extracted sample that is waiting in an auto-injector. It is evident that a practical approach must be taken to ensure sample throughput as well as high recovery of metabolites (3). Therefore, detecting the threshold of change for the type of tissue to be analyzed becomes a necessity, that could be related to each plant species (35) and is also justifiable at the level of plant organ (18). Table 1 illustrates the injection schedule. The time count began with the addition of extraction solvent to the ground floret samples until the time of their injection.

Table 1. Cumulative time sequence for injections at 25 °C

Time point	**Injection time (hr:min)[a]**
1	5:15
2	6:30
3	7:45
4	9:00
5	10:15
6	11:30
7	12:45
8	27:15

[a]Time in hours and minutes taken for each time point over 3 consecutive days

Extract Stability at Room Temperature (25 °C)

Sample reproducibility

The reproducibility of the data acquired daily from ground floret samples stored at -80 °C was demonstrated by overlaying TIC plots for all runs (23,36). Samples for day 1 (red), day 2 (blue) and day 3 (green) correspond to each day in Figure 1. Overall, samples appeared

consistent, with a time drift of 0.1 minutes. Intensities overall appear similar except from minute 25 onwards, when a slight decrease of the signals are seen as analysis day progressed. It can be seen that samples signals in this experiment were stable overall.

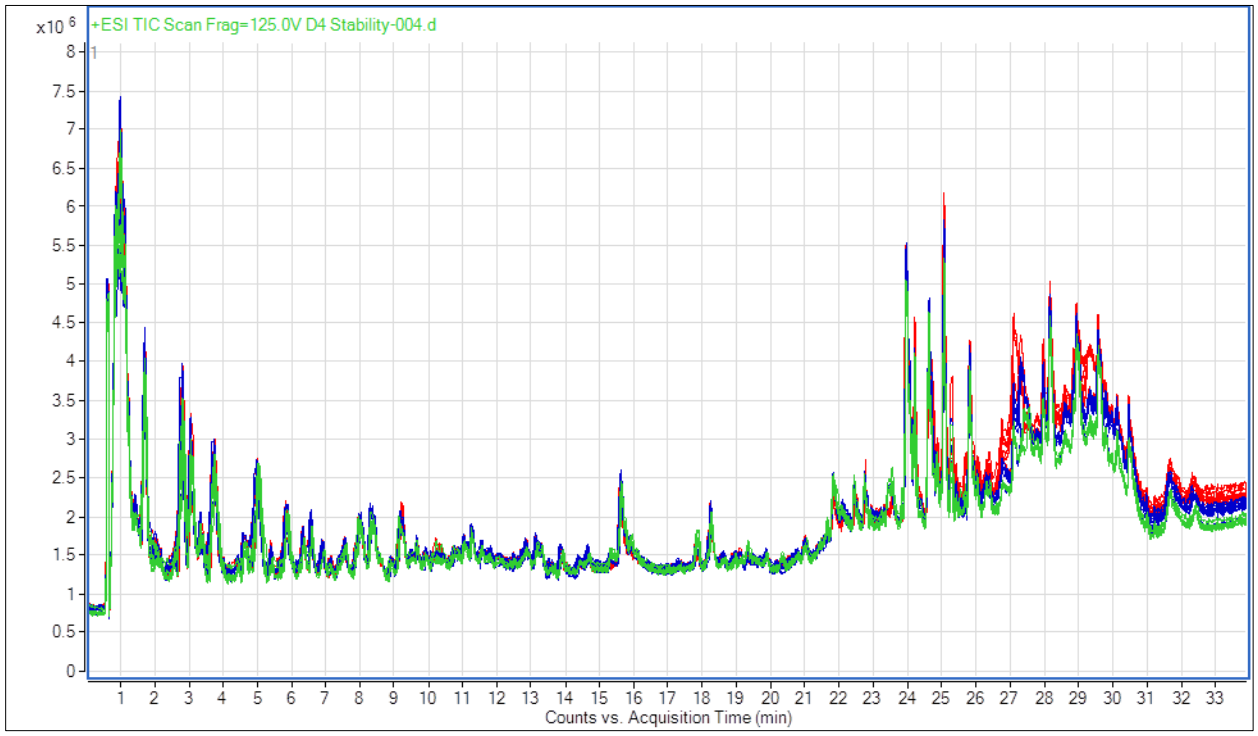

Figure 1. Overlaid TIC plot for Steele-ND at -80 °C analyzed 3 consecutive days (counts per seconds vs time in min.). Each color represents a day: red= day 1; blue= day 2; green= day 3.

Data pre-processing

The blanked features served as an input for a Venn diagram, PCA and volcano plot analyses. A total of 870 extracted features (m/z with retention times) were compiled after blanking and filtering. PCA of the ground sample stored at -80 °C was performed in order to identify any patterns. In Figure 2, storage day can be seen forming distinct clusters. Interestingly, a marked regular tendency of the time points is replicated in each day. To verify the consistency of the features detected each day, a Venn diagram in Figure 3 was used to show how many of those features were unique each day. The majority of features (95.6%) are common to all days, with only a few shared ones that diminished as the day progressed. The decay of features

overtime was evaluated by using the common pool from the 3 day runs. This effectively disregarded any other molecule that entered by small differences due to preparation. Figure 4 shows the general tendency of the time points after combining the data from the 3 days PCA. The most noticeable grouping is seen from 4 (9:00 hr) to 7 (12:45 hr). Points 1 (5:15 hr), 2 (6:30 hr.) and 3 (7:45 hr) are far on the X axis but are not as separated as with time point 8 (27:15 hr).

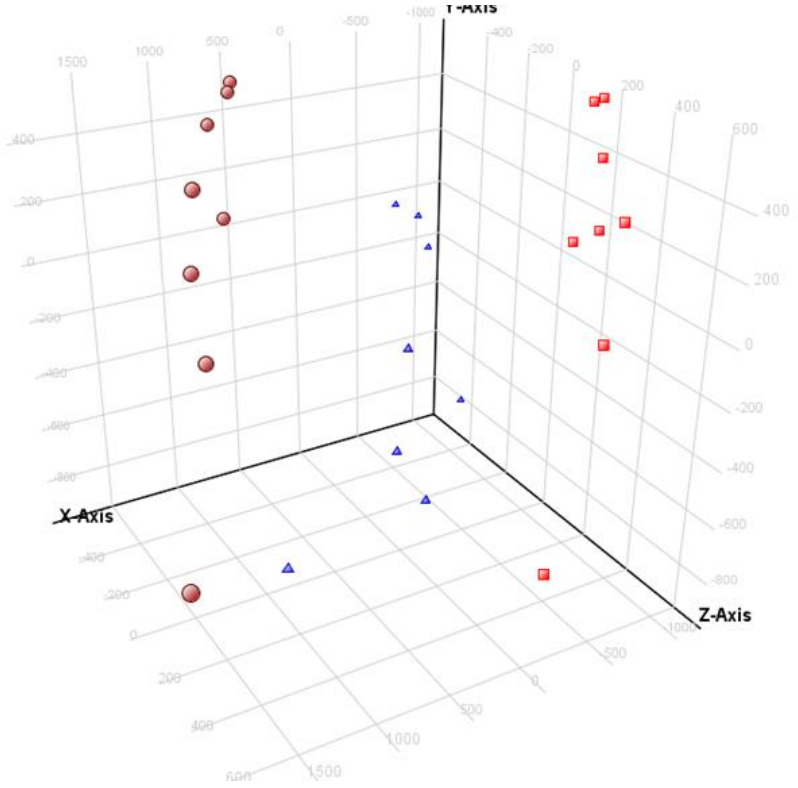

Figure 2. PCA of Steele-ND samples at -80 in 3 analytical days. The top of Y axis corresponds to the first injections. The most distant points correspond to the last injections. Each color represents a day: red= day 1; blue= day 2; brown= day 3. Each point represents 2 samples.

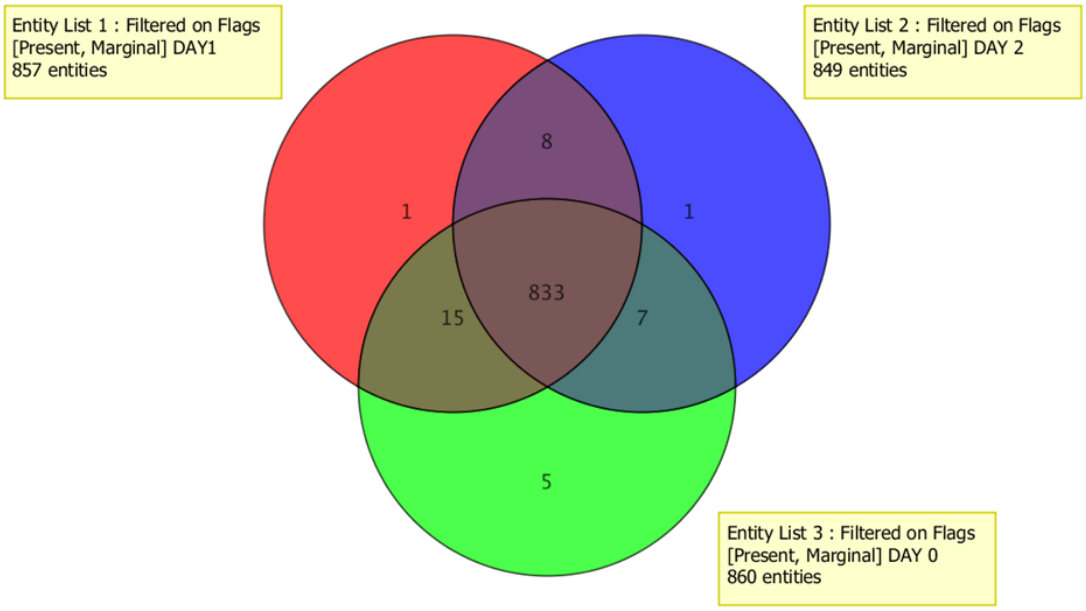

Figure 3. Venn diagram representing features of 3 days of analysis. Common compounds for the three days represent 95.6% of the total. Green= day 1; red= day 2; blue= day 3.

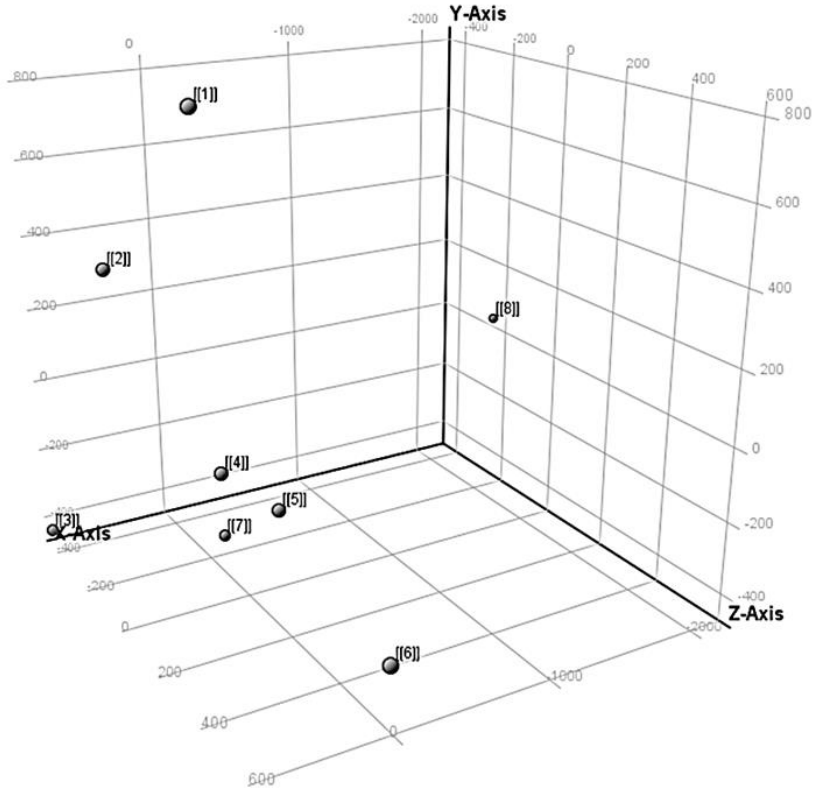

Figure 4. PCA score plot of Steele-ND wheat florets sample analyzed at 25 °C. Numbers 1 to 7 represent consecutive injections in the first 13 hours. Point 8 represent the same sample analyzed after 26 hours. Each point on the plot corresponds to 6 total samples analyzed in 3 days. Time points (hour): 1= 5:15; 2= 6:30; 3= 7:45; 4= 9:00; 5= 10:15; 6= 11:30; 7= 12:45; 8= 27:15.

Analytical window determination

To identify which time point was the first in which significant changes occurred to the extract, a series of volcano plots comparing the initial and subsequent injections was evaluated. A volcano plot consists of a scatter plot in which the "x" axis corresponds to the log10 of the *p*-value; the "y" axis refers to the log2 of the fold change. This arrangement allows distinguishing features with a biological significance fold-change; and also a statistical significance. In this manner, it takes both magnitude of change and variability into consideration (32). In this study, volcano plots were used to determine any change that could be significantly different to the original sample profile. The plots seen in Figure 5 starting from pair 1 Vs 4 show features that are statistically significant (above a horizontal green line) and important in magnitude (> or = to a fold change of 2 vertical green lines).

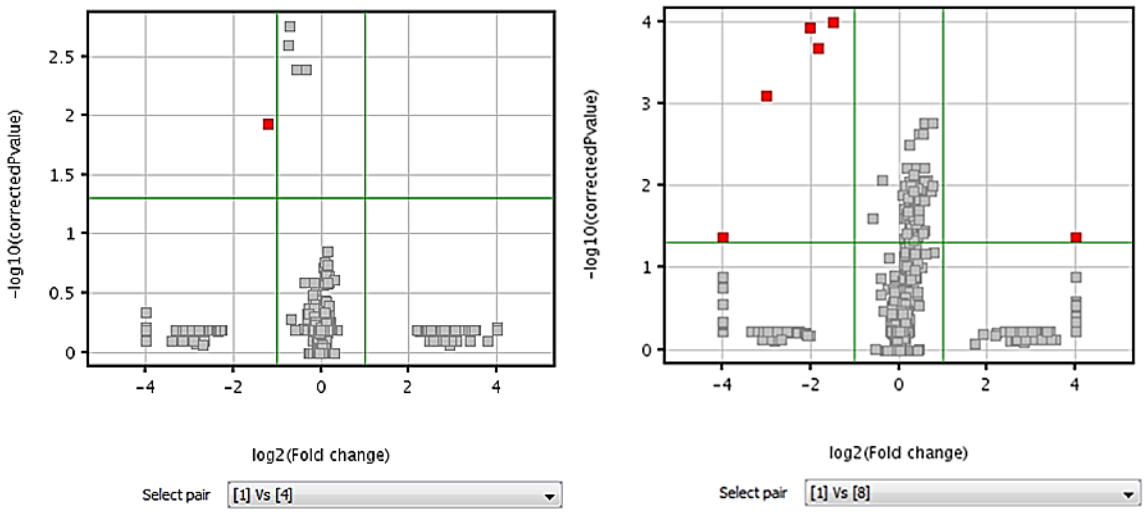

Figure 5. Volcano plots of Steele-ND wheat florets extracts analyzed at 25 °C. Volcano plot on the left represents time point 1 vs time point 4, were the first significant difference was detected (9:00 hours). A significant compound (242.0425 Da) was consistently found in all analyzed times. The volcano plot on the right (1 vs 8), represents the same sample analyzed after 27:15 hours. Additional significant compounds can be seen represented in red. Upper-left quadrant represents a compound significantly higher in any of the later time points. Features found in the upper-right quadrant represent those being higher in time point 1. No significant compounds were found in previous comparisons (1 vs 2 or 3rd time point).

These compounds were represented in red for each quadrant of the volcano plot. If the comparison is X vs. Y, the compounds higher in X will be visualized on the right quadrant. There were no significant compounds in pairs 1 Vs 2 or 1 Vs 3 (plots not shown). As time progressed, a marked increase in significant compounds is detected. Interestingly, comparison 1 Vs 8 shows also a feature higher in 1 than 8. This could represent a compound that decreased drastically in injection 8th, thus showing higher in injection 1. In contrast, a report with *Brassica nigra* leaf tissue showed no appreciable effect in drift, intensity or mass accuracy up to 240 hours when using an auto injector at 20 °C (4). The same auto sampler temperature was applied to barley metabolomics studies (37), and a lower one (10 °C) to wheat metabolite comparisons (10) although no stability data is shown.

Relevant significant features that are seen in the volcano plots were: isotopic mass 242.0402 Da/ rt 4.31 min. was found significant in pair 1 Vs 4 through 8. Features significant in pair 1 vs 6 through 8 corresponded to isotopic mass 297.0894 Da/ rt 3.20 min and mass 205.0737 Da/ rt 10.37 min. An additional feature in pair 1 vs 8 correspond to isotopic mass 242.1055 Da/rt 10.21 min. The mass higher in time point 1 than time point 8 corresponded to isotopic mass 598.4018 Da/ rt 25.17 min. A cumulative time effect in number and intensity of molecules is evident for the extracts in this kind of tissue; therefore an estimated cut-off decision could be made depending on the type of study to be performed or if a specific metabolic target is at risk of being lost. In our case, due to the untargeted nature of this approach, any loss is important as it reflects a 2 fold change significant difference for a potentially relevant metabolite.

As part of their study in human biofluids, Gika, *et al.* (36) verified the stability of urine samples inside an auto-injector at 4 °C. They compared the TIC of quality control samples by visually inspecting the fingerprints, but relied on multivariate methods such as PCA score plots

to compare the actual differences. They also found masses that increased or decreased in intensity later in the runs. The increased signals found in our study could be degradation products that intensify over time until they were detectable and determined through statistical tests. An example of one is seen in Figure 6.

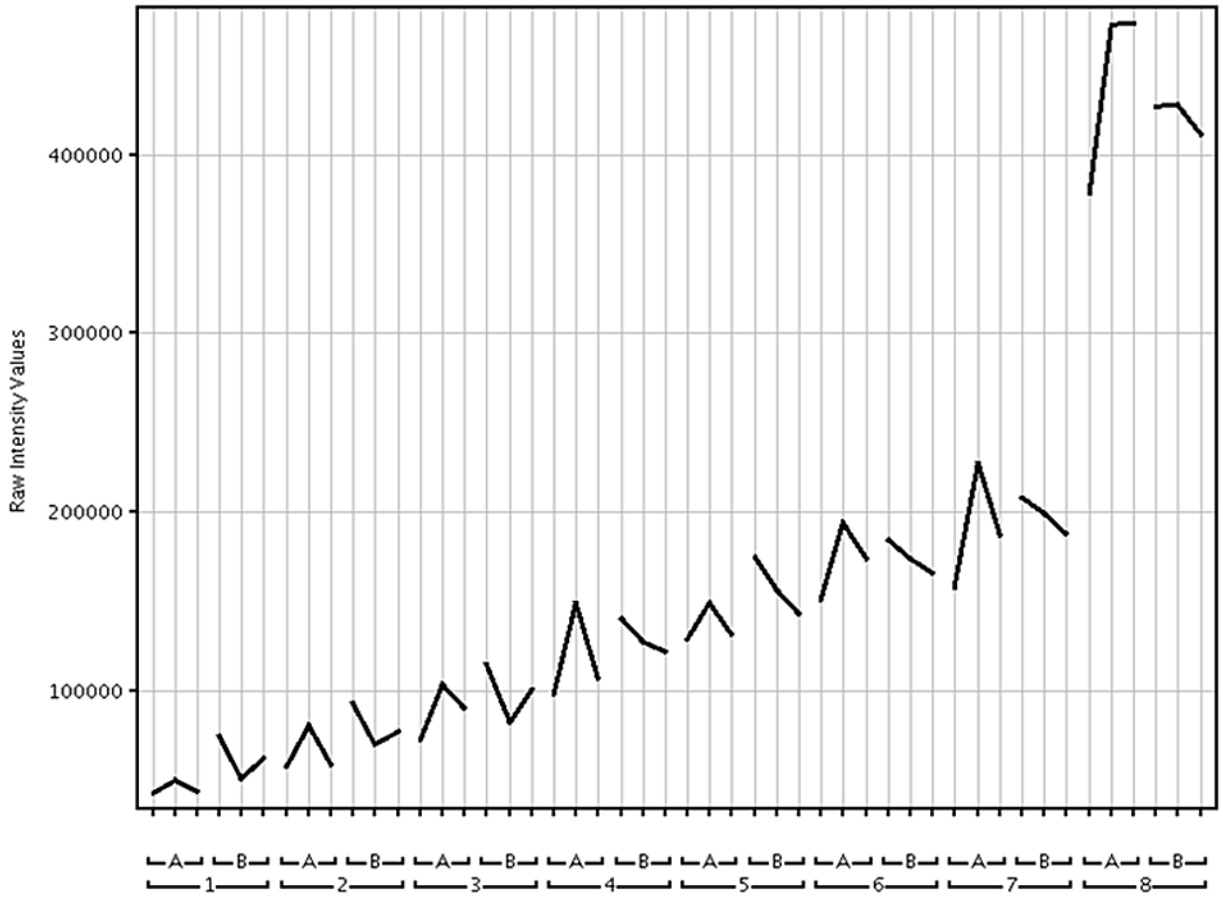

Figure 6. Intensity graph of a feature found in a 25 °C volcano plot 1 vs 4 (higher in 4). The feature was common from time point 4 till 8. Intensities were plot against each injection in succession for 3 days. Isotopic mass was 242.04025 Da with a retention time of 4.308 min. Time points (hour): 1= 5:15; 2= 6:30; 3= 7:45; 4= 9:00; 5= 10:15; 6= 11:34; 7= 12:45; 8= 27:15.

For practical purposes, it was observed that for Steele-ND metanolic extracts analyzed at 25 °C, the maximum analytical time without appreciable changes should be 7:45 hours. The amount of samples and repeats should be fitted accordingly with this window time. This matches the concept that, aside from samples being randomly analyzed, they should be processed in

reduced batches since several samples processed at a single time may increase the error (2); making it rational to do particular adjustments depending on the sample type (18,35).

As mentioned before, oxidation events are prone to occur after the sample has been altered (11). Since samples were stored crushed in a normal air atmosphere, it makes sense that such events might happen and alter the chemistry of the samples. As a solution, crushing and extracting prior to the analysis would seem a good step to improve the overall quality at the cost of analytical time. Another improvement to prevent decay in the auto injector could be reflected by decreasing the temperature, to help preserve the quality of the sample during analysis for a longer time. Such experiments would decide the programing and repetitions of the samples to be analyzed per run cycle.

Conclusion

The effect of time on the stability of extracted wheat floret samples was investigated over analytical time. The use of PCA coupled with volcano plots helped to define the maximum time before the sample started to change in an auto-sampler. For Steele-ND wheat floret extracts analyzing in a 25 °C environment, a maximum stable analytical time (from extraction to injection) was found to be 7:45 hours. The time found in this study should not be taken for any other type of sample nor analytical pipeline. However, the approach could be applied to determine the work logistics in a metabolite profiling study with the aim of producing confident results.

References

1. Dunn, W. B., and Ellis, D. I. (2005) Metabolomics Current analytical platforms and methodologies. *Trends in analytical chemistry : TRAC* **24**, 285-293

2. Khakimov, B., Bak, S., and Engelsen, S. B. (2014) High-throughput cereal metabolomics: Current analytical technologies, challenges and perspectives. *Journal of Cereal Science* **59**, 393-418

3. Theodoridis, G. A., Gika, H. G., Want, E. J., and Wilson, I. D. (2012) Liquid chromatography-mass spectrometry based global metabolite profiling: a review. *Analytica chimica acta* **711**, 7-16

4. De Vos, R. C., Moco, S., Lommen, A., Keurentjes, J. J., Bino, R. J., and Hall, R. D. (2007) Untargeted large-scale plant metabolomics using liquid chromatography coupled to mass spectrometry. *Nature protocols* **2**, 778-791

5. Gunnaiah, R., Kushalappa, A. C., Duggavathi, R., Fox, S., and Somers, D. J. (2012) Integrated metabolo-proteomic approach to decipher the mechanisms by which wheat QTL (Fhb1) contributes to resistance against Fusarium graminearum. *PloS one* **7**, e40695

6. Baker, J. M., Hawkins, N. D., Ward, J. L., Lovegrove, A., Napier, J. A., Shewry, P. R., and Beale, M. H. (2006) A metabolomic study of substantial equivalence of field-grown genetically modified wheat. *Plant Biotechnology Journal* **4**, 381-392

7. Curtis, T. Y., Muttucumaru, N., Shewry, P. R., Parry, M. A. J., Powers, S. J., Elmore, J. S., Mottram, D. S., Hook, S., and Halford, N. G. (2009) Effects of Genotype and Environment on Free Amino Acid Levels in Wheat Grain: Implications for Acrylamide Formation during Processing. *Journal of agricultural and food chemistry* **57**, 1013-1021

8. Beleggia, R., Platani, C., Nigro, F., De Vita, P., Cattivelli, L., and Papa, R. (2013) Effect of genotype, environment and genotype-by-environment interaction on metabolite profiling in durum wheat (Triticum durum Desf.) grain. *Journal of Cereal Science* **57**, 183-192

9. Graham, S. F., Amigues, E., Migaud, M., and Browne, R. A. (2009) Application of NMR based metabolomics for mapping metabolite variation in European wheat. *Metabolomics* **5**, 302-306

10. Matthews, S. B., Santra, M., Mensack, M. M., Wolfe, P., Byrne, P. F., and Thompson, H. J. (2012) Metabolite profiling of a diverse collection of wheat lines using ultraperformance liquid chromatography coupled with time-of-flight mass spectrometry. *PloS one* **7**, e44179

11. Ryan, D., and Robards, K. (2006) Analytical Chemistry Considerations in Plant Metabolomics. *Separation & Purification Reviews* **35**, 319-356

12. Kim, H. K., and Verpoorte, R. (2010) Sample preparation for plant metabolomics. *Phytochemical Analysis* **21**, 4-13

13. Fiehn, O. (2001) Combining Genomics, Metabolome Analysis, and Biochemical Modelling to Understand Metabolic Networks. *Comparative and Functional Genomics* **2**, 155-168

14. Sumner, L. W., Mendes, P., and Dixon, R. A. (2003) Plant metabolomics: large-scale phytochemistry in the functional genomics era. *Phytochemistry* **62**, 817-836

15. Álvarez-Sánchez, B., Priego-Capote, F., and Luque de Castro, M. D. (2010) Metabolomics analysis I. Selection of biological samples and practical aspects preceding sample preparation. *TrAC Trends in Analytical Chemistry* **29**, 111-119

16. Villas-Boas, S. G., Nielsen, J., Smedsgaard, J., Hansen, M. A. E., and Roessner-Tunali, U. (2007) *Metabolome Analysis: An Introduction*, Wiley

17. Sumner, L. W., Amberg, A., Barrett, D., Beale, M. H., Beger, R., Daykin, C. A., Fan, T. W., Fiehn, O., Goodacre, R., Griffin, J. L., Hankemeier, T., Hardy, N., Harnly, J., Higashi, R., Kopka, J., Lane, A. N., Lindon, J. C., Marriott, P., Nicholls, A. W., Reily, M. D., Thaden, J. J., and Viant, M. R. (2007) Proposed minimum reporting standards for chemical analysis Chemical Analysis Working Group (CAWG) Metabolomics Standards Initiative (MSI). *Metabolomics* **3**, 211-221

18. Fiehn, O., Wohlgemuth, G., Scholz, M., Kind, T., Lee do, Y., Lu, Y., Moon, S., and Nikolau, B. (2008) Quality control for plant metabolomics: reporting MSI-compliant studies. *The Plant journal : for cell and molecular biology* **53**, 691-704

19. Lauridsen, M., Hansen, S. H., Jaroszewski, J. W., and Cornett, C. (2007) Human Urine as Test Material in 1H NMR-Based Metabonomics: Recommendations for Sample Preparation and Storage. *Analytical Chemistry* **79**, 1181-1186

20. Dunn, W. B., Broadhurst, D., Ellis, D. I., Brown, M., Halsall, A., O'Hagan, S., Spasic, I., Tseng, A., and Kell, D. B. (2008) A GC-TOF-MS study of the stability of serum and urine metabolomes during the UK Biobank sample collection and preparation protocols. *International journal of epidemiology* **37 Suppl 1**, i23-30

21. Deprez, S., Sweatman, B. C., Connor, S. C., Haselden, J. N., and Waterfield, C. J. (2002) Optimisation of collection, storage and preparation of rat plasma for 1H NMR spectroscopic analysis in toxicology studies to determine inherent variation in biochemical profiles. *Journal of pharmaceutical and biomedical analysis* **30**, 1297-1310

22. Teahan, O., Gamble, S., Holmes, E., Waxman, J., Nicholson, J. K., Bevan, C., and Keun, H. C. (2006) Impact of Analytical Bias in Metabonomic Studies of Human Blood Serum and Plasma. *Analytical Chemistry* **78**, 4307-4318

23. Abdel Rahman, A. M., Pawling, J., Ryczko, M., Caudy, A. A., and Dennis, J. W. (2014) Targeted metabolomics in cultured cells and tissues by mass spectrometry: Method development and validation. *Analytica chimica acta* **845**, 53-61

24. Tikunov, Y., Lommen, A., de Vos, C. H., Verhoeven, H. A., Bino, R. J., Hall, R. D., and Bovy, A. G. (2005) A novel approach for nontargeted data analysis for metabolomics. Large-scale profiling of tomato fruit volatiles. *Plant physiology* **139**, 1125-1137

25. t'Kindt, R., Morreel, K., Deforce, D., Boerjan, W., and Van Bocxlaer, J. (2009) Joint GC-MS and LC-MS platforms for comprehensive plant metabolomics: repeatability and sample pre-treatment. *Journal of chromatography. B, Analytical technologies in the biomedical and life sciences* **877**, 3572-3580

26. Moco, S., Bino, R. J., Vorst, O., Verhoeven, H. A., de Groot, J., van Beek, T. A., Vervoort, J., and de Vos, C. H. (2006) A liquid chromatography-mass spectrometry-based metabolome database for tomato. *Plant physiology* **141**, 1205-1218

27. Frohberg, R. C., Mergoum, M., Miller, J. D., and Stack, R. W. (2005) Registration of 'Steele-ND' wheat. *Crop Science* **45**, 1163

28. Ransom, J., Mergoum, M., Simsek, S., Acevedo, M., Friesen, T., McMullen, M., Zhong, S., Eriksmoen, E., Halvorson, M., Hanson, B., Martin, G., Schatz, B. (2011) North Dakota Hard Red Spring Wheat Variety Trial Results for 2011 and Selection Guide. (Station, N. N. D. A. E. ed., NDSU, North Dakota

29. Puri, K. D., and Zhong, S. (2010) The 3ADON population of Fusarium graminearum found in North Dakota is more aggressive and produces a higher level of DON than the prevalent 15ADON population in spring wheat. *Phytopathology* **100**, 1007-1014

30. Zadoks, J. C., Chang, T. T., and Konzak, C. F. (1974) A decimal code for the growth stages of cereals. *Weed Res.* **14**, 415-421

31. Hamzehzarghani, H., Kushalappa, A. C., Dion, Y., Rioux, S., Comeau, A., Yaylayan, V., Marshall, W. D., and Mather, D. E. (2005) Metabolic profiling and factor analysis to discriminate quantitative resistance in wheat cultivars against fusarium head blight. *Physiological and Molecular Plant Pathology* **66**, 119-133

32. Agilent Technologies, I. (2013) Mass profiler professional Workshop. in *Course Number R2260A Student Manual*, Agilent technologies, Inc, Alpharetta, GA

33. De Vos, R. H., Schipper, B., and Hall, R. (2012) High-Performance Liquid Chromatography–Mass Spectrometry Analysis of Plant Metabolites in Brassicaceae. in *Plant Metabolomics* (Hardy, N. W., and Hall, R. D. eds.), Humana Press. pp 111-128

34. Sobolev, A. P., Brosio, E., Gianferri, R., and Segre, A. L. (2005) Metabolic profile of lettuce leaves by high-field NMR spectra. *Magnetic Resonance in Chemistry* **43**, 625-638

35. Salimen, J. P. (2003) Effects of sample drying and storage, and choice of extraction solvents and analysis method on the yield of birch leaf hydrolyzable tannins. *Journal of chemical ecology* **29**, 1289-1305

36. Gika, H. G., Theodoridis, G. A., and Wilson, I. D. (2008) Liquid chromatography and ultra-performance liquid chromatography-mass spectrometry fingerprinting of human urine: sample stability under different handling and storage conditions for metabonomics studies. *Journal of chromatography. A* **1189**, 314-322

37. Bollina, V., Kumaraswamy, G. K., Kushalappa, A. C., Choo, T. M., Dion, Y., Rioux, S., Faubert, D., and Hamzehzarghani, H. (2010) Mass spectrometry-based metabolomics application to identify quantitative resistance-related metabolites in barley against Fusarium head blight. *Molecular plant pathology* **11**, 769-782

PAPER 2. TIME COURSE METABOLITE PROFILING OF FUSARIUM HEAD BLIGHT INFECTED HARD RED SPRING WHEAT USING ULTRA HIGH PERFORMANCE LIQUID CHROMATOGRAPHY COUPLED WITH QUADRUPOLE TIME OF FLIGHT/MS

Abstract

Wheat is one of the most important food crops worldwide. Its overall value is greatly reduced by fungal infections such as from *Fusarium graminearum*, the causal agent of Fusarium Head Blight. Although effective breeding using known resistant cultivars that incorporate resistance through the use of quantitative trait loci has reduced the losses, more knowledge is needed to assess the effectiveness of this process as well as to develop rapid screening methodologies that identify resistant genes. Since the metabolome is the most dynamic system, metabolite profiling technology may provide new insights in finding or explaining FHB resistance mechanisms. By analyzing a near isogenic lines (NIL) with contrasting *Fhb1* alleles and three wheat varieties using UHPLC-QTOF/MS technology, a time course resulting in 61 relevant metabolites was studied. Some compounds were shared between the NIL and the varieties; however, the cultivars also showed some unique metabolites. The presence of 1 metabolite as resistant related constitutive late in the time course was detected. Tentative identification was performed by using online tools and Tandem MS resources. Overall, results confirm the presence of hydroxycinnamic acid amides conjugated with polyamine derivatives (HCAA) which have been shown to induce thickening of cell wall. These compounds are shared by resistant and susceptible genotypes with no difference in intensities but vary in time as early or late occurring. Findings of "susceptibility indicator" molecules were also considered. This

suggests that for the near isogenic line studied here, HCAA were a normal part of host reaction, while potentially important metabolites for the host resistant reaction develop later after 48 hours after inoculation.

Introduction

Wheat (*Triticum aestivum* L.) represents a major crop in the world. However, its value is reduced greatly by fungal infections and mycotoxins (1). Fusarium Head Blight (FHB) is one which has the greatest significance worldwide, being one of the most destructive wheat diseases having both negative economic and health impacts (2). The disease manifests itself as premature bleaching of the wheat heads (3) and the deposition of toxins such as deoxynialenol. The resulting low yield and quality has resulted in millions of dollars in losses per year in the USA (4). Many species of *Fusarium* are globally important pathogens of wheat. FHB is mainly caused by *Fusarium graminearum* Schawabe (telemorph: *Gibberella zeae* (Schweinitz) Petch) and *Fusarium culmorum* (W.G. Smith) Saccardo (3), with *F. graminearum* being the dominant fungal species causing FHB in North America (5,6).

Fusarium head blight is of primary concern because these fungi produce a number of secondary metabolites within infected grain that are toxic to humans and animals. The most prevalent *Fusarium* mycotoxins in wheat are the trichothecenes such as deoxynivalenol (DON) and nivalenol (NIV) (7,8).

Breeding wheat cultivars for resistance is the most practical way to manage this disease in the long-term (9). There is known variation for resistance to FHB, with examples having high and low resistance. However, no wheat or barley variety is completely immune (10,11). It is considered that type II resistance (resistance to disease spread within the spike) is the most used in wheat (12). Aside from type II resistance seen on cultivar sources like Sumai3 and Niang

(13,14), the genetics of the other types of resistance remain to be fully elucidated. Sumai3 is widely used as a breeding source for resistance due to a quantitative trait loci (QTL) on chromosome 3BS or *Fhb1*, that has been identified to provide a high type II resistance in the range of 15-60% of phenotypic variation (15). Although breeders have used QTL's in marker assisted selection, this strategy might fail in some cases to transfer the expected level of traits (16).

Past studies have linked specific metabolites to particular genomic locations. They have found that a set of genes regulating metabolic pathways through enzymatic reactions produce metabolites that constitute a unique phenotype (17,18). In summary, the metabolome is the ultimate expression of genes (19). Metabolomics has the objective to identify and quantify the totality of metabolites in biological systems (17). Non-targeted metabolomics techniques have been used to study resistance of wheat against *F. graminearum* (20,21). The resistance modes of action have been associated with the phenypropanoid, terpenoid and fatty acid pathways; which are involved in plant defense signaling, antimicrobial activity and cell wall thickening. Ideally, subjects with nearly identical genetic backgrounds should be used in the study of metabolites and their role in resistance since differences in the metabolic pool could be the result of different plant genetic makeup (22). A recent report used near isogenic lines of wheat with contrasting FHB susceptible/ resistant alleles in an attempt to reduce complex whole genome epistatic interactions and highlight the relevance of a resistant QTL on chromosome 2DL (23). The previous *Fusarium* resistance studies used GC-MS technology to detect the metabolites. GC-MS is mostly used in the analysis of volatile organic compounds with a required derivatization step for the detection of non-volatile/polar metabolites. On the other hand, LC-MS methods cover a more ample spectrum of metabolites without the need of derivatization. The key in resolution

and mass accuracy of the peaks depends on the type of mass analyzer (24). In addition LC-MS has been proven a popular choice being used for its capacity to separate and detect a wide set of molecules with high sensitivity (25). The choice of ion separation methods is also greater in LC-MS compared with GC-MS. Mass analyzers like Quadrupole Time of Flight (QTOF) offer high mass accuracy coupled with an ample *m/z* scanning range, 50 - 1200 *m/z*, and selected ions monitoring (24). A concrete example of a comprehensive untargeted protocol using an Ultra-high performance LC-MS for the analysis of *Arabidopsis* resulted in the detection of several hundred metabolites (26). Non targeted metabolo-proteomics approaches have used 2D gel electrophoresis combined with LC-MS/MS strategies in order to elucidate wheat defense systems in a FHB infection (27). In addition, the phenylpropanoid pathway compounds, in particular the hydroxycinnamic acid amides, conjugates of phenol polyamines compounds, were seen to be present in higher concentrations on resistant wheat lines. They further confirmed this by detection of relevant role of oxidative burst and accumulation of key enzymes. It was concluded that the resistance provided by *Fhb1* was mainly due to regulation of the phenylpropanoid pathway.

The selection of metabolites conferring resistance based solely on their increase in number could be misleading. A limited host infection may yield in turn a few compounds as a result of plant resistance (22). On the other hand, some genomic and proteomic wheat studies have focused on observing the onset of pathogenesis-related proteins (28), transcripts in early and late stages (29) or expression patterns in a time course fashion (30). The advantage of these approaches gives insight to expand the knowledge of the resistant genes, although not making a direct link with the end metabolites.

Our objective in this work was to determine the occurrence of significant and biologically relevant compounds present early in FHB infected wheat NIL with contrasting *Fhb1*alleles. Also, to consider the relationship that exists between the NIL time course model and three wheat cultivars varying the levels of resistance to FHB.

Experimental Procedures

Statistical Design

The experiments were organized in a randomized complete blocks design (RCBD) and consisted of three blocks (replications) with the wheat genotypes within blocks being randomized. For the wheat varieties there were 2 treatments inoculations: water (mock) or with the pathogen within a single time point for each of the three cultivars (low, medium and high resistance). For the near isogenic line (NIL), the experiment contained 2 contrasting alleles of *Fhb1* QTL for FHB resistance and 2 inoculations of spikelets: one with the pathogen another with water, plus a 5 point time course. A biological sample for metabolite profiling consisted of a pooled sample of 16 spikelets to be harvested 24 hours after inoculation (hai) in wheat varieties; or in a time course of 0, 6, 12, 24 and 48 hai for the NIL. Wheat varieties or NIL were planted simultaneously in each block to yield a minimum of 6 pooled samples or biological repetitions per treatment per block. Each block was planted giving a space of 2 weeks before the next one. Figure 7 and 8 summarize the experiments.

The FHB symptoms on pathogen inoculated/mock inoculated wheat spikelets were assessed over a period of 21 days after inoculation (dai) using a visual scale to estimate the severity of FHB in wheat (31)

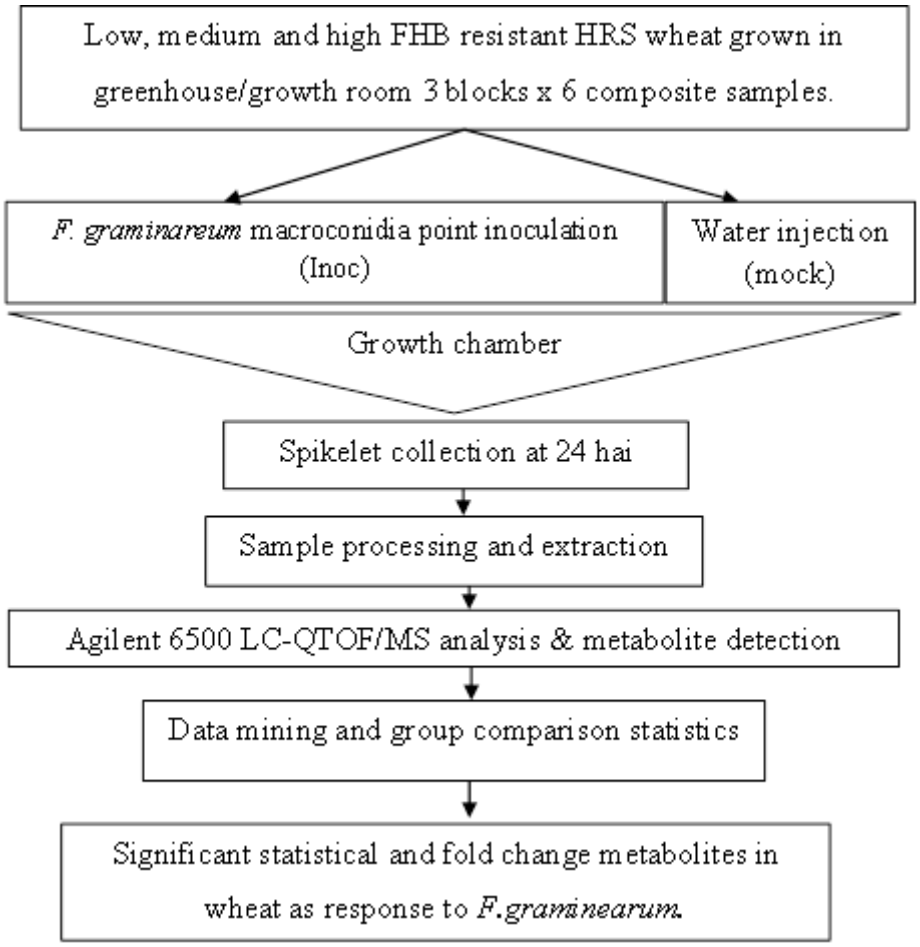

Figure 7. General diagram of metabolic profiling experiments in hard red spring wheat florets inoculated with *F. graminearum*.

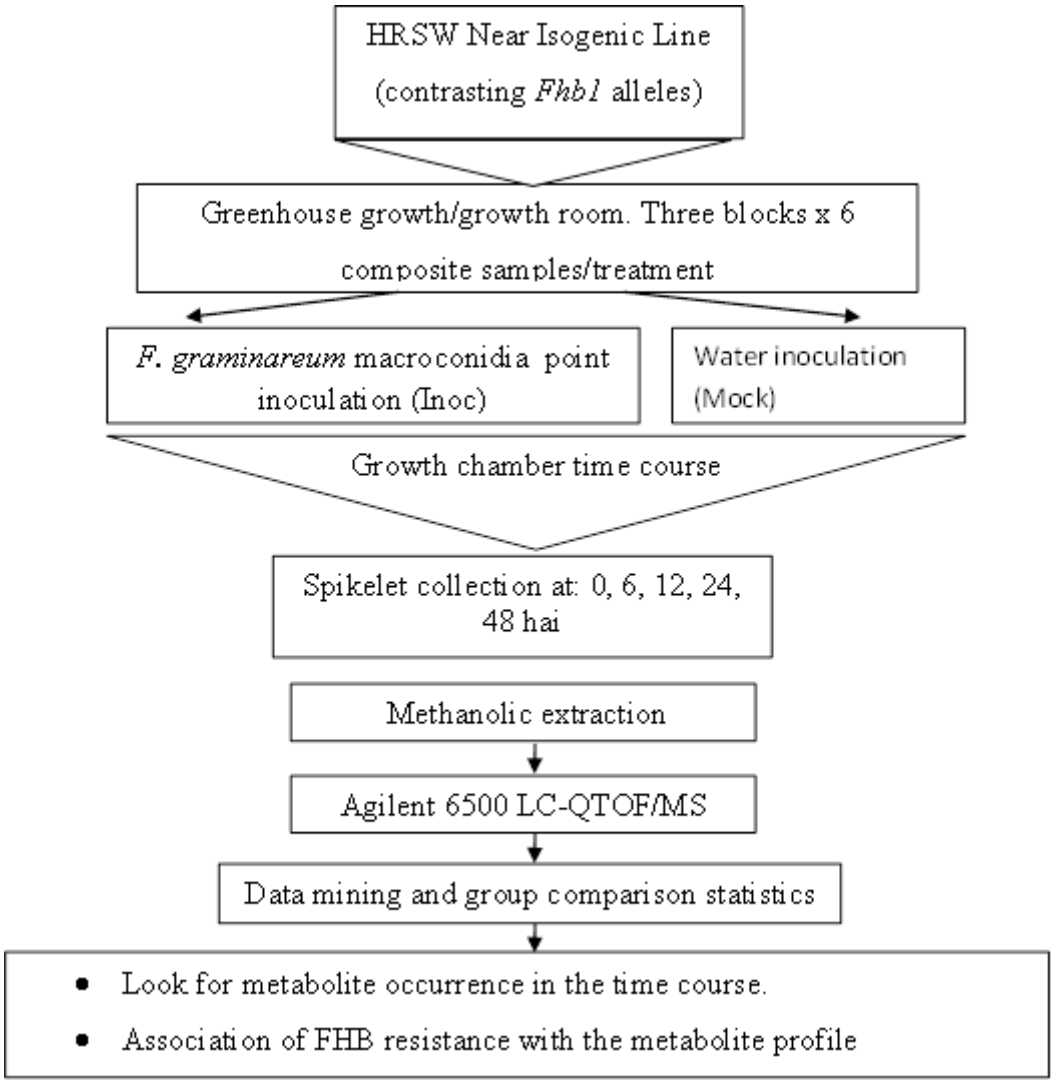

Figure 8. General diagram of metabolic profiling as a resistance screening tool in wheat near isogenic line with contrasting *Fhb1* alleles.

Wheat Planting, Inoculation and Sampling

Seed

The near isogenic line (NIL) was kindly provided by Dr. James Anderson of the Department of Agronomy and Plant Genetics at the University of Minnesota. The selection was based on its resistance to FHB and growth characteristics. NIL Pair 19 was composed of contrasting *Fhb1* alleles, one being susceptible (NIL-S) and the other resistant (NIL-R). The pair

pedigree corresponds to: 72055 55 260-28-1-6 S/S 63-4/MN97448; 72056 56 260-28-1-4 S/S 63-4/MN97448, derived from a cross between Sumai 3/Stoa 63–4//MN97448. The average QTL effect on disease severity due to *Fhb1* is reported at 64% for this specific pair (32).

Seeds of the hard red spring wheat (HRSW) varieties Glenn, Steele-ND and Reeder were obtained from Dr. Senay Simsek, Department of Plant Sciences of the North Dakota State University. Samples were selected based on resistance to FHB (33). Glenn pedigree consisted of: ND 2831/'Steele-ND' (PI 634981). ND 2831 is a hard red spring experimental line developed by the NDSU breeding program from the cross 'Sumai 3'(PI 481542)/'Wheaton'(PI 469271)//'Grandin'(PI 531005)/3/ND 68826 (34). Glenn is considered moderately resistant to FHB (33).

Steele-ND pedigree consisted of: 'Parshall' (PI 613587)/5/ 'Grandin' (PI 531005)/3/IAS[20.sup.*]4/H567.71//'Amidon' (PI 527682)/ 4/[Grandin.sup.*]2/'Glupro' (PI 592759)27 (35). It is classified as intermediate to FHB (33).

Reeder pedigree consisted of: IAS-20*4/H-567.71//STOA/3/ND-674 (36). It is derived from a complex cross of a Brazilian line, Stoa, Grandin and GluPro (37).This variety is classified as susceptible to FHB (33).

Planting

Wheat was sown in 3.8 cm Ray Leach Cone-Tainers, planting 1 seed in each cone. Sunshine Mix #1/LC1 Soil was used for planting. The plant density was set at 70 cones per rack. After emergence, 8 beads of Multicoat 4 fertilizer (Haifa group, Israel) were applied to the top soil of each cone. The racks containing the cones were kept in water trays filled with reverse osmosis water. Greenhouse temperature was set at 25 ± 2 °C with a 16:8 hour (light : day) photoperiod until booting stage.

When the first awns were visible (GS= 47-49) (38), wheat plants were incubated in a growth room with conditions similar to the greenhouse, with the exception that the light intensity was regulated to ≈15000 lm/m^2. The purpose of this was to stabilize the plants by having a constant light intensity while avoiding temperature swings.

Inoculation and sample collection

At the reach of anthesis (GS=60-69 Zadoks scale) (29) the varieties/lines were inoculated with a *F. graminearum* strain isolated from Foster, North Dakota in 2008 named Fg08-001. The isolate was provided by Dr. Shaobin Zhong from the Department of Plant Pathology at North Dakota State University. It is regarded as a strain with a 3-acetyl Deoxynivalenol (3ADON) chemo-type (39). Growth and inoculation with *F. graminearum* macorconida was applied as described elsewhere (20,39). A 10 µl of the macroconidial *F. graminearum* suspension (100 conidia per µl) was inoculated between the palea and lemma of four central spiklets of four independent spikes (Figure 9). Treated spikelets were marked by cutting the awns of the respective spikelet. Plant incubation was performed in a mist chamber with 28.5 +/- 0.5 °C, with a spaying rate of 20 seconds at 15 minutes intervals to ensure 90 to 95% RH for fungal colonization. For the NIL, following inoculation the plants were incubated depending on the treatment for 6, 12, 24 or 48 hours respectively. A 0 hour sample collection was performed immediately after inoculation. A total of 720 plants were inoculated with the pathogen, with an equal number of plants were mock inoculated. For the wheat varieties, following inoculation, all treated plants were incubated in a mist chamber for 24 hours. A total of 144 plants for each variety were inoculated, with an equal number of mock treated plants being also processed. A sample was composed of four replicated sets of four florets, each set being represented by a single plant's spike, giving a total of 16 pooled florets in a sample (20). Florets were collected in

labeled #1 Kraft paper coin envelopes (2-1/4 x 3-1/2) submerged immediately in liquid nitrogen. Frozen tissue was stored in an ultra-freezer at -80±1 °C until use.

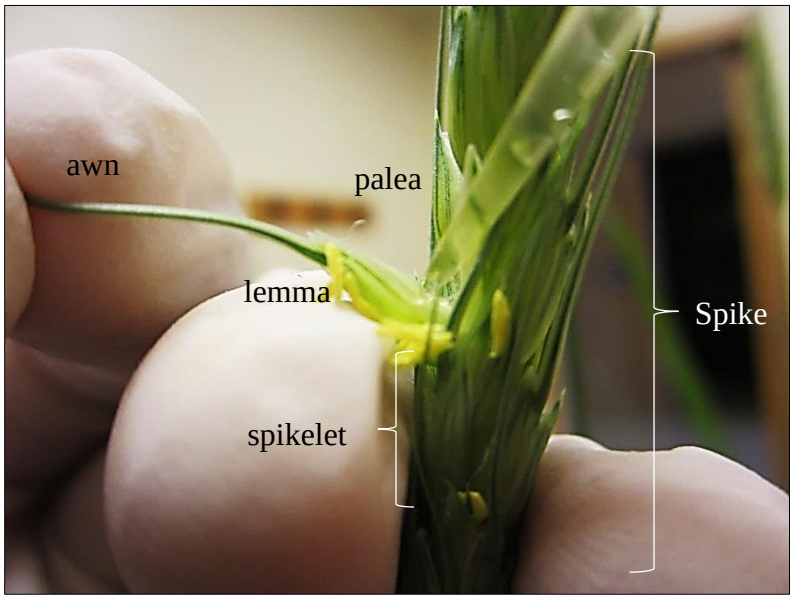

Figure 9. Floret inoculation with *F. graminearum* macroconidial suspension. When the incubation time was fulfilled, sixteen inoculated florets (4 florets collected from 4 spikes) were gathered to compose a sample.

Severity

To evaluate FHB severity, an extra 40 plants from each block were set aside and were point inoculated at a single spikelet located at the middle of the spike (29). These plants were incubated for 24 hours. Disease severity assessment was carried out by evaluating at 21 days after inoculation (dai). A spikelet showing discoloration, browning, necrosis or visible mycelia was considered diseased. The FHB severity percentage was assessed as the number of diseased spikelets in a spike by utilizing a pictorial scale as seen in Figure 10 (31).

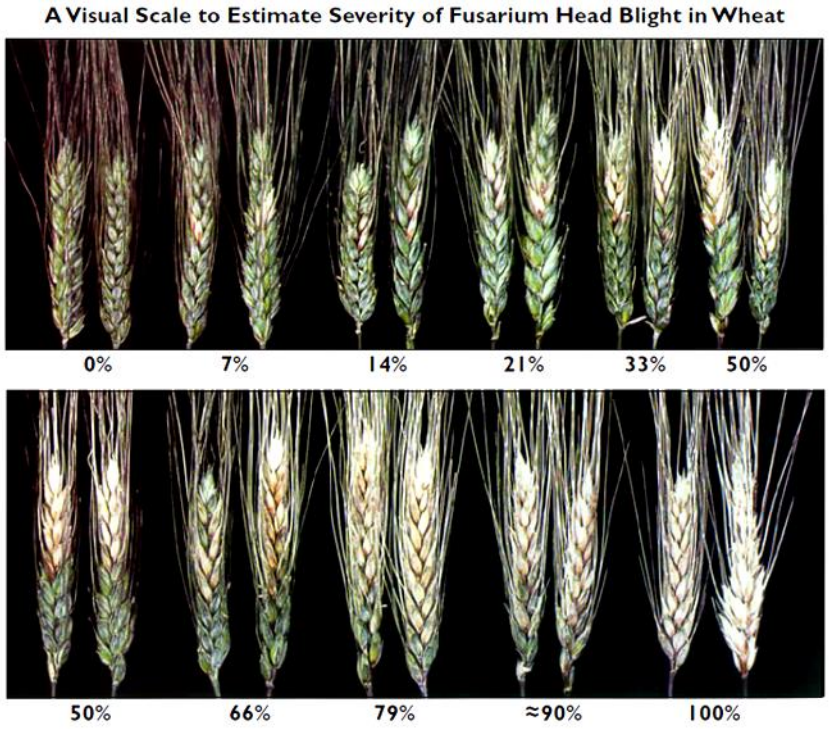

Figure 10. Visual scale to estimate the severity of FHB in wheat. Adapted from (Stack and McMullen, 1995).

Sample Extraction

The process of selecting which samples to be prepared was randomly generated. Before each run, the frozen tissue was crushed into a fine powder utilizing a washed (2% phosphate-free detergent followed by a two-step distilled water soaking/rinse-cycles in two days) heat-treated (4 hr. at 590 °C) ceramic pestle and mortar sitting on dry ice. Tissue thawing was avoided by carefully pouring a small volume of liquid nitrogen onto the sample during crushing and weighing.

Samples prepared for small molecules analysis were extracted based on the methods developed by De Vos et al. (2007) (26) and t'Kindt et al. (2009) (40) with modifications. Tissue extracts were prepared freshly each day before analysis. The ground powder was transferred into a pre-frozen 1.5 ml micro tubes by weighing 300 mg ±5% of the sample powder. Cryogenic conditions were kept by submerging the tube and spatula into liquid nitrogen. Sample extraction

solution (80:20 methanol/water HPLC grade) stored at -80 °C was added in a 3:1 volume/fresh weight ratio. Tubes were stirred in pulses using a vortex shaker for 10 seconds. Next, each sample was submerged in a Branson 2510 sonicator bath (Branson ultrasonics corp.) at 25 °C for 15 minutes set on maximum frequency (40 kHz), this followed by two centrifuge cycles of 10 min each at 3,000g at 6±1 °C. Supernatant for each sample were filtered through a 0.2-µm PTFE filter by using 3 ml. disposable syringes into new 1.8-ml amber glass vials with Teflon caps. The blank vials were prepared in the same way as the samples, except they only contained extraction solution. All samples were analyzed immediately after their extraction.

Sample Analysis

Metabolite analysis was conducted using an UHPLC-ESI-QTOF/MS 6540 series (Agilent Technologies, Inc.) utilizing Mass Hunter Workstation software-LC/MS Acquisition for 6200 series TOF/6500 QTOF version B.05.00 /build 5.05.042.0.

The Infinity 1290 UHPLC section (Agilent Technologies, Inc.) was composed of a G44227A flex cube, G4220A binary pump, G1210B Iso pump, G1316C TCL and a G4226A sampler unit. A Zorbax Eclipse plus C-18 column (1.8 µm; 2.1 x 100mm) was utilized. Reverse phase conditions were maintained at 40 °C with a flow rate of 0.4ml/min. The mobile phase consisted of 0.1% of formic acid (solvent A) and Acetonitrile with 0.1% of formic acid (solvent B).

A step gradient elution profile was used starting with 5% B for 0.75 min; increasing from 5% to 16% B between 0.75 to 6 min; from 16 to 35% B between 6 to 10 min; from 35% to 95% B from10 to 25 min; going back from 95% to 5% B from 25 min to 28 min. Post-run time was set at 2 minutes to clean the column. The injection volume was 2 µl. A blank sample was run two

times before the beginning of a series of injections and at the end of the run. A needle wash of 3 seconds with needle seat black flush was included.

The UHD Accurate-Mass MS general acquisition settings and MS-TOF settings were left as default except for the parameters described in the supplemental material (TOF/Q-TOF Mass Spectrometer section). Reference mass solution was prepared using an API-TOF Reference Mass Solution Kit (Supelco/Agilent Part No. G1969-85001). It consisted of 1.0 ml Ammonium Trifluoroacetate (100 μM); 2.0 ml purine (10 μM); 0.8ml (2.5 μM) Hexakis (1H, 1H, 3H-tetrafluoropropoxy) phosphazine; dissolved in 500 ml of 95% Acetonitrile: 5% water. Reference masses (positive mode) 121.050873 and 922.009798 Da.

The MS TOF settings were: fragmentor at 125V; 65V for skimmer; 750 V for OCT 1RF Vpp. The mass range that was employed for detection went from 80 to 1100 m/z (4GHz). Acquisition rate was set at 1.5 spectra /sec. The rest of parameters can be seen in Appendix A. The results of the analysis were acquisition files in *.d extension.

A run cycle consisted of 4 vials: One vial containing extraction solvent (blank) was injected two times; another 2 vials contained biological composite samples in randomized order: one mock and the other pathogen inoculated; lastly, a vial containing a solution made of 20μl (2.25mg/ml) of genistein (Sigma Aldrich, G6649) (mass 270.05282 Da) in 880 μl of extraction solution (80:20 methanol/water) used as check standard. Unique file names were individually assigned and were sequential for the particular day/run. Three injections for each sample (technical reps) were analyzed. The total time of analysis per run was approximately 5:40 hours. Sample vials were held at 4 °C for the duration of the analysis cycle.

Data Pre-processing

The general sequence of the data processing and metabolite discovery involve a series of processes that are described throughout this section, the statistical analyses section and the compound annotation section. A flow diagram of this can be seen in Figure 11.

Raw *.d files from the Mass Hunter acquisition software were processed using Mass Hunter Workstation Qualitative analysis ver. B.5.00 Build 5.0.519.0 (MH Qual software) (Agilent Technologies, Inc.) Within this software, the Molecular Feature Extraction (MFE) algorithm provided a *naïve* finder that is effective as a first way to scrutinize UHPLC QTOF/MS raw data. The algorithm was set accordingly for small molecules discovery. The adjusted parameters can be found in Appendix A (Find by Molecular Feature section). Pre-processing was assisted by the DA reprocessor software ver. B.05.00 (Agilent Technologies, Inc.) which converted *d files to *cef files.

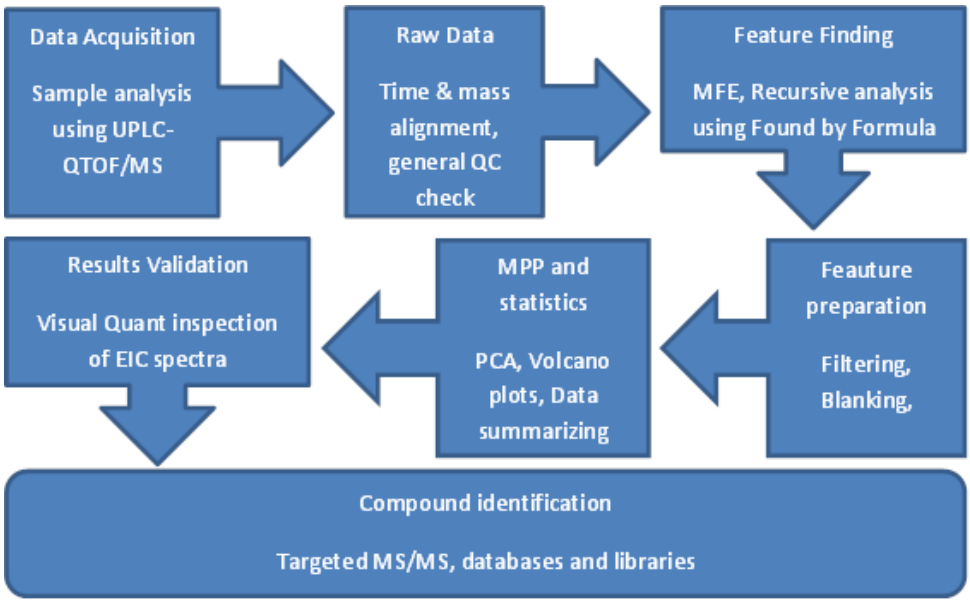

Figure 11. General sequence of metabolite discovery.

Mass and time alignment

The retention time (RT) window was estimated on the MH Qual software, by overlaying the raw peaks or the total ion current (TIC) scan within each day/block, and clicking the apex of the left-most peak of a zoomed –in plot. This time was recorded and subtracted to the right-most peak of another TIC. Comparative sample plots were assembled at this stage The output ".cef" files were aligned for time and mass using Mass Profile Professional ver. 12.1 Build 170166 (Agilent Technologies, Inc) or MPP. The compound alignment option was modified as to set a retention time window of 0.15 minutes. A filter by flags option was selected at 10% to discard some of the artifacts generated by the last processes. Flags are attributes that denote feature quality. Selected options can be: "present" (mass was detected), "absent" (no mass detected) and "marginal" (signal saturated). The filter finds masses based on the quality of these flags in the sample files. A recommended setting involves detecting the present and marginal features found in at least 2 out of 20 or less sample files. The features that pass the filter will be collected in a new list for further processes. The masses that were only found once in the entire data file are likely to be artifacts and will be discarded. Due to the number of files (more than 20) a 10% of the total sample files seemed to work well according to the manufacturer (41). The resulting aligned data was exported for recursion analysis using a single *.cef file.

Recursion analysis

This step was performed in the MH Qual program after completing the MFE run, mass and time alignment. Utilizing this approach reduces in great amount the false positive entities generated by the MFE. The algorithm "find by formula" included: options, chromatograms and mass spectra. The unique *.cef file generated by the alignment process was used as template to start the recursion analysis. The specific settings can be found in Appendix A (Find Compounds

by Formula section). The MH Qual software was again assisted by the DA re-processor program and was used in the same fashion as mentioned before. After the recursion analysis, the new output sample *.cef files were loaded to the MPP software for statistical analyses.

Statistical Analyses

Blank subtraction and filtering

Before data analysis, blanks were subtracted from the samples. This operation was necessary to effectively subtract the features (potential compounds) found in the blanks from the samples. It was performed using MPP software. Data was transform to log2 and a filter by flags at 10% was applied before performing a Venn diagram to separate and save the entities unique to the experimental samples. The list was then filtered again by frequency at 100% to remove any inconsistently detected features that were not extracted or those generated by MFE. This filter limits the analysis to compounds found in a minimum percentage of samples in a particular condition (genotype, collection time, etc.). Since the list being processed is almost the final one, a 100% of the features should appear in at least on condition. The resulting final list was then used for statistical analyses.

Interpretations

In order to do statistical analyses in MPP software, it is required to create "interpretations" using the experiments parameters to answer particular questions. The parameters defining the wheat varieties interpretations were: variety (Glenn, Steele-ND or Reeder), treatment (inoculated or mock), block (1 – 3), sample number (1 – 6). For NIL, additional parameters were: collection time (0, 6, 12, 24, 48 hours) and genotype (susceptible or resistant) instead of variety. Interpretations were made by combining different parameters to

perform blanking or do other preliminary comparisons. Principal component analysis, Volcano plots and other comparisons were made.

Principal component Analysis

PCA plots were constructed after filtering by flags 10% to evaluate the samples as a quality control check. An interpretation with the proper parameters was needed for its construction.

Volcano plots

This statistical test was very useful for visualizing differences between any two conditions. It was perform using the MPP software. This arrangement allows distinguishing masses with a fold-change (magnitude of change) as a biological significance; and also statistical significance (takes both magnitude of change and variability into consideration). A twofold change in magnitude represents a relevant change and is equal to the absolute ratio between the normalized average intensities of condition 1/condition 2. Benjamini-Hochberg FDR multiple testing correction was added for p-value correction. The *p*-value cut off was set to 0.05. The fold change cut-off was set at 2. The abundance difference (raw, abs) cut-off was set to lower the number of false positives originated by the process. A value of 500 was enough to eliminate meaningless fold change differences. In the case of the NIL pair, the interpretation of "Block-Genotype-Treatment-Collection time (non-averaged)" was selected. This allowed having grouping without the level of separation from sample 1 to 6, thus considering a mixed pool at the level of sample for each category. For the wheat varieties, a "Block-wheat type-treatment." interpretation was chosen. The option "exclude missing values from calculation of fold change and p-value" was selected. This was important to avoid greater errors from missing values. The *t*-test selected was non -paired unequal variance since the experimental conditions were not

tested within each individual (unpaired comparisons). It may also correct for differences between variances.

For the NIL, the defined tests of hypotheses were: RM vs SM, RI vs RM, SI vs. SM, RI vs. SI, were: “R” stands for resistant, “S” stands for susceptible, “M” for mock and “I” for inoculated. Table 2 provides the classifications. The features were then classified as either pathogenesis related (PR) or resistance related (RR). A PR compound would be elevated in the comparison of the resistant inoculated to the resistant mock (R I > RM), making it PRr; or in the comparison of the susceptible inoculated versus the susceptible mock (S I > SM) would be classified as PRs in susceptible genotype. Any entity that had higher abundance in the resistant genotype than in a susceptible such as RI > SI or ((RI > RM) > (SI > SM)) was considered a RR induced (RRi). If the result was higher in RM on Mock inoculation as RM > SM, then it was considered as RR constitutive (RRc) (42). Any metabolite detected in the comparison RM < SM or RI < SI were potentially considered a result from manipulation. These comparisons were made for each collection time and for each block. Each passing entity was visually verified for the profile plot and spectrum. The first option used was to visually verify that the “raw intensity” of the candidate entity really was more/less double of that in the comparing group. The second option was used to verify if the composite spectrum of a given entity was really consistent of 3 and a minimum of 2 ion peaks. If one of the two options was not satisfactory, the entity was not taken into account for the sub-list. Multiple entity lists were made by selecting the compounds that were statistically significant (above a horizontal green line) and biologically important (greater than or equal to a twofold change, vertical green lines).

Table 2. Volcano plot comparisons and group classification.

Pathogenesis related (PR)		**Resistant Related (RR)**	
PR resistant (PRr)	PR susceptible (PRs)	RR induced (RRi)	RR constitutive (RRc)
RI>RM	SI>SM	RI>SI; ((RI>RM)>(SI>SM)	RM>SM
Down regulated			
RI<RM	SI<SM	RI<SI	RM<SM

RI=NIL Resistant inoculated; SI=NIL susceptible inoculated; RM=NIL resistant mock; SM=NIL susceptible mock.

Visual inspection of spectra

To reduce the number of false negatives in the entity lists that could have been generated at the level of the volcano plots, it was necessary to visually compare the EIC (extracted ion chromatogram) from each original acquisition file. This was performed by using the *m/z* of each candidate compound in Mass Hunter Qual. The comparisons were made according to the pairs used in the volcano plot testing. A candidate compound had to have a two- fold difference in area for at least 4 out of the 6 biological samples per comparison pair to be used in the analysis.

Compound Annotation

Accurate mass identification

The resulting entity lists were then annotated using the "ID browser software". This software is integrated into the MPP main software. It uses four different reference internet databases [Kyoto Encyclopedia of Genes and Genomes (KEGG); Chemical Abstracts Service (CAS), Human metabolome database (HMDB) and Lipid Maps (LMP)] as well as a unique Agilent /Metlin database. The elements and limits for formula generation were set according to the Identify Compounds section in Appendix A. An alternative way to set the chemical elements and excluding the rest can be found elsewhere (43). The results of the potential identifications

were collected in an Office Excel spreadsheet to serve as starting point and as a reference start point for the Tandem MS confirmation.

Tandem MS

The use of MS/MS was chosen to aid in the identification of the candidate compounds. This technique was employed using the same UHPLC-MS QTOF equipment. After setting the tandem MS/MS, a set of samples from the previous experiments were analyzed to obtain a fragmentation spectrum of each of the candidate compounds. These spectra used as fragmentation ions and abundances, were compared to the ones found in online libraries and literature.

The general settings for the MS/MS section at the acquisition level were mostly the same for the MS1 method previously described. However, the particular Targeted MS/MS settings were as follow: Absolute threshold was set to 5 and relative threshold % was set to 0.01. The acquisition was set to targeted MS/MS option; acquisition rate/time for the MS section was set at 8 spectra/ s; acquisition rate for the MS/MS section was set to 4 spectra/ s. Time between MS1 spectra was set to 5s.

Collision energies (CE) were fixed to 10, 20 and 35 or 40 Volts. The use of one or another energy profile depended on the fragmentation patterns. The targeted compound list was selected according to the mass of the candidate compounds that resulted from the comparisons of the NIL pair and wheat varieties. In all cases the delta retention time was set to 0.2 minutes.

The acquired data files were analyzed in the MH Qual Software using the "find by targeted MS/MS" algorithm. The settings for these parameters can be found at Appendix A (Find By Targeted MS/MS section).

Using online tools for putative identification

The fragments that compose each of the compounds spectra, consisting of *m/z* and abundances, were used as raw data input for online *in silico* identification. The CE spectrum selection (1 out of 4 CE), was the one that had a lower MS/MS precursor ion abundance percentage compared to the original MS precursor ion. Abundance below 20 but more than 5% was preferred, however this was not always possible to obtain. Another criterion was to select the CE that had product ions that could not be encountered in the original acquisition spectrum but repeated the pattern in the rest of the CE spectra. This paired with a good abundance of the product ions determined the best choice to use for a particular compound.

Three *in silico* fragmentation computer assisted identification libraries were used. These were: Metfrag, Metlin MS/MS spectrum match and Mass Bank metabolite prediction. They were selected because they have the option to compare the query to its database resulting in a score and number of matching peaks.

Metfrag: Parent ion was used according to the m/z of result as [M+H]+; precursor tolerance ppm was set at 5; the molecular formula used same as Targeted MS/MS output; biological compounds option was used; number of structures in the output was limited to 100. The rest was left to default. The results were collected as a score, number of matching spectrum peaks, potential structure and name of compound.

Metlin: A maximum of 30 product ion peaks out of the total could be selected. The selection was based on abundance but included the base peak for the compound in question. Positive mode was always selected; collision energy was set accordingly to the spectrum that was selected; tolerance precursor (ppm) was set to 5. Everything else was left as default. The results were collected as a score, number of matching spectrum peaks, potential structure and

name of compound. Massbank: Precursor m/z was set; positive mode selected always, Cut-off set at 0; tolerance at 0.005. The results were collected as a number of matching spectrum peaks, potential structure and name of compound.

Results

Severity Evaluations

Disease spread of FHB in HRS wheat cultivars and NIL pair was considered a crucial step to confirm the validity of the FHB inoculation model, as well as to ensure proper samples for metabolite profiling. Infected and mock spikes were screened daily during the disease development period of 21 days. The *F. graminearum* strain used in this study gave early signs of infection, usually in less than 5 dai, depending on the host type. However the final measurement was taken at 21dai. Signs that the wheat spikes developed FHB were seen as discoloration or browning around the inoculation floret. For a susceptible line or variety, this browning tended to spread towards the upper end of the spike from the point of inoculation. In time, the rachis also showed signs of necrosis. Extreme cases were observed as complete desiccation of the spike (Figure 12). For the more resistant individuals, the signs of infection tended to remain close to the inoculation point. Average plot severity values for wheat cultivars were: Glenn = 27.13%; Steele-ND = 43.29%; Reeder 50.98%. Severity values for Pair 19 NIL were: susceptible (*non-Fhb1*) allele = 64.25%; resistant (*Fhb1*) allele = 4.73%. All control plants (non-treated), as well as the mock treated plants resulted free from disease.

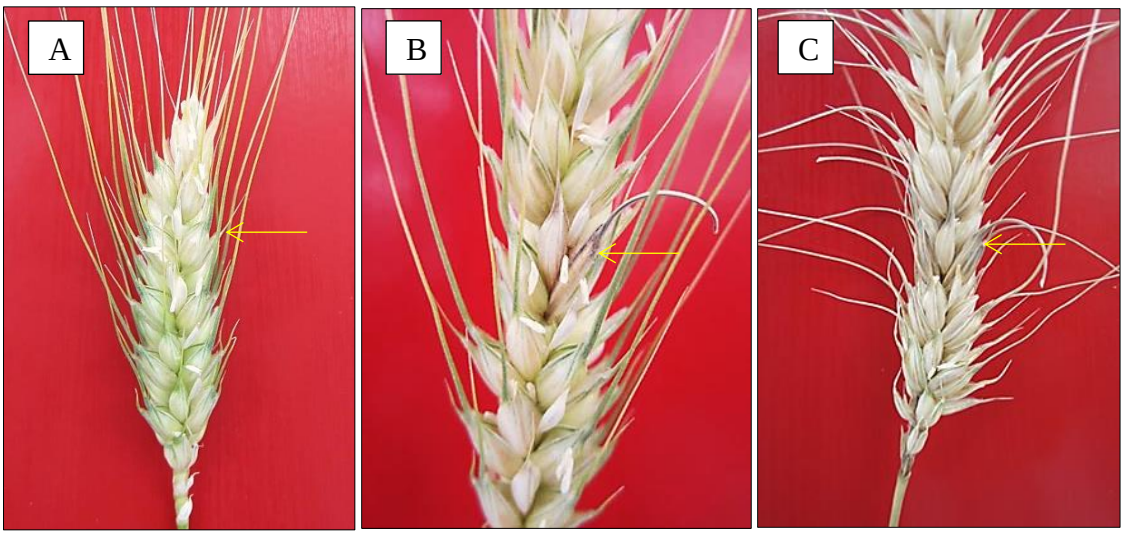

Figure 12. Disease spread after 21dai: A) no spread, mock inoculated. B) Resistant wheat with an infected floret. C) Susceptible wheat spike with the entire spike showing blight. Indication of disease as browning of spiklets and dropping of awns. Yellow arrow shows the inoculation point.

UHPLC-QTOF/MS System Verification

The daily routine inspection of the UHPLC-QTOF/MS system involved several steps: system stabilizing until correct pressure, cleaning the ESI source from organic buildup, flushing the pumps with acetonitrile:acidified water mix of 50:50 and blanking 3 times or until a stable baseline was reached. At that point, calibration with the internal reference mass solution (see sample analysis section) was performed, in which a difference of less than 1 ppm was expected. This assured that the proper conditions to begin an analysis run were met. Genistein, an isoflavone found commonly in soybeans (44) was used as standard to verify the analytical system's performance throughout all experimental runs. Figure 13 shows the raw total ion current (TIC) plots stacked together with an extracted ion chromatogram (EIC) of the standard isolated and labeled. In all 288 injections over the course of the analyses cycles, genistein had an average mass of 270.052876 +/- 1.06x10-4 Da, and an average retention time of 10.90458 +/- 0.0118 min which is well within the experimental error of 0.2 min.

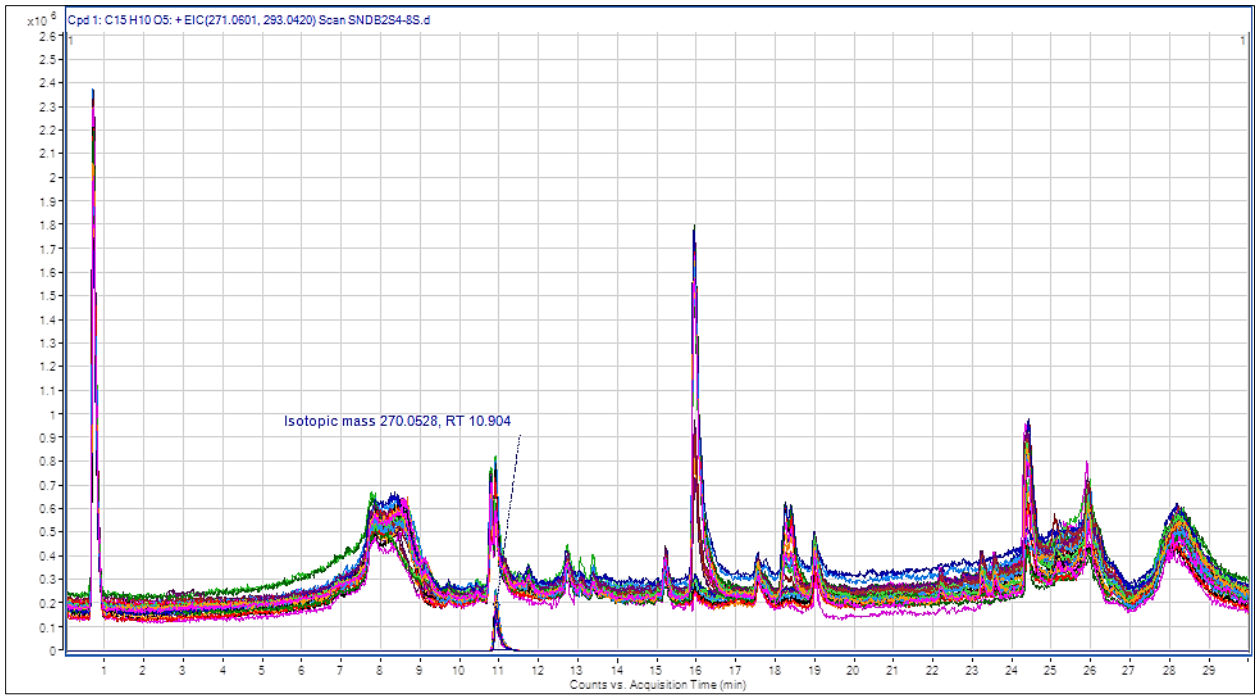

Figure 13. Check standard plot. TIC stacked standard injections used across all experiments. The EIC peaks located below the main stack show the genistein standard (Isotopic mass 270.0528 Da; retention time of 10.904 min.).

Metabolite Discovery Workflow

After processing the samples in the UHPLC-QTOF/MS, the next step was to perform pattern recognition of the molecules detected by using statistical multivariate analyses. The data sets contained features that in turn have a mass, retention time and intensity (22). In summary, the data produced by the acquisition step was processed by the molecular feature extractor (MFE) and find by ion (FBI) algorithms. These two programs function as preparation steps to detect attributes of quality that distinguish features from noise. Once the data was prepared, the next step was to import it into the mass profiler professional (MPP) software. Here the features were aligned by mass and retention time, after which additional filtering was performed to meet quality control. After subtracting the blanks (compounds found in solvent) from the samples, the filtered masses were subjected to significance and fold change analyses. The compounds that passed were examined by comparing their extracted ion chromatograms (EIC) area with a visual

inspection to confirm their intensity change in magnitude (2 fold change). A final list of metabolites was compiled that could then be explored for identification with online databases using exact mass or by performing fragmentation via tandem MS(41).

For the NIL pair, a total of 1260 raw acquisition files were obtained using a non-targeted metabolite profiling approach. The initial alignment for mass and retention time resulted in 747 features. After applying a filter by flags at 10%, which considers attributes of quality signal detected or signal saturated, the yield resulted in 677 features. Following blank subtraction and a filter by frequency at 100% (removes false positive compounds) resulted in a total of 534 metabolites to be used in statistical analyses as seen in Figure 14.

A major part of the analyses involved employing volcano plots that compared plants with different alleles (NIL-R and NIL-S) collection times (0, 6, 12, 24, 48 hai) and treatment (inoculated or mock) for statistic and magnitude significant molecule discovery. An example of the volcano plots as early (0 hai) or late (48 hai) can be seen in Figure 15.

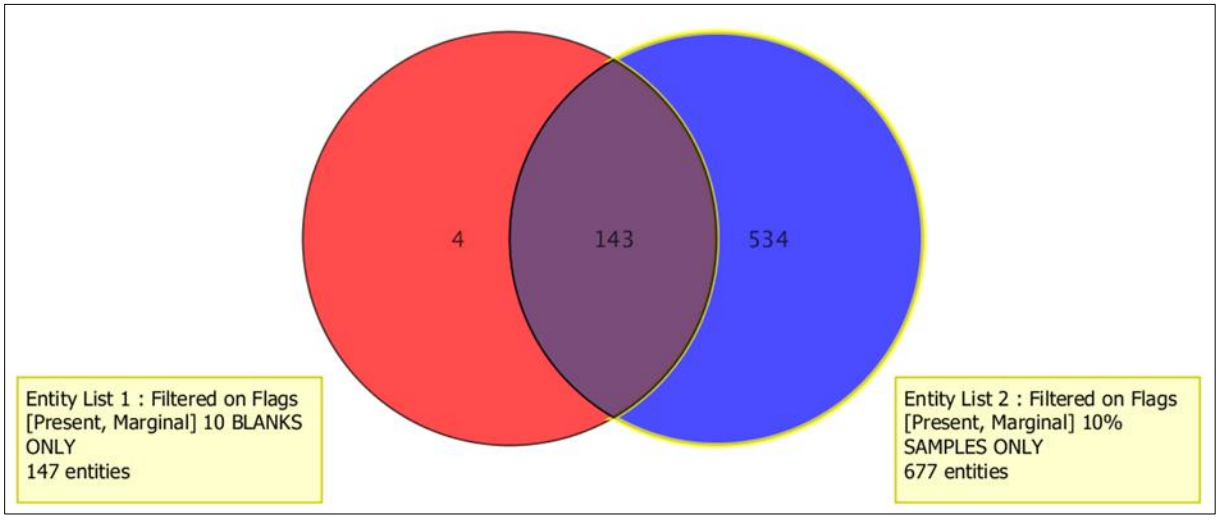

Figure 14. Blank subtraction using a Venn diagram. Features that are in the blue semi-circle highlighted in yellow only appear within NIL samples. The red semi-circle and shared purple area correspond to the blank (extraction solvent) features.

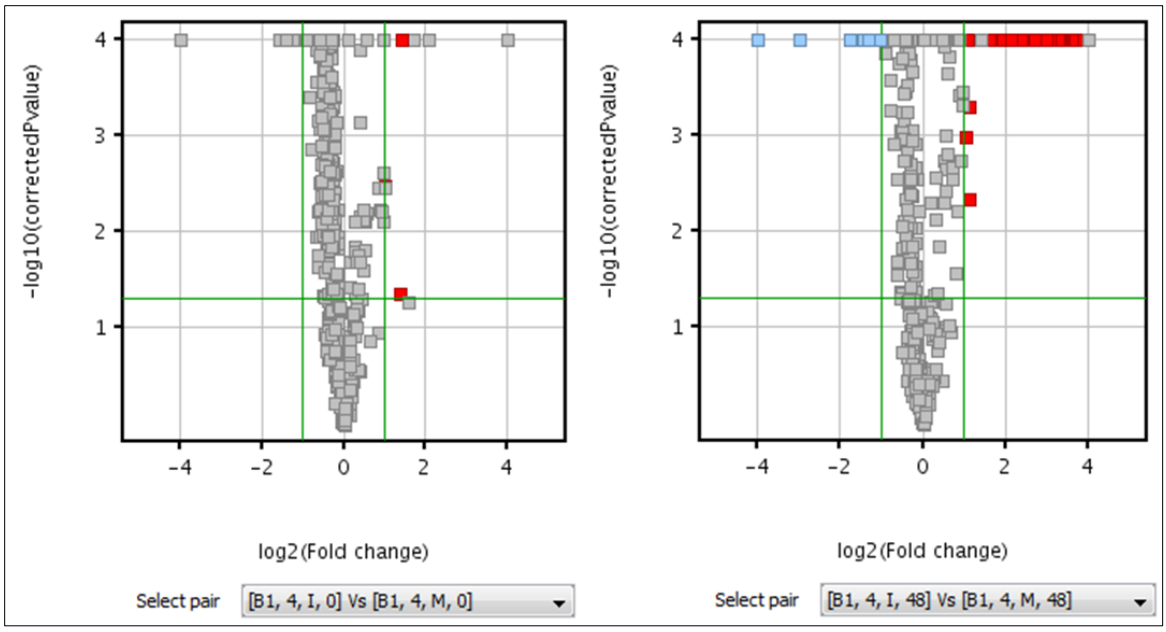

Figure 15. Volcano plots of two comparisons in NIL. The left plot is an early inoculated RI (B1, 4, I, 0) vs RM (B1, 4, M, 0) at 0 hai. Right plot shows a RI (B1, 4, I, 48) vs RM (B1, 4, M, 48) at 48 hai. The red dots represent features that are higher on the RI than RM (up-regulated). The blue dots represent features higher in RM than RI (down-regulated. The *p*-value <0.5; Fold change was 2.0.

The metabolites that passed the statistical significance and fold change criteria were further inspected visually in each biological sample by comparing their individual EIC (extracted ion chromatogram) plots to disqualify any false positive entity. An example of this can be seen in Figure 16. The metabolites were arranged in an Excel worksheet specifying the occurrence time of each.

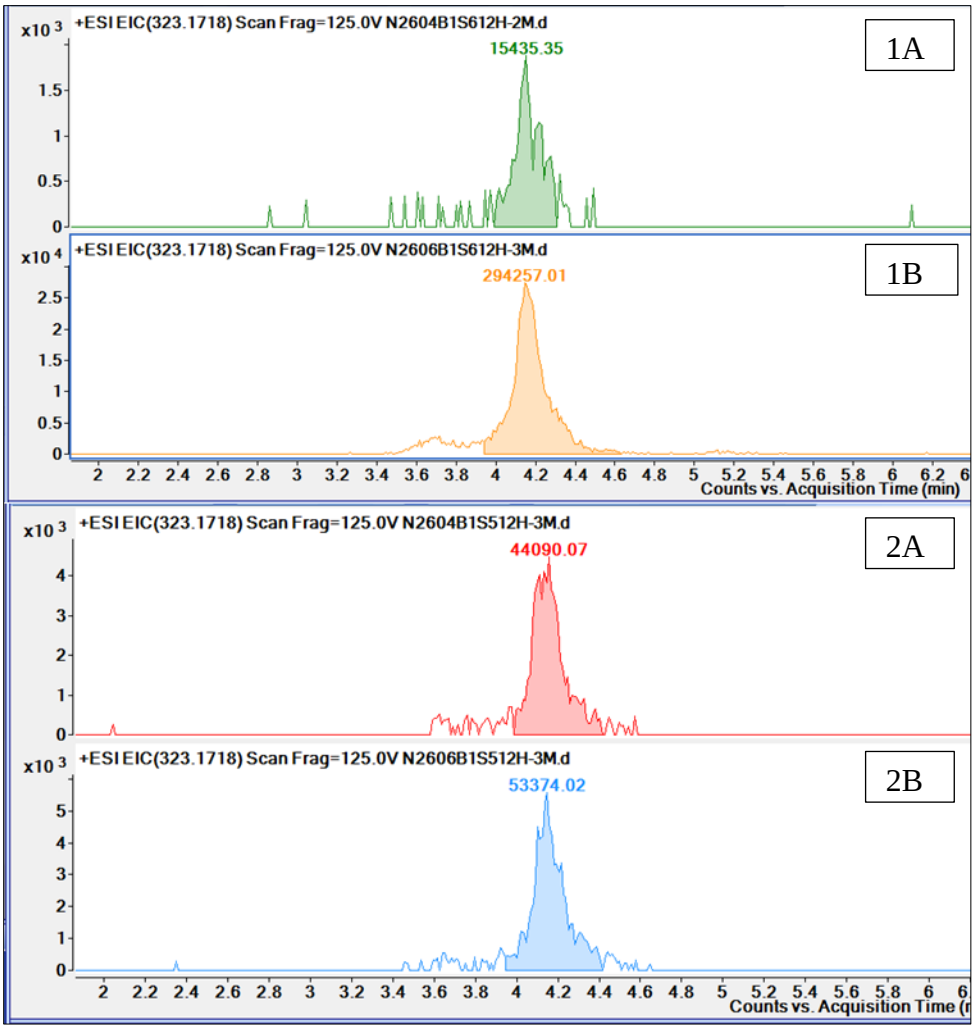

Figure 16. Quantitative visual inspection of EIC plots in samples 5 and 6. Comparison RM < SM found mass 323.1718 Da being higher in the susceptible line for samples corresponding to12 hai. For sample 5, when the EIC counts are compared in plots 1A (resistant) vs 1B (susceptible), the *t*-test finding was confirmed since the count in 1B is more than 2 times higher than 1A. For plots 2A and 2B, this is not true. For any compound, a minimum confirmation of 4 out of 6 samples was necessary. For this mass, a total of 5 out of 6 samples backed up the statistical decision to consider this compound as real.

The number of metabolites that passed the last criteria were 61 distinct compounds, with many being shared between comparisons as shown in Figure 17.

In the case of the three wheat varieties, the initial acquisition resulted in a total of 376 raw acquisition data files using a non-targeted metabolite profiling approach. The initial alignment in mass and retention time resulted in 896 features. After applying a filter on flag at

10% (detects attributes of quality signal detected or signal saturated) the resulting yield was 787 features. The following blank subtraction and a filter by frequency at 100% (to remove any false positive compound) gave a final yield of 634 metabolites to be used in statistical analyses (Figure 18). Volcano plots were employed to compare varieties as inoculated vs. mock after a 24 hour incubation period following inoculation. The metabolites that passed the statistical significance and fold change criteria were further inspected in the same manner as with the NIL metabolites. These metabolites can be seen in Figure 17.

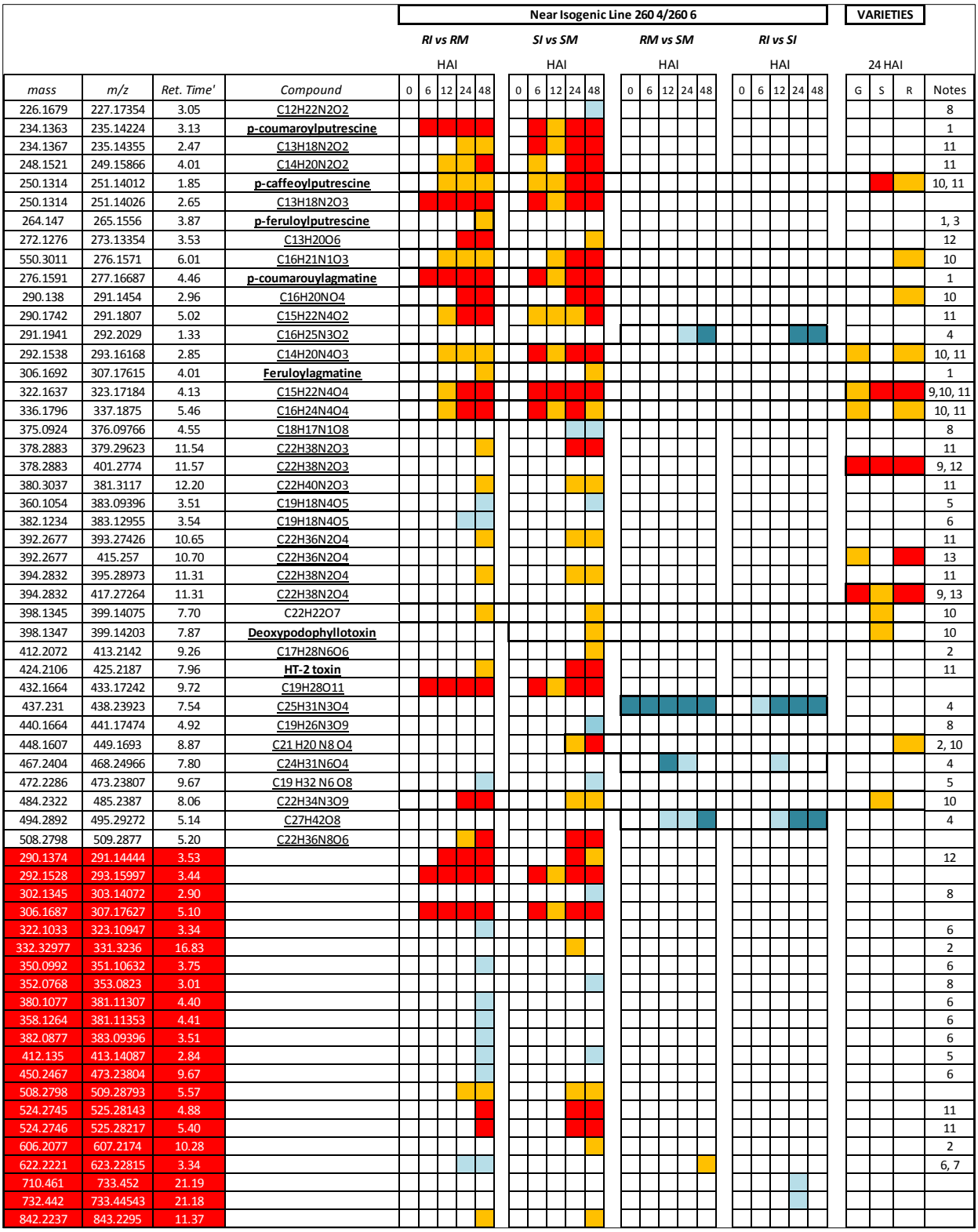

Figure 17. Selected metabolites found in wheat NIL and Wheat varieties with contrasting levels of resistance to FHB. Metabolite selection involved separating compounds by volcano plot with a p-value <0.05 and a Fold change ≥ 2.

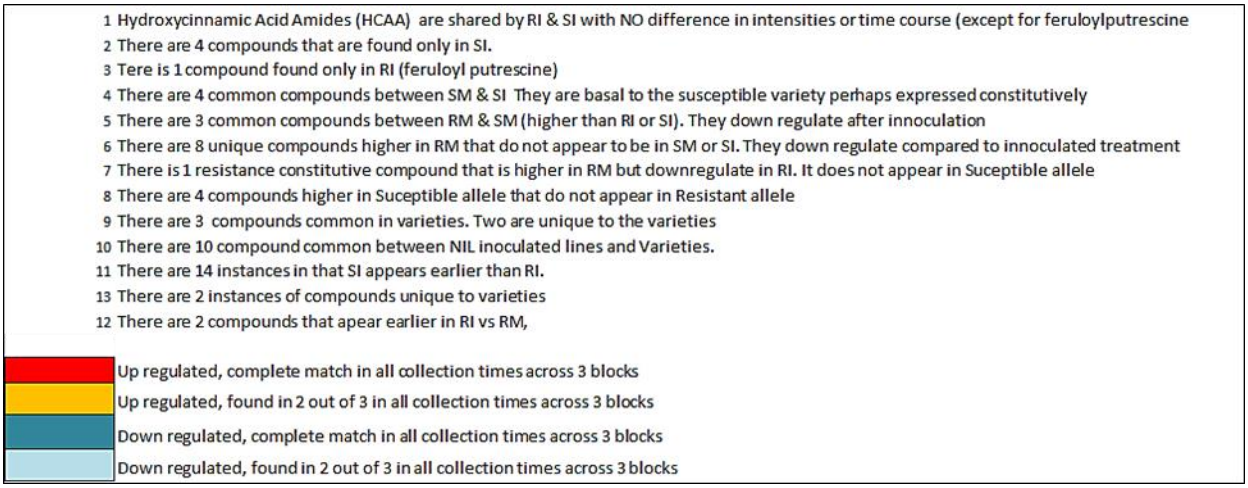

Figure 17. Selected metabolites found in wheat NIL and Wheat varieties with contrasting levels of resistance to FHB. Metabolite selection involved separating compounds by volcano plot with a *p*-value <0.05 and a Fold change ≥ 2 (continued).

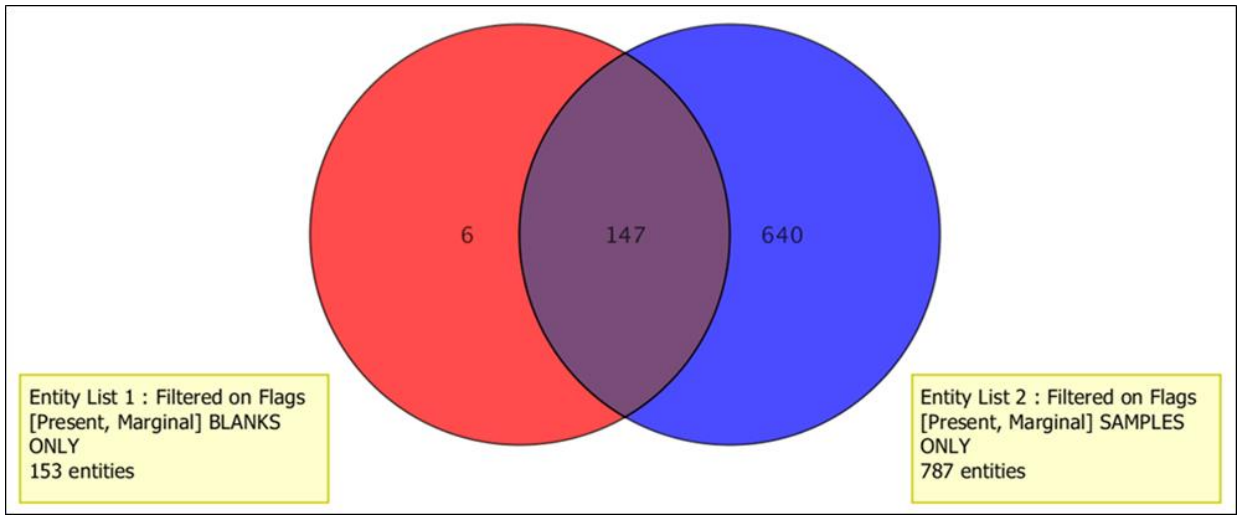

Figure 18. Venn diagram of blank subtraction of wheat varieties. Features that are in the blue semi-circle only appear within wheat varieties samples. A subset of these entities was made for further statistical analyses.

NIL with contrasting alleles and time course comparison metabolite profile

Although the MS/TOF dynamic range selected was 80 -1200 Da at 4GHz, after pre-processing and applying *t*-tests, the final metabolite mass range was between 227– 842 Da. The tentative identification of compounds was performed with the aid of the internal ID browser software (Agilent Technologies, Inc), internet databases and fragmentation pattern libraries.

Pathogenesis related compounds were mostly shared by the two main comparisons: RI vs RM and SI vs SM, with a few exceptions. Compounds with a mass difference less than 5 ppm to that of the reference and fragmentation patterns most closely matching those in the database were: *p*-coumaroylputrescine, caffeoylputrescine, feruloylputrescine, *p*-coumarouylagmatine, feruloylagmatine, deoxypodophyllotoxin and HT-2 toxin. Fragmentation patterns of each of the putatively identified compounds can be seen in Figures 19 to 25. The fragment 147.0437-147.0441Da corresponded to the deprotonized *p*-coumaric acid structure, the basic phenylpropanoid skeleton to which a polyamine (putrescine or agmatine) is later attached. This was common across the phenylpropanoid derived metabolites detected by tandem MS, and is seen commonly starting at 10 V CE onwards, except for feruloylputrescine (Figure 21), in which the deprotonized ferulic acid fragment is the most prominent signal at 177.0547 Da.

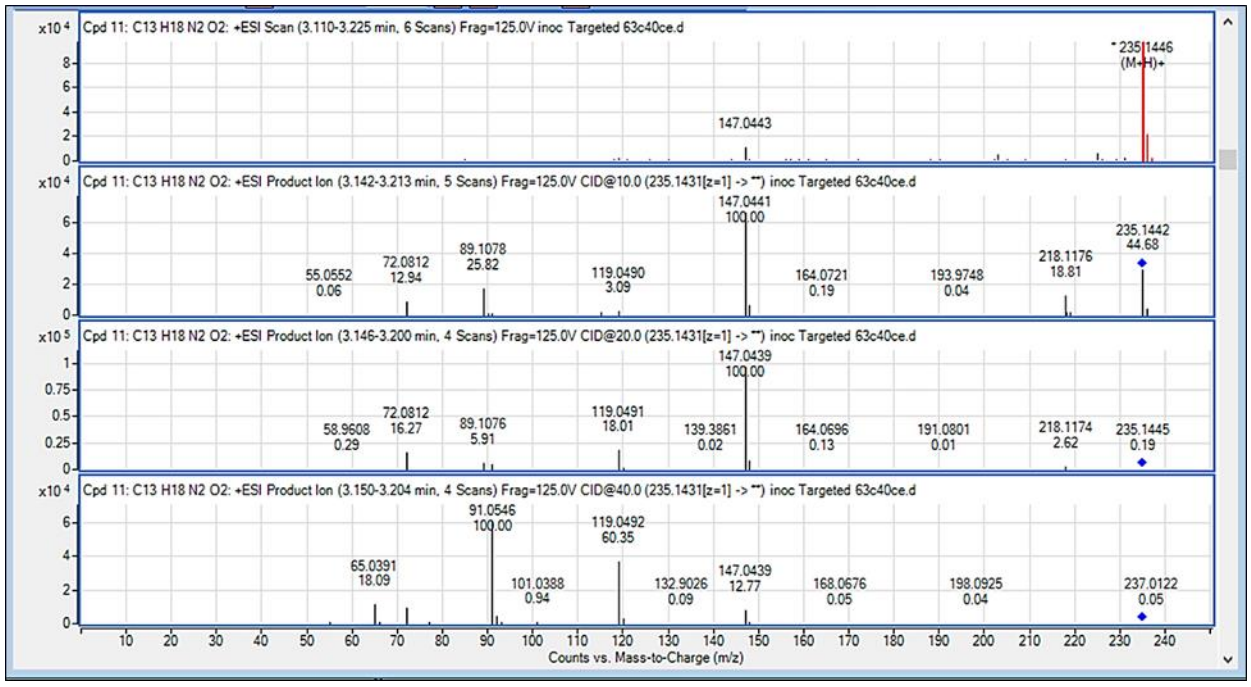

Figure 19. Fragmentation MS/MS scan of mass 234.1363 Da putatively identified as *p*-coumaroylputrescine. The first plot represents the parent MS1 scan followed by 10, 20 and 40 Volts as collision energies.

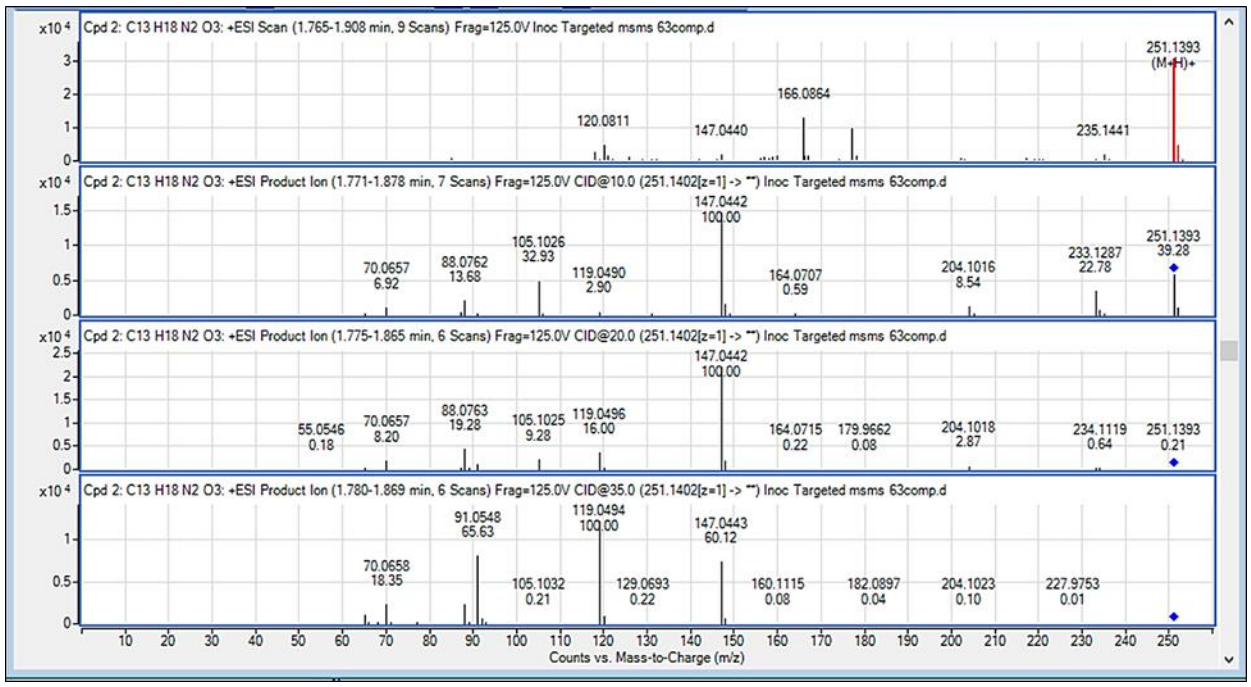

Figure 20. Fragmentation MS/MS scan of mass 250.1314 Da putatively identified as p-caffeoylputrescine. The first plot represents the parent MS1 scan followed by 10, 20 and 35 Volts as collision energies.

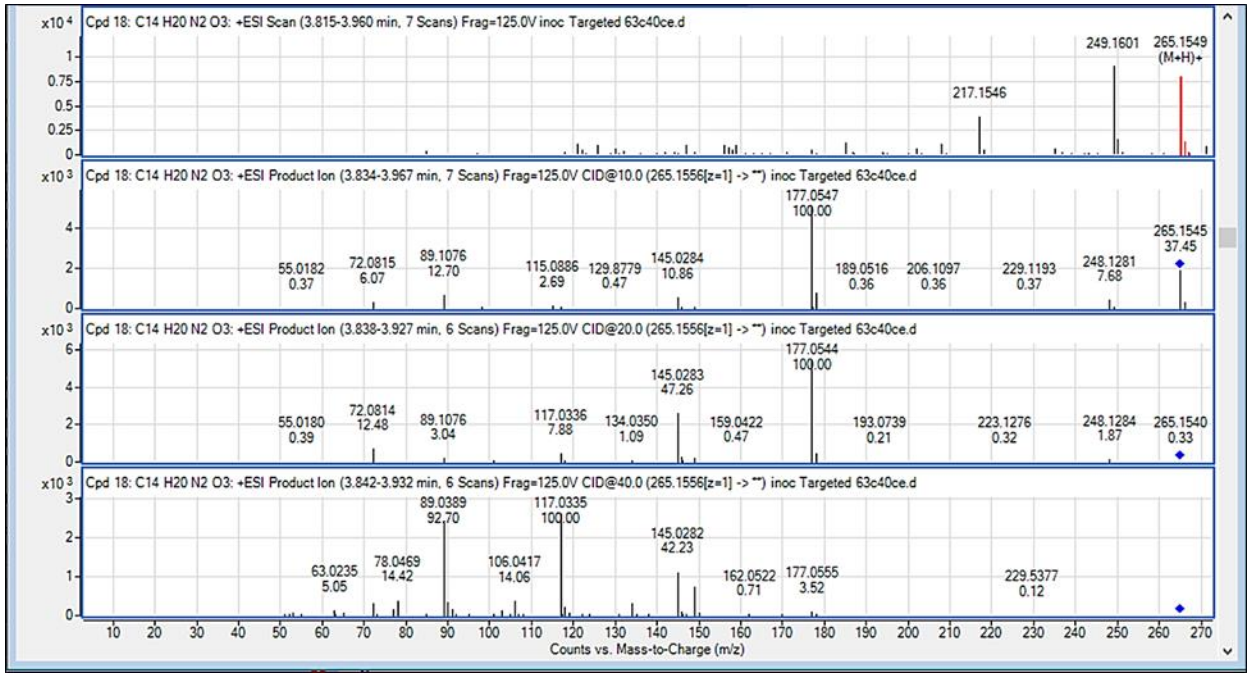

Figure 21. Fragmentation MS/MS scan of mass 264.1470 Da putatively identified as p feruloylputrescine. The first plot represents the parent MS1 scan followed by 10, 20 and 40 Volts as collision energies.

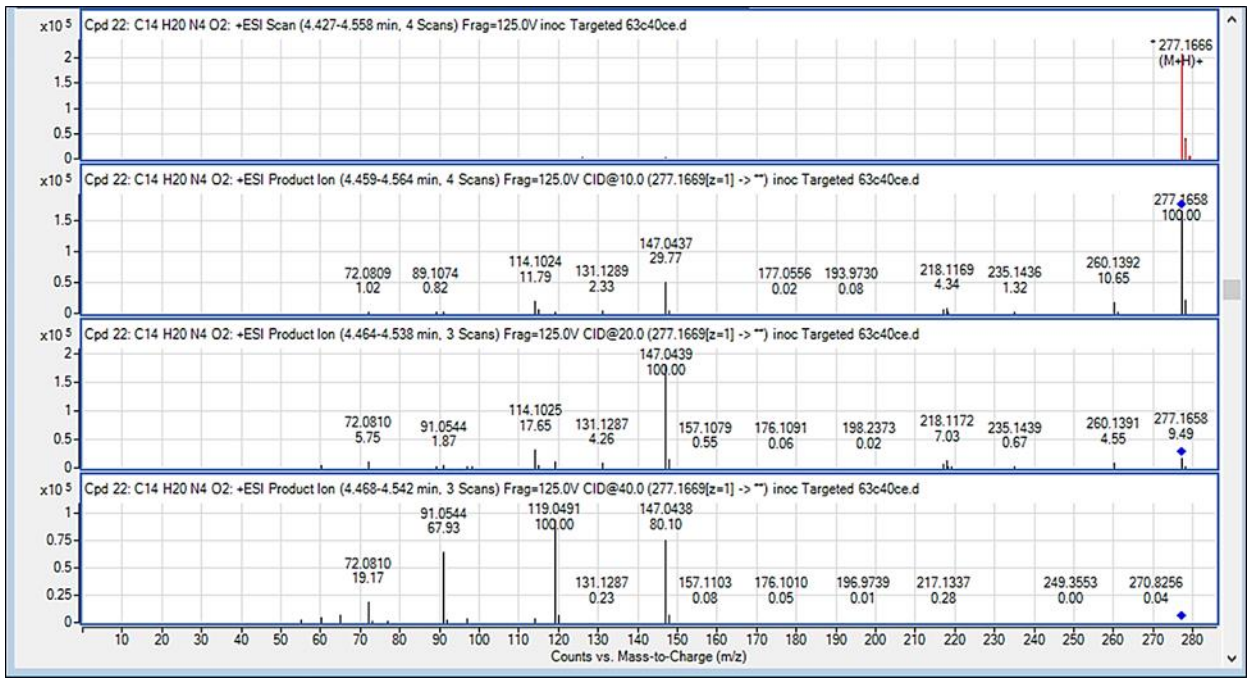

Figure 22. Fragmentation MS/MS scan of mass 276.1591 Da putatively identified as p-coumarouylagmatine. The first plot represents the parent MS1 scan followed by 10, 20 and 40 Volts as collision energies.

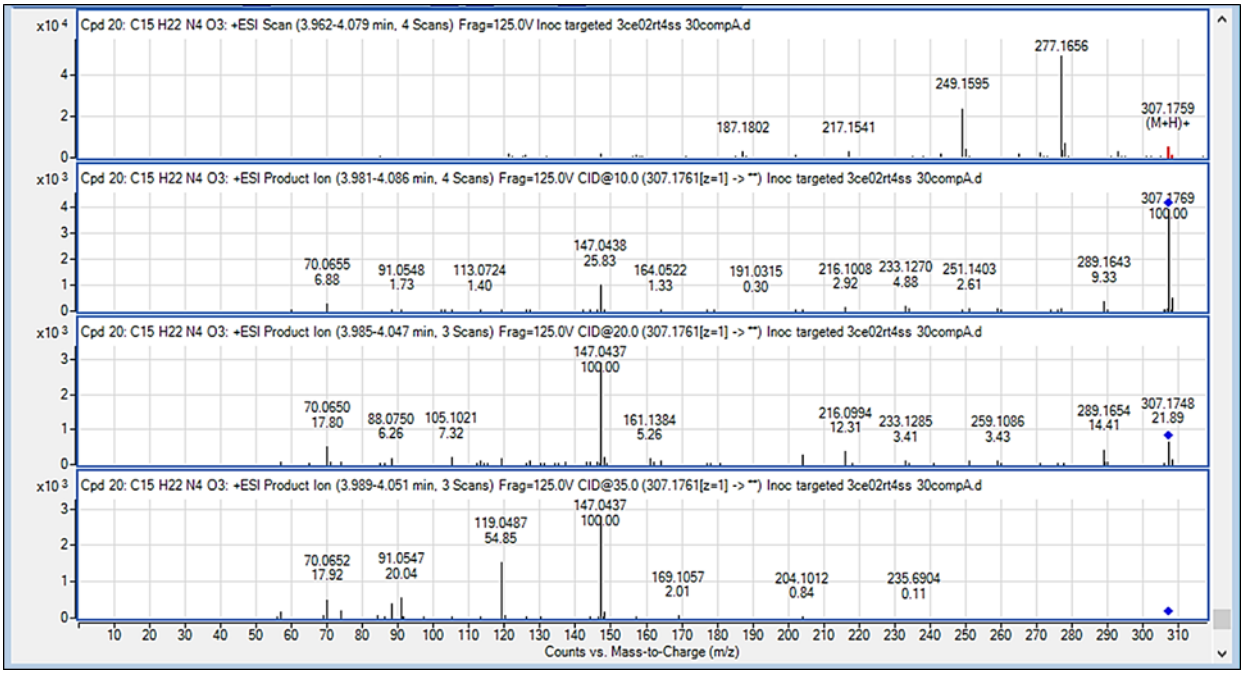

Figure 23. Fragmentation MS/MS scan of mass 306.1692 Da putatively identified as p-feruloylagmatine. The first plot represents the parent MS1 scan followed by 10, 20 and 35 Volts as collision energies.

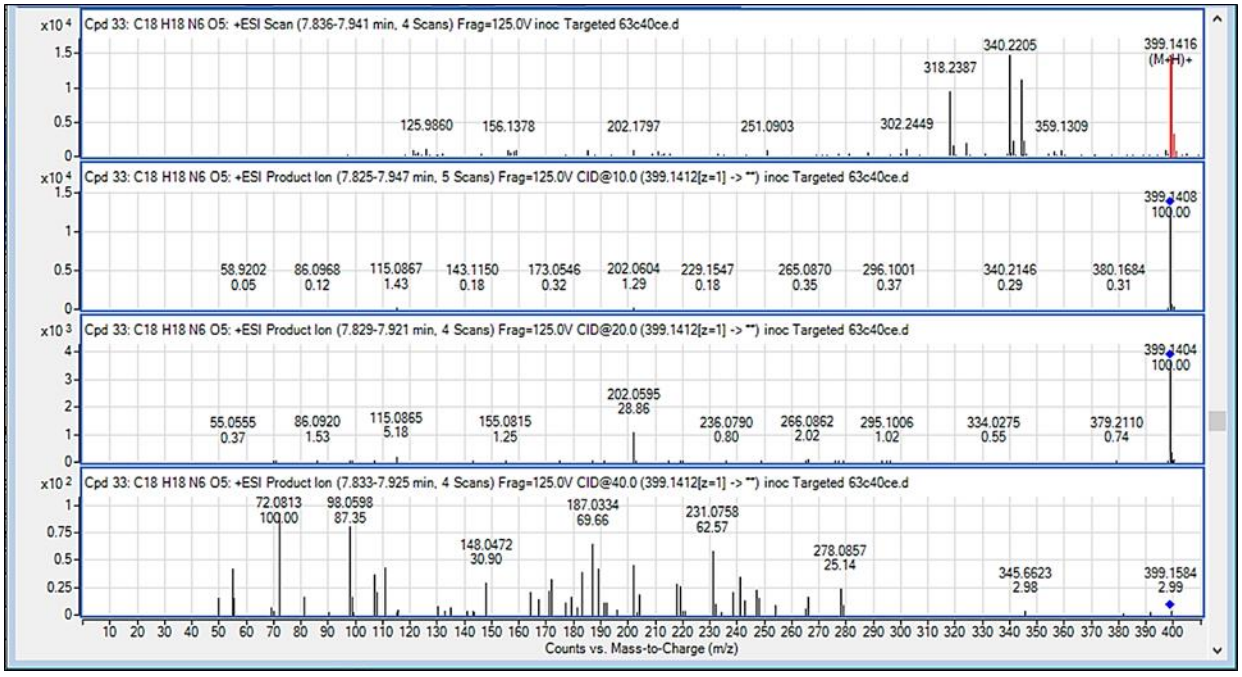

Figure 24. Fragmentation MS/MS scan of mass 398.1397 Da putatively identified as Deoxypodophyllotoxin. The first plot represents the parent MS1 scan followed by 10, 20 and 35 Volts as collision energies.

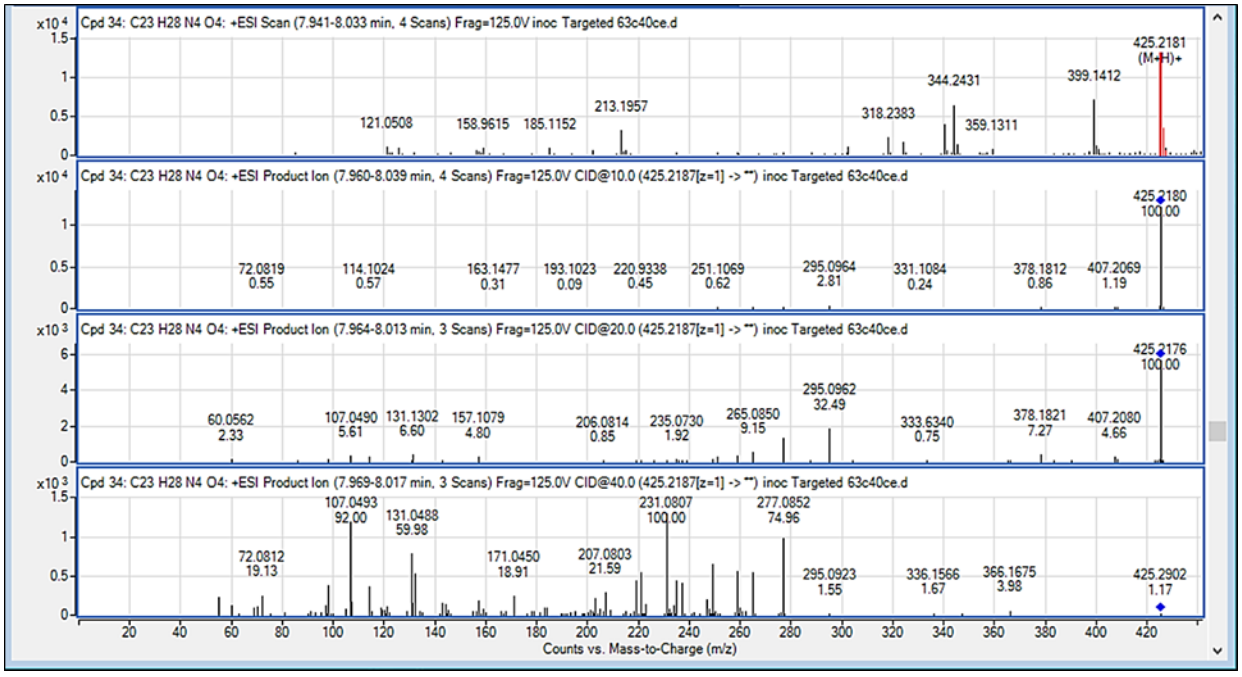

Figure 25. Fragmentation MS/MS scan of mass 424.2106 Da putatively identified as HT-2 toxin. The first plot represents the parent MS1 scan followed by 10, 20 and 35 Volts as collision energies.

Pathogenesis related resistant (PRr) metabolites were higher in the resistant inoculated when compared with the resistant mock (RI >RM), with a total of 31 compounds. The metabolite feruloylputrescine was unique to RI and was considered RRi. Pathogenesis related susceptible (PRs) metabolites were estimated as the compounds that were greater in the susceptible inoculated samples than in mock samples (SI>SM), resulted in 35 compounds. Within this comparison, there is one compound that can only be found in the susceptible inoculated group (322.32977 Da).

Resistant related constitutive (RRc) refers to the compounds higher in the resistant mock samples when compared to the susceptible mock (RM>SM). Only one compound was found with an isotopic mass of 622.2221Da. It was also found higher in resistant mock when compared to resistant inoculated (RI<RM). There are 14 instances in that compounds occur earlier in PRs than PRr, but only 2 compounds in that the inverse situation occurs. This suggests potential susceptibility factors. The overall abundance of the PR metabolites comprised the majority of the unique metabolites found or 57.37%.

The rest of the comparisons found down –regulated metabolites: comparison of two treatments within the same allele in RI<RM=11 and SI<SM=8. Within these two comparisons, 3 compounds are shared and were unique to them (Figure 17, note 5). There are 8 unique compounds higher in RM that do not appear to be in SM or SI (Figure 17, note 6). There are 5 compounds higher in the susceptible allele that do not appear in resistant allele (Figure 17, note 8).

Four compounds were different in the comparison between mock treated alleles (RM<SM), while the comparison between inoculated contrasting alleles, RI<SI, resulted in six compounds. Four of the down-regulated compounds were shared between these two

comparisons. They seemed to be basal to the susceptible variety (Figure 17, note 4). The fact that the only compound (437.231 Da) in all metabolites detected appeared at 0 hours, is a good reason to consider compounds down regulated in this category in potentially being part of the plant reaction to manipulation, since they appear higher in the NIL-S line regardless of the type of treatment. A number of 21 masses from the total 61 compound set could not be matched for an empirical formula nor spectra library in online databases, they are depicted red in Figure 17.

Wheat varieties comparison metabolite profile

The three hard red spring wheat varieties were selected based on their degree of resistance to FHB. A three dimensional PCA was used to compare their overall clustering prior to further statistical analysis (Figure 26). Wheat varieties results can be seen to the right of Figure 17. There are 3 compounds common to all the wheat varieties; from those compounds, 2 are not found in the NIL, but are unique to the wheat varieties. There are 10 compounds shared between NIL inoculated lines and wheat inoculated varieties: two were upregulated in Reeder in the RI and SI samples; one in Reeder in the SI sample; two were up regulated in Steele-ND in the RI and SI samples; one in Steele-ND shared with SI; two in Glenn and Reeder in the RI and SI samples; one was unique to Glenn and Reeder; one was unique to Steele-ND and Reeder in RI and SI respectively; and one was found in Glenn, Steele-ND and Reeder in the RI and SI samples (Figure 17 notes 9 and 10).

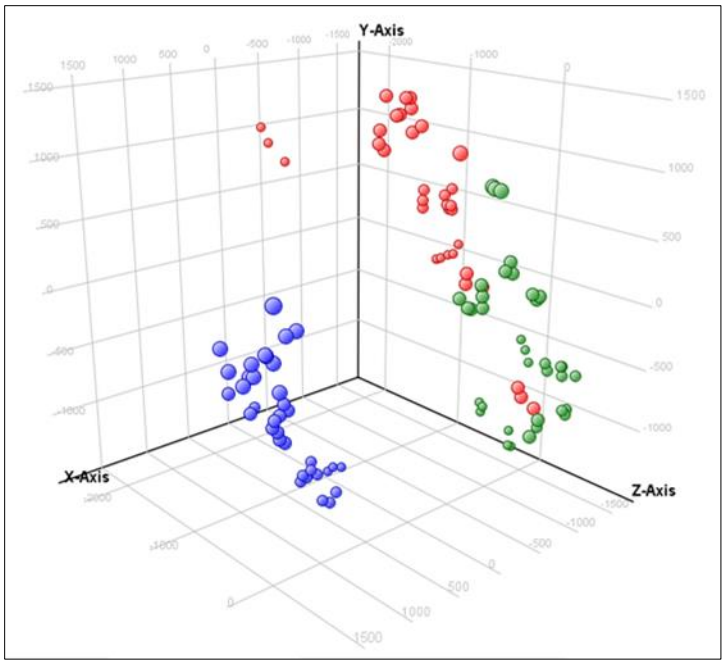

Figure 26. Unsupervised 3D PCA plot of HRSW varieties: Glenn (red) and Steele-ND (green) share a similar space in the plot, while Reeder (blue) can be seen apart from both. Averaged interpretation combining three blocks.

Discussion

UHPLC QTOF/MS System Verification

The accuracy and reproducibility of the data acquired by the UHPLC QTOF/MS system was assured by daily flushing the UHPLC pumps, cleaning the ionization source and calibrating the MS with an internal reference mass solution. Recalibration was performed only if the mass difference was higher than 1.0 ppm, however, it was usual to obtain a value of 0.2 ppm. The use of an internal or external standards to monitor performance has been recommended to visualize potential events such as drift, which can be detrimental for the quality of the results in a long term study (45) One way is to use a mixture of samples and run it as a QC analyte. This approach has been used in the medical field of metabolomics (46). The applicability to include a QC sample however, may depend on its stability; if the nature of the extraction is not stable (as verified in our case) then, this would be unreliable for long analytical cycles. Another option is

the use of standards. In our case we decided in using two chemical standards that could cover a good range of mass detection. One of them, adonitol, a pentose alcohol (153.0684 Da) was difficult to recuperate when spiked in the samples. We were also concern in a potential matrix effects that could eclipse the detection of meaningful metabolites. Genistein, an isoflavone found in soybeans (44,47), was analyzed along the other samples to verify the complete system accuracy for retention time and mass. It dissolved well in a mixture of methanol: water 80%, while being stable at 4 °C. Its mass and retention time were in range for being used in this study. Overlaying the TICs intensity/time plots has been proven to be a good method to verify the consistency of detections (48,49). In addition, the comparison of the entire 288 check standard injections throughout all experiments resulted in a maximum time drift of +/- 0.0118 min and a mass difference of 0.1962 ppm , thus being less than the stipulated time window of 0.2 min (41) and mass difference of less than 5 ppm (25).Additionally, the shape of the extracted ion chromatogram for this particular compound was consistent (Figure 13). Therefore, in addition to the system's own internal mass standards, the stability of the instrument over the total time used was sufficient.

FHB Severity in NIL and Wheat Varieties

Anatomical features associated with type II resistance include smaller diameter vessel elements, denser vascular bundles in the rachis and shorter internodes in the upper part of rachis joints with stronger thick cortical sclerenchyma and cell walls (50). Also, cells and structures around the lesion can become thicker and denser 10.5 days after inoculation (51). Thus a clear involvement of post-inoculation defense response in the resistant wheat has to take place in preventing fungal spread in our experiments, since the susceptible *Fusarium*-inoculated line/variety showed increasing levels of necrosis across the 21dai.

Severity in wheat varieties

The wheat varieties were selected for their variable levels of FHB type II resistance. The visual assessment results revealed that the FHB severity in the wheat varieties selected for this study are in agreement with those previously reported, in which Glenn is the most resistant and Reeder the least (33). When our visual severity percentage results are compared with those of the greenhouse variety registration severity results, it is possible to see the following: Glenn gave a 27.13% severity compared to the16% severity seen in the variety registration; Reeder resulted in a 50.98% severity compared to a 42% severity seen in the variety registration. In both varieties, there is a similar tendency, however, our Steele-ND results indicate a severity of 43.29% which differs from the literature reference of 25% (34). Another experiment that used the original *Fusarium* strain Fg08-001 and Steele-ND variety, reports a 42.4%, which agrees with our result (39). The potential reasons are the use of a different pathogen isolate, the inoculation technique (spraying vs. point inoculation) or an effect of both. As an alternative explanation may lay on previously reports observing that variation in spread results appears to be very small in highly resistant and highly susceptible cultivars, with the most variation seen in intermediate levels of resistance, as is the case of Steele-ND (52,53).

PCA, an unsupervised multivariate statistical method, provide a simplified representation of the data by reducing its dimensionality, it can also include the visualization of clusters with separation in classes and outliers (22,25). The grouping of features in a PCA does not mean statistical significance, but it is a clear way to visualize the tendencies in a data set. By taking the three wheat varieties pool of metabolites and applying the proper interpretation (data inquiry) that only verified what corresponded to each cultivar, a PCA plot was created. By doing this, the similarities or differences of each cluster (cultivar in this case) were observed according to

covariance. The fact that Steele-ND forms part of the pedigree of Glenn (34) is taken as a basis to explain the clustering of both in the PCA plot, confirming this relationship (Figure 26). Reeder appeared as an overall distinct cluster.

Severity in NIL pair

Near isogenic lines were especially effective for the objectives of this study. Due to their breeding that fixes their genetic background, the effects on a pair can be then attributed to a specific QTL or the absence of it (32). For this study, the NIL pair was selected depending on ease of growth, maturation, availability and most importantly, upon the known contribution of their *Fhb1* QTL effect. Four isolines pairs with above 48% QTL effect were tried, being pair 19 (32) the one with best growth qualities: large spike, stout stalk while reaching anthesis in 5 weeks after planting. This last attribute was important for the logistics of the greenhouse operation. For the NIL pair selected, our study confirmed that the FHB severity was clearly distinct between the resistant (*Fhb1*, NIL-R) and the susceptible (non-*Fhb1*, NIL-S), in such a way that the QTL effect was higher than reported previously for the wheat NIL pair 19 at 94% (32). Again, the difference in inoculum strain is suspected. Nonetheless, the fact that the effect of FHB severity in each of the two alleles was clearly distinguishable should further validate the use of this NIL pair. Overall, the selected wheat cultivars with varying levels of resistance and NIL, proved to be a good model for the detection of metabolites involved in FHB response.

Metabolite Detection

Because metabolomics analyses can result in large data collections (54), it is necessary to pre-process the data before differential analysis. The removal of noise signals using filtering, peak alignment, normalization and blanking helped to reduce non-reproducible signals. The remaining features can then be compared with statistical methods between experimental

treatments (55). In contrast with previous FHB infected wheat metabolite profile studies (21,23,56), in which the number of compounds detected were between 117 - 214, a comparatively larger number of compounds were found after pre-processing; 534 for the NIL and 634 for the wheat varieties. One major difference is that in the previous studies GC-MS was used, whereas in this study a UHPLC-QTOF/MS was used. LC-MS has a high capacity for separating and detecting a wide variety of molecules with higher sensitivity (25), does not alter the sample by derivatization and does not degrades heat sensitive compounds as GC (57). In addition, the UHPLC unit used in this study incorporated an electro spray ionization (ESI) source which was able to perform in polarity switch mode, enabling it to increase the number of detected compounds at a cost of cycles time (57). Positive mode can effectively ionize a wide range of medium polar and polar molecules, like polyamines, alkaloids and anthocyanins (58). Organic acids, carbohydrates, semi-polar metabolites like glucosinolates, polyphenols and other glycosylated compounds are best detected in negative mode (25,58). In our initial trials using negative ionization mode, the detection level was only of a few features per sample, meaning that the molecules extracted with the methanol: water at 80% were better suited to be ionized in positive mode. Single ionization profiles can be performed depending on the compound classes in interest (59), thus for this study only medium polarity metabolites were targeted. In addition to the low discovery rate of metabolites in negative mode, switching polarity seemed difficult to incorporate due to higher analytical times with lower instrument sensitivity. Another factor was that floret extracts had a low stability. Positive ionization mode was therefore the only ionization mode used for this study.

Metabolomics experiments that follow the FHB development on wheat over a time course are few, most using a single collection time being 24 hai (20,21,23), 48 hai (56) or 72 hai

(27,42). This approach takes a "snap-shot" of the events happening for that particular time in the host-pathogen interaction. A time course approach was taken to study the germination of *F. culmorum* macroconidia and its colonization of wheat (60). By using microscopy in samples collected over time, the spores were shown to germinate between 6 and 12 hours with hyphal growth on the inner floret structures like palea and lemma within 48 hai. Genetic expression of FHB infection has also been studied in a time course fashion in wheat and barley (30,61). Their findings on the wheat-*Fusarium* interactions were divided in 3 stages depending on abundance of transcripts: early stage, at 6 hai (4%); intermediate stage from 12-24 hai (13%) and late stage from 48-72 hai (63%)(30). In barley, the majority of the transcripts were detected above the 72 hai (61). Our results agree with theirs, as the metabolites in the NIL pair appear to increase in quantity over the course of the treatments, also no significant metabolites related to resistance were found at 0 hai, Since our time course metabolite profiling did not involve analysis outside of the 48 hai limit, it was not possible to determine later response compounds.

The *Fhb1* QTL has been related to the resistance of FHB spread on wheat, which has been attributed to the activation of the phenylpropanoid, terpenoid, fatty acids metabolism and detoxification of DON to DON-3G (22). More than half of the compounds observed in the current experiments appeared to be commonly shared between the NIL pathogen related resistant (PRr), pathogen related susceptible (PRs) and the wheat varieties. A few of these metabolites were putatively identified as part of hydroxycinnamic acid, conjugated with polyamine derivatives. These compounds have been shown to be participant in resistance due to *Fhb1* QTL, being intermediate compounds that over accumulate and cause thickening of the host cell walls (20,27,56). Their synthesis is activated as a response to stress, including pathogen infection and elicitor treatment (62) and could be one reason that they appear early in our results. It should be

noted that in our experiments, the intensities of the metabolites shared between the pathogenesis related resistant or susceptible categories (PRr or PRs) were found to not have any significant difference when verified in a *t*-test volcano plot ($p < 0.05$; FC=2) at any time point. A prominent exception was the compound *p*-feruloylputrescine, detected late at 48 hai. It was the only resistant related induced (RRi) metabolite seen in the list. This result agrees with previous findings (27). Gunnaiah *et al*., detected feruloylputrescine as the highest fold-change RRi metabolite after 72 hai, only below 8'-Hydroxyabscisate. The rest of the HCAA were also detected and classified as PRr and RRi; whereas in our study the same metabolites were only classified as PRr since they were also found in the susceptible line.

Two other compounds appeared 12 hours earlier in the resistant NIL than in its susceptible counterpart and may be considered RRi compounds: 272.1276 Da/3.53 min and 290.1374 Da/3.52 min. All this suggest that the RRi metabolites are important against FHB spread start to appear after 48 hai. Additional support on this point was provided by the detection of a resistant related constitutive compound (RRc) 622.2221 Da/3.34 min at 48 hai, which increases late regardless of the inoculum (pathogen or water) and only in the resistant NIL allele.

Molecules known to enhance the hyphal growth of *Fusarium*, such as betaine and choline are contained in wheat anthers (63,64). In our results, one compound was found to be shared by the susceptible Reeder variety and the NIL-S upregulated SI > SM comparison, or PRs. This compound 448.1607 Da/ 8.87 min, is unique and does not appear to be in the NIL-R or the other two resistant varieties, and can be potentially considered as an indicator of susceptibility to FHB along with the other unique NIL-S compound 606.2067 Da/ 10.28 min.

It is known that individual mycotoxins appear to influence virulence depending on host (65). A molecule putatively identified as HT-2 toxin appeared earlier in the NIL-S than NIL-R.

The fragmentation patterns of this mass did not match as close as with other molecules mentioned before, but can very well represent a tricothecene. Diacetoxyscirpenol, DON, and HT-2 toxin share early biosynthesis pathways but then branch out from calonectrin to a series of hydroxylations and acetylations in *F. sporotrichioides* (66). The *Fhb1* QTL is associated with the biotransformation of DON to DON-3 glucoside reducing the compound toxicity to the plant (67), and may present an explanation to the late occurrence in the NIL-R compared to the NIL-S. It is know that polyamines such as putrescine and its precursor agmatine can stimulate the production of DON *in vitro* (68). We encountered metabolites that contained polyamines, although not the free forms, the peaks in the tandem MS matched the known monoisotopic mass of putrescine (88.151 Da). A probable factor of not detecting it may be due to being close to the lower limits of detection (80-1200 Da at 4GHz), or that the shunt phenylpropanoid pathway was directing them towards the synthesis of HCCA with conjugated polyamines. It is tempting to visualize that the pool of free polyamines product of plant degradation by *Fusarium* can in turn stimulate DON synthesis *in planta*, with the consequence of causing cell death (69), however, there is no report of this stimulation happening in a natural environment. The presence of DON was not tested in our study, although is something that might be of interest as another way of visualizing resistance.

The majority of the compounds detected were not identified. All metabolites detected had an accurate mass, intensity and a retention time. However, only 7 entities (11.47%) met the tentative criteria of accurate mass matching less than 5 ppm, empirical formula and fragmentation patterns found with online libraries. Thirty three compounds (54.1%) had fragmentation data and empirical formula, with no positive match for mass, formula or fragmentation patterns. The 21 compounds left (34.42%) had only mass and retention time. Thus

an 88.52% are without identification. This is a known disadvantage of LC based technology, in that the lack of reproducibility of fragmentation spectra between instruments complicates the creation of mass spectral libraries based on LC-MS data (22). As an option, fragmentation libraries for LC-MS methods are usually made in-house.

The data presented here supports previous findings in which the resistance reaction of the host plant to *Fusarium graminearum* infection is complex and involves a multitude of early and late responses. The compounds tentatively identified as HCAA that appear early in the time course, are a common initial response to the infection in both resistant and susceptible alleles. Finding of unidentified compounds appearing late in the resistant pair time course indicate that the plant might develop its defense further after the initial 48 hai. In particular, the ones labeled as "resistant indicator" and "susceptible indicator" might be helpful in a screening of FHB response. The lack of positive identification made it difficult to explore biosynthetic pathways. In spite of this, it should be possible to use this methodology to perform assays that can explore other experimental options (alternative times, neighboring tissues to inoculation point, DON detection) in order to have a wider scope on the chemical species involved in a time course FHB infection model.

References

1. Beyer, M., Verreet, J.-A., and Ragab, W. S. M. (2005) Effect of relative humidity on germination of ascospores and macroconidia of Gibberella zeae and deoxynivalenol production. *International journal of food microbiology* **98**, 233-240

2. Steffenson, B. J. (2003) Fusarium head blight of barley: impact, epidemics, management, and strategies for identifying and utilizing genetic resistance. in *Fusarium Head Blight of Wheat and Barley* (Leonard K. J., B. W. R. ed.), APS press, St. Paul, MN. pp 241-295

3. Parry, D. W., Jenkinson, P., and McLeod, L. (1995) Fusarium ear blight (scab) in small grain cereals—a review. *Plant Pathology* **44**, 207-238

4. Nganje, W. E., Bangsund, D. A., Leistritz, F. L., Wilson, W. W., and Tiapo, N. M. (2004) Regional Economic Impacts of Fusarium Head Blight in Wheat and Barley. *Applied Economic Perspectives and Policy* **26**, 332-347

5. Gale, L. R. (2003) Population biology of Fusarium species causing head blight of grain crops. in *Fusarium Head Blight of Wheat and Barley* (Bushnell, K. J. L. a. W. R. ed.), American Phytopathological Society, St. Paul, MN. pp

6. Shaner, G. E. (2003) Epidemiology of Fusarium head blight of small grain cereals in North America. in *Fusarium Head Blight of Wheat and Barley* (Bushnell, K. J. L. a. W. R. ed.), American Phytopathological Society, St. Paul,MN. pp 84-119

7. Placinta, C. M., D'Mello, J. P. F., and Macdonald, A. M. C. (1999) A review of worldwide contamination of cereal grains and animal feed with Fusarium mycotoxins. *Animal Feed Science and Technology* **78**, 21-37

8. McMullen, M., Jones, R., and Gallenberg, D. (1997) Scab of Wheat and Barley: A Re-emerging Disease of Devastating Impact. *Plant Disease* **81**, 1340-1348

9. Miedaner, T. (1997) Breeding wheat and rye for resistance to Fusarium diseases. *Plant Breeding* **116**, 201-220

10. Rudd, J. C., Horsley, R. D., McKendry, A. L., and Elias, E. M. (2001) Host Plant Resistance Genes for Fusarium Head Blight. *Crop Sci.* **41**, 620-627

11. Anderson, J. A. (2007) Marker-assisted selection for Fusarium head blight resistance in wheat. *International journal of food microbiology* **119**, 51-53

12. Bushnell, W. R. (2003) Hitstology and physiology of Fusarium head blight. in *Fusarium Head Bligth of Wheat and Barley* (Leonard K. J., B. W. R. ed.), American Phytopathological Society, St. Paul, MN. pp 44-83

13. Bai, G., and Shaner, G. (2004) Management and resistance in wheat and barley to fusarium head blight. *Annu Rev Phytopathol* **42**, 135-161

14. Anderson, J. A., Stack, R. W., Liu, S., Waldron, B. L., Fjeld, A. D., Coyne, C., Moreno-Sevilla, B., Fetch, J. M., Song, Q. J., Cregan, P. B., and Frohberg, R. C. (2001) DNA markers for Fusarium head blight resistance QTLs in two wheat populations. *Theoretical and Applied Genetics* **102**, 1164-1168

15. Yang, Z., Gilbert, J., Fedak, G., and Somers, D. J. (2005) Genetic characterization of QTL associated with resistance to Fusarium head blight in a doubled-haploid spring wheat population. *Genome* **48**, 187-196

16. Collard, B. C. Y., Jahufer, M. Z. Z., Brouwer, J. B., and Pang, E. C. K. (2005) An introduction to markers, quantitative trait loci (QTL) mapping and marker-assisted selection for crop improvement: The basic concepts. *Euphytica* **142**, 169-196

17. Schauer, N., and Fernie, A. R. (2006) Plant metabolomics: towards biological function and mechanism. *Trends in plant science* **11**, 508-516

18. Keurentjes, J. J. B., Fu, J., de Vos, C. H. R., Lommen, A., Hall, R. D., Bino, R. J., van der Plas, L. H. W., Jansen, R. C., Vreugdenhil, D., and Koornneef, M. (2006) The genetics of plant metabolism. *Nat Genet* **38**, 842-849

19. Allwood, J. W., and Goodacre, R. (2010) An introduction to liquid chromatography–mass spectrometry instrumentation applied in plant metabolomic analyses. *Phytochemical Analysis* **21**, 33-47

20. Hamzehzarghani, H., Kushalappa, A. C., Dion, Y., Rioux, S., Comeau, A., Yaylayan, V., Marshall, W. D., and Mather, D. E. (2005) Metabolic profiling and factor analysis to discriminate quantitative resistance in wheat cultivars against fusarium head blight. *Physiological and Molecular Plant Pathology* **66**, 119-133

21. Hamzehzarghani, H., Paranidharan, V., Abu-Nada, Y., Kushalappa, A. C., Dion, Y., Rioux, S., Comeau, A., Yaylayan, V., and Marshall, W. D. (2008) Metabolite profiling coupled with statistical analyses for potential high-throughput screening of quantitative resistance to fusarium head blight in wheat. *Canadian Journal of Plant Pathology* **30**, 24-36

22. Balmer, D., Flors, V., Glauser, G., and Mauch-Mani, B. (2013) Metabolomics of cereals under biotic stress: current knowledge and techniques. *Frontiers in plant science* **4**, 82

23. Hamzehzarghani, H., Paranidharan, V., Abu-Nada, Y., Kushalappa, A. C., Mamer, O., and Somers, D. (2008) Metabolic profiling to discriminate wheat near isogenic lines, with quantitative trait loci at chromosome 2DL, varying in resistance to fusarium head blight. *Canadian Journal of Plant Science* **88**, 789-797

24. Khakimov, B., Bak, S., and Engelsen, S. B. (2014) High-throughput cereal metabolomics: Current analytical technologies, challenges and perspectives. *Journal of Cereal Science* **59**, 393-418

25. Theodoridis, G. A., Gika, H. G., Want, E. J., and Wilson, I. D. (2012) Liquid chromatography-mass spectrometry based global metabolite profiling: a review. *Analytica chimica acta* **711**, 7-16

26. De Vos, R. C., Moco, S., Lommen, A., Keurentjes, J. J., Bino, R. J., and Hall, R. D. (2007) Untargeted large-scale plant metabolomics using liquid chromatography coupled to mass spectrometry. *Nature protocols* **2**, 778-791

27. Gunnaiah, R., Kushalappa, A. C., Duggavathi, R., Fox, S., and Somers, D. J. (2012) Integrated metabolo-proteomic approach to decipher the mechanisms by which wheat QTL (Fhb1) contributes to resistance against Fusarium graminearum. *PloS one* **7**, e40695

28. Muthukrishnan, S., Liang, G., Trick, H., and Gill, B. (2001) Pathogenesis-related proteins and their genes in cereals. *Plant Cell, Tissue and Organ Culture* **64**, 93-114

29. Pritsch, C., Muehlbauer, G. J., Bushnell, W. R., Somers, D. A., and Vance, C. P. (2000) Fungal Development and Induction of Defense Response Genes During Early Infection of Wheat Spikes by Fusarium graminearum. *Molecular Plant-Microbe Interactions* **13**, 159-169

30. Steiner, B., Kurz, H., Lemmens, M., and Buerstmayr, H. (2009) Differential gene expression of related wheat lines with contrasting levels of head blight resistance after Fusarium graminearum inoculation. *TAG. Theoretical and applied genetics. Theoretische und angewandte Genetik* **118**, 753-764

31. Stack, R. W., and McMullen, M. P. (1995) *A Visual Scale to Estimate Severity of Fusarium Head Blight in Wheat*, NDSU Extension Service

32. Pumphrey, M. O., Bernardo, R., and Anderson, J. A. (2007) Validating the QTL for Fusarium Head Blight Resistance in Near-Isogenic Wheat Lines Developed from Breeding Populations. *Crop Science* **47**, 200

33. Ransom, J., Mergoum, M., Simsek, S., Acevedo, M., Friesen, T., McMullen, M., Zhong, S., Eriksmoen, E., Halvorson, M., Hanson, B., Martin, G., Schatz, B. (2011) North Dakota Hard Red Spring Wheat Variety Trial Results for 2011 and Selection Guide. (Station, N. N. D. A. E. ed., NDSU, North Dakota

34. Mergoum, M., Frohberg, R. C., Stack, R. W., Olson, T., Friesen, T. L., and Rasmussen, J. B. (2006) Registration of 'Glenn' Wheat. *Crop Science* **46**, 473-474

35. Frohberg, R. C., Mergoum, M., Miller, J. D., and Stack, R. W. (2005) Registration of 'Steele-ND' wheat. *Crop Science* **45**, 1163

36. GRIS. (2012) Reeder.

37. Schneiter, A., and Hulse, D. (1999) NDSU Releases Reeder Hard Red Spring Wheat Variety.

38. Zadoks, J. C., Chang, T. T., and Konzak, C. F. (1974) A decimal code for the growth stages of cereals. *Weed Res.* **14**, 415-421

39. Puri, K. D., and Zhong, S. (2010) The 3ADON population of Fusarium graminearum found in North Dakota is more aggressive and produces a higher level of DON than the prevalent 15ADON population in spring wheat. *Phytopathology* **100**, 1007-1014

40. t'Kindt, R., Morreel, K., Deforce, D., Boerjan, W., and Van Bocxlaer, J. (2009) Joint GC-MS and LC-MS platforms for comprehensive plant metabolomics: repeatability and sample pre-treatment. *Journal of chromatography. B, Analytical technologies in the biomedical and life sciences* **877**, 3572-3580

41. Agilent Technologies, I. (2013) Mass profiler professional Workshop. in *Course Number R2260A Student Manual*, Agilent technologies, Inc, Alpharetta, GA

42. Kumaraswamy, K. G., Kushalappa, A. C., Choo, T. M., Dion, Y., and Rioux, S. (2011) Mass spectrometry based metabolomics to identify potential biomarkers for resistance in barley against fusarium head blight (Fusarium graminearum). *Journal of chemical ecology* **37**, 846-856

43. Kind, T., and Fiehn, O. (2007) Seven Golden Rules for heuristic filtering of molecular formulas obtained by accurate mass spectrometry. *BMC bioinformatics* **8**, 105

44. Walter, E. D. (1941) Genistin (an Isoflavone Glucoside) and its Aglucone, Genistein, from Soybeans. *Journal of the American Chemical Society* **63**, 3273-3276

45. Theodoridis, G., Gika, H. G., and Wilson, I. D. (2008) LC-MS-based methodology for global metabolite profiling in metabonomics/metabolomics. *TrAC Trends in Analytical Chemistry* **27**, 251-260

46. Gika, H. G., Theodoridis, G. A., Wingate, J. E., and Wilson, I. D. (2007) Within-Day Reproducibility of an HPLC−MS-Based Method for Metabonomic Analysis: Application to Human Urine. *Journal of Proteome Research* **6**, 3291-3303

47. Wu, J.-G., Ge, J., Zhang, Y.-P., Yu, Y., and Zhang, X.-Y. (2010) Solubility of Genistein in Water, Methanol, Ethanol, Propan-2-ol, 1-Butanol, and Ethyl Acetate from (280 to 333) K. *Journal of Chemical & Engineering Data* **55**, 5286-5288

48. Abdel Rahman, A. M., Pawling, J., Ryczko, M., Caudy, A. A., and Dennis, J. W. (2014) Targeted metabolomics in cultured cells and tissues by mass spectrometry: Method development and validation. *Analytica chimica acta* **845**, 53-61

49. Gika, H. G., Theodoridis, G. A., and Wilson, I. D. (2008) Liquid chromatography and ultra-performance liquid chromatography-mass spectrometry fingerprinting of human urine: sample stability under different handling and storage conditions for metabonomics studies. *Journal of chromatography. A* **1189**, 314-322

50. Yu, Q., and Liu, T. (1996) Pathological anatomy of rachis in wheat varieties with resistance against scab. *Journal of the Heilongjiang August first Land reclamation University* **8**, 42 - 45

51. Ribichich, K. F., Lopez, S. E., and Vegetti, A. C. (2000) Histopathological Spikelet Changes Produced by Fusarium graminearum in Susceptible and Resistant Wheat Cultivars. *Plant Disease* **84**, 794-802

52. Mesterházy, Á. (1997) Methodology of resistance testing and breeding against Fusarium head blight in wheat and results of this selection. *Cereal Research Communications*, 631 - 637

53. Foroud, N. A., and Eudes, F. (2009) Trichothecenes in Cereal Grains. *International Journal of Molecular Sciences* **10**, 147-173

54. Fiehn, O. (2001) Combining Genomics, Metabolome Analysis, and Biochemical Modelling to Understand Metabolic Networks. *Comparative and Functional Genomics* **2**, 155-168

55. Hall, R., and Hardy, N. (2012) Practical Applications of Metabolomics in Plant Biology. in *Plant Metabolomics* (Hardy, N. W., and Hall, R. D. eds.), Humana Press. pp 1-10

56. Paranidharan, V., Abu-Nada, Y., Hamzehzarghani, H., Kushalappa, A. C., Mamer, O., Dion, Y., Rioux, S., Comeau, A., and Choiniere, L. (2008) Resistance-related metabolites in wheat againstFusarium graminearumand the virulence factor deoxynivalenol (DON). *Botany* **86**, 1168-1179

57. Bedair, M., and Sumner, L. W. (2008) Current and emerging mass-spectrometry technologies for metabolomics. *TrAC Trends in Analytical Chemistry* **27**, 238-250

58. Hanhineva, K., Rogachev, I., Kokko, H., Mintz-Oron, S., Venger, I., Karenlampi, S., and Aharoni, A. (2008) Non-targeted analysis of spatial metabolite composition in strawberry (Fragariaxananassa) flowers. *Phytochemistry* **69**, 2463-2481

59. Allwood, J. W., De Vos, R. C. H., Moing, A., Deborde, C., Erban, A., Kopka, J., Goodacre, R., and Hall, R. D. (2011) Plant Metabolomics and Its Potential for Systems Biology Research: Background Concepts, Technology, and Methodology. in *Methods in Enzymology* (Daniel Jameson, M. V., and Hans, V. W. eds.), Academic Press. pp 299-336

60. Kang, Z., and Buchenauer, H. (2000) Cytology and ultrastructure of the infection of wheat spikes by Fusarium culmorum. *Mycological Research* **104**, 1083-1093

61. Boddu, J., Cho, S., Kruger, W. M., and Muehlbauer, G. J. (2006) Transcriptome Analysis of the Barley-Fusarium graminearum Interaction. *Molecular Plant-Microbe Interactions* **19**, 407-417

62. Hahlbrock, K., and Scheel, D. (1989) Physiology and Molecular Biology of Phenylpropanoid Metabolism. *Annual Review of Plant Physiology and Plant Molecular Biology* **40**, 347-369

63. Strange, R. N., Majer, J. R., and Smith, H. (1974) The isolation and identification of choline and betaine as the two major components in anthers and wheat germ that stimulate Fusarium graminearum in vitro. *Physiological Plant Pathology* **4**, 277-290

64. Strange, R. N., and Smith, H. (1971) A fungal growth stimulant in anthers which predisposes wheat to attack by Fusarium graminearum. *Physiological Plant Pathology* **1**, 141-150

65. Maier, F. J., Miedaner, T., Hadeler, B., Felk, A., Salomon, S., Lemmens, M., Kassner, H., and SchÄFer, W. (2006) Involvement of trichothecenes in fusarioses of wheat, barley and maize evaluated by gene disruption of the trichodiene synthase (Tri5) gene in three field isolates of different chemotype and virulence. *Molecular plant pathology* **7**, 449-461

66. McCormick, S. (2003) The role of DON in pathogenicity. in *Fusarium head blight of wheat and barley* (Leonard K. J., B. W. R. ed.), The American Phytopathological Society, St. Paul, MN. pp 165-183

67. Lemmens, M., Scholz, U., Berthiller, F., Dall'Asta, C., Koutnik, A., Schuhmacher, R., Adam, G., Buerstmayr, H., Mesterházy, Á., Krska, R., and Ruckenbauer, P. (2005) The Ability to Detoxify the Mycotoxin Deoxynivalenol Colocalizes With a Major Quantitative Trait Locus for Fusarium Head Blight Resistance in Wheat. *Molecular Plant-Microbe Interactions* **18**, 1318-1324

68. Gardiner, D. M., Kazan, K., and Manners, J. M. (2009) Nutrient profiling reveals potent inducers of trichothecene biosynthesis in Fusarium graminearum. *Fungal Genetics and Biology* **46**, 604-613

69. Desmond, O. J., Manners, J. M., Stephens, A. E., Maclean, D. J., Schenk, P. M., Gardiner, D. M., Munn, A. L., and Kazan, K. (2008) The Fusarium mycotoxin deoxynivalenol elicits hydrogen peroxide production, programmed cell death and defence responses in wheat. *Molecular plant pathology* **9**, 435-445

GENERAL CONCLUSION

The results in the present work represent the stability of the samples to be analyzed, and the metabolite profiling of FHB infected hard red spring wheat utilizing UHPLC-QTOF/MS analytical approach. Preliminary work to support the quality of subsequent studies is an aspect that is often overlooked in research. By covering this basic aspect, it was possible to have an increased certainty in the detection and classification of the molecules that occur in a FHB time course wheat infection. MS/MS fragmentation data helped to confirm some of the compounds detected (11.47%). Although the metabolites in wheat produced as response to *F. graminearum* inoculation were detected, the lack of resources such as online databases and availability of standards, made it challenging to foresee pathways that went beyond the patterns of resistance/infection and the well-known phenylpropanoid pathway. However, it was possible to develop an analytical and data mining methodology to perform metabolite profiling of medium polarity compounds in wheat florets utilizing a UHPLC-QTOF/MS. Also, a simple way to verify the stability of the extracted samples was incorporated. It was also possible to distinguish the metabolites that are synthesized as a result of the infection treatments to wheat varieties and NIL with contrasting alleles for *Fhb1*. These were: resistant related induced, resistant related constitutive and pathogenesis related. It was specially reveling to observe the early occurrence pattern of metabolites.

Some recommendations for future studies can be forwarded. The addition of more than one NIL would be beneficial to increase the certainty of the metabolites that are directly involved with the *Fhb1* QTL, as the effect of this locus is not absolute and the genetic background might still play a small role in the metabolites being detected.

The inclusion of incubation times of 72, 96 and 120 hours would provide more data to aid in the profiling of metabolites that participate in the process of resistance. This could also be extended to include several days that pair with the usual FHB spread time verification of 21 dai. In addition to the time extension, the use of diverse solvent polarities for tissue extraction and the inclusion of a negative mode in the QTOF analyses may expand the range and the number of compound classes detected per run. The sample collection might extend to other tissues like the rachis or neighbor florets up or down the inoculation point to aid in the detection of metabolites involved in the spread of the disease.

DON analysis might reveal when the toxin can first be detected after the inoculation in the infected tissue, and at what point the plant detoxifies it or not. The design of the experiment should pay attention to details that increase the identification of the features found, specifically to associate the detected molecules to the biological pathways that generated them. Lastly, due to the scarce database information in the metabolomics of wheat and the limitations of the current state of the art, it is evident that collaborative research with the fields of genomics and proteomics would bring more and better insight to clarify the molecular intricacies of the *Fusarium* head blight disease.

APPENDIX A. UPHLC QTOF-MS DATA ACQUISITION AND MASS HUNTER QUALITATIVE METHOD REPORT

Acquisition Method Report

Agilent Technologies

TOF/Q-TOF Mass Spectrometer

Component Name	MS Q-TOF	**Component Model**	G6540A
Ion Source	AJS ESI	**Stop Time (min)**	No Limit/As Pump
Can wait for temp.	Enable	**Fast Polarity**	N/A
MS Abs. threshold	200	**MS Rel. threshold(%)**	0.010
MS/MS Abs. threshold	5	**MS/MS Rel. threshold(%)**	0.010
Tune File	AutoTune.tun		

Time Segments

Time Segment #	Start Time (min)	Diverter Valve State	Storage Mode	Ion Mode
1	0	MS	Centroid	AJS ESI

Time Segment 1

Acquisition Mode MS1

Min Range (m/z)	80
Max Range (m/z)	1100
Scan Rate (spectra/sec)	1.50

Source Parameters

Parameter	Value
Gas Temp (°C)	300
Gas Flow (l/min)	7
Nebulizer (psig)	30
SheathGasTemp	225
SheathGasFlow	12

Scan Segments

Scan Seg #	Ion Polarity
1	Positive

Scan Segment 1

Scan Source Parameters

Parameter	Value
VCap	4000
Nozzle Voltage (V)	0
Fragmentor	125
Skimmer1	65

ReferenceMasses

Reference Masses

<Positive>
121.0508730
922.0097980

Name: HiP Sampler **Model:** G4226A

Enable needle seat back flush Yes

Auxiliary

Injection

Injection Mode	Injection with needle wash
Injection Volume	2.00 µL

Needle Wash

Needle Wash Location	Flush Port
Wash Time	3.0 s

Figure A1. TOF mass spectrometer parameters.

Acquisition Method Report

Name: Binary Pump **Model:** G4220A

Flow	0.400 ml/min
Low Pressure Limit	0.00 bar
High Pressure Limit	600.00 bar
Posttime Mode	Time set
Posttime	2.00 min

Timetable

	Time	Function	Parameter
1	0.75 min	Change Solvent Composition	Solvent composition A: 95.00 % B:5.00 %
2	6.00 min	Change Solvent Composition	Solvent composition A: 84.00 % B:16.00 %
3	10.00 min	Change Solvent Composition	Solvent composition A: 65.00 % B:35.00 %
4	25.00 min	Change Solvent Composition	Solvent composition A: 5.00 % B:95.00 %
5	28.00 min	Change Solvent Composition	Solvent composition A: 95.00 % B:5.00 %

	Channel	Ch. 1 Solv.	Name 1	Ch2 Solv.	Name 2	Selected	Used	Percent
1	A	100.0 % ACN in Water V.02		100.0 % ACN in Water V.02		Ch. 2	Yes	95.00 %
2	B	100.0 % Acetonitrile V.02		100.0 % Acetonitrile V.02		Ch. 2	Yes	5.00 %

Name: Column Comp. **Model:** G1316C

Left Temperature Control

Temperature Control Mode	Temperature Set
Temperature	40.00 °C

Post Time

Posttime Mode	1.00 min
Posttime	Time set

Figure A2. Timetable parameters.

Qualitative Data Analysis Method Report

Find Compounds

Find by Molecular Feature

MFE processing and ion species settings

Retention time range:	0.5 - 29
Restrict m/z range:	False
Use peaks with height >=	600
Positive ions:	
Modifier	+H
Modifier	+Na
Negative ions:	
Modifier	-H
Salt dominated positive ions:	False
Include representative raw spectrum for each compound	False
Assume unidentified ions are radical ions	False
Target data type	Small molecules (chromatographic)
Neutral Species Definitions	
Include representative raw spectrum for each compound	False
Extract ECC	False
Extract MFE spectrum	False
Typical RT peak width	False
min	0.200
Smoothing	True
times peak width	0.200
Smoothing	True
length	50.000
Remove spikes	False
max spike width	0.250
Smooth peaks	True
times peak width	1.000
Remove wide peaks	False
min peak width	10.000
Display only the largest	False
Extract MS/MS Spectrum	False
Average MSMSSpectrum per CE	False
Single m\z Expansion mode	Asymmetric (m/z)
Tolerance	20.00
Tolerance	0.05
Tolerance Unit	ppm
Deisotope MS/MS spectrum	True

Charge state assignment settings

Isotope spacing tolerance(m/z)	0.0025
Isotope spacing tolerance(ppm)	7.0
Maximum charge state	2
Limit assigned charge states to a maximum of:	True
Isotope model	Common organic molecules
Treat ions with unassigned charge as singly-charged	False

Figure A3. Find by molecular feature parameters.

MFE result filters

Peak height (counts) >=	5000
Restrict retention times:	False
Charge states:	1 - 1
Restrict to neutral losses:	False
Filter mass list	False

MS/MS spectrum peak filter settings

MFE result options

Delete previous compounds	True
Highlight all compounds	False

MFE database location

Database Path	D:\Mass Hunter\PCDL\default.csv

Find Compounds by Formula

Find by Formula - Options

Find Compounds by Formula options

Formula source to confirm	Worklist	
Use Absolute Mass Tolerance		FALSE
Retention Time Tolerance	0.35	
Single Mz expansion mode:	Symmetric (ppm)	
Expected retention time	1.5	
Search Fields	Mass, Optional Retention Time	
Relative Mass Tolerance	10	
Single ppm width:	35	
Cef Path		
Automatically increase for isomeric compounds		TRUE
Do not match if score is		TRUE
Reject score threshold	60	
Do not match if the (unobserved) second ion's abundance is expected to be		TRUE
Reject second ion threshold	300	
Prefer profile for raw spectra, if available		TRUE
Clip extracted raw spectra		TRUE
Extracted spectrum expansion mode	Symmetric (m/z)	
Asymmetric low width	5	
Asymmetric high width	10	
Single width	5	
Extract MS/MS spectrum		FALSE
Average MS/MS spectrum for all CE's		FALSE
Precursor tolerance	20	
Precursor tolerance	0.05	
Tolerance unit	ppm	
Deisotope MS/MS spectrum		TRUE
Include structure		FALSE
Warn if score is		TRUE
Warn if the (unobserved) second ion's abundance is expected to be		TRUE
Warn score threshold	75	
Warn single ion threshold	50	
Smooth EIC before integration		FALSE

Database location settings

Database Path	C:\Mass Hunter\PCDL\default.csv

Probable Pos Species settings

Positive ions:	
Modifier	+H
Modifier	+Na
Positive Neutral Loss:	
Positive Charge State Range	2

Figure A4. Find by formula-options parameters.

Identification Scoring

MS mass coeff (m Da)	2
MS mass coeff (ppm)	5.6
MS/MS mass coeff (MDa)	5
MS/MS mass coeff (ppm)	7.5
MS isosope abundance	7.5
Retention time:	0.5
Isotope abundance score	60
Mass score	100
Isotope spacing score	50
Retention time score	0
MS/MS score weight	50

Find compounds results settings

Delete previous compounds	TRUE
Highlight all compounds	FALSE

Find by Formula - Chromatograms

Find Compounds by Formula options

Formula source to confirm	Worklist
Use Absolute Mass Tolerance	FALSE
Retention Time Tolerance	0.35
Single Mz expansion mode:	Symmetric (ppm)
Expected retention time	1.5
Search Fields	Mass, Optional Retention Time
Relative Mass Tolerance	10
Single ppm width:	35
Cef Path	
Automatically increase for isomeric compounds	TRUE
Do not match if score is	TRUE
Reject score threshold	70
Do not match if the (unobserved) second ion's abundance is expected to be	TRUE
Reject second ion threshold	200
Prefer profile for raw spectra, if available	TRUE
Clip extracted raw spectra	TRUE
Extracted spectrum expansion mode	Symmetric (m/z)
Asymmetric low width	5
Asymmetric high width	10
Single width	5
Extract MS/MS spectrum	FALSE
Average MS/MS spectrum for all CE's	FALSE
Precursor tolerance	20
Precursor tolerance	0.05
Tolerance unit	ppm
Deisotope MS/MS spectrum	TRUE
Include structure	FALSE
Warn if score is	TRUE
Warn if the (unobserved) second ion's abundance is expected to be	TRUE
Warn score threshold	75
Warn single ion threshold	50
Smooth EIC before integration	FALSE

Chromatogram smoothing settings

Smoothing function:	Gaussian
Function width:	15
Gaussian width:	5

MS Integrator selection

Integrator Selection	Agile

Find by Formula Chromatogram peak filter settings

Peak height(counts) >=	3000
Limit to largest:	5

Figure A5. Find by formula-chromatograms parameters.

Find by Formula - Mass Spectra

MS Peak spectrum extraction settings

Average scans above (%):	10
TOF saturation limit (%):	10
Restrict saturation m/z range:	FALSE
MS background source:	None
Also evaluate with no background	FALSE
Never return an empty spectrum	TRUE
Tof saturation mz range option	In the m/z ranges used in the chromatogram

MS TOF peak finder settings

Detect Maximum Spike Width	2
Detect Required Valley	0.7

Charge state assignment settings

Isotope spacing tolerance(m/z)	0.0025
Isotope spacing tolerance(ppm)	7
Maximum charge state	2
Limit assigned charge states to a maximum of:	TRUE
Isotope model	Common organic molecules
Treat ions with unassigned charge as singly-charged	FALSE

Identify Compounds

Search Database

Database search settings

Use Absolute Mass Tolerance	False
Relative Mass Tolerance	5.00
Retention Time Tolerance	0.100
Maximum Hits	10
Maximum number of peaks to search when peaks are not specified graphically:	5
Search "neutral" database entries for masses from simple ions	False

Database location settings

Database Path	C:\Mass Hunter\PCDL\Metlin_AMRT_PCDL.cdb

Probable Pos Species settings

Positive ions:	
Modifier	+H
Modifier	+Na
Positive Neutral Loss:	
Positive Charge State Range	1 - 1
Positive Dimer	False
Positive Trimer	False

Figure A6. Find by formula-mass spectra parameters.

Search Accurate Mass Library

LC Spectral library search settings

Spectral library path:	
Limit to the best	False
Maximum hits per compound:	10
Search criteria	Collision Energy, Fragmentation Voltage, Polarity, Scan Type, Instrument Type, Precursor Ion
Search method	Reverse
Ce Tolerance	2.00
Precursor Ion m/z ppm	10.0
Precursor Ion m/z m Da	2.0000
Product ion m/z ppm	20.0
Product ion m/z m Da	2.0000
Minimum forward match score:	25.00
Minimum reverse match score:	80.00

Spectral library selection settings

Spectral library path:	C:\Mass Hunter\PCDL\Metlin_AM_PCDL.cdb
Apply to search database path	False

Peak filters used by spectral library search

Peak height (counts) >=	100
Peak height (%) >=	0.500

Generate Formulas

Formula calculator settings

MS nitrogen rule:	even electron
Positive ions:	H
Negative ions:	H
Element Limits	
C	3 to 60
H	0 to 120
O	0 to 30
N	0 to 30
Maximum neutral mass for which formulas should be calculated:	950.0000
Minimum score	50.000
Maximum MS mass error	False
Require DBE from	False
Maximum number of hits	False
MS Mass Coeff (MDa)	2.0
MS Mass Coeff (Ppm)	5.6
MS MS Mass Coeff (MDa)	2.5
MS MS Mass Coeff (Ppm)	7.5
MS isotope abundance	7.5
Formula generation rules	B0201

Charge state assignment settings

Isotope spacing tolerance(m/z)	0.0025
Isotope spacing tolerance(ppm)	7.0
Maximum charge state	2
Limit assigned charge states to a maximum of:	True
Isotope model	Common organic molecules
Treat ions with unassigned charge as singly-charged	False

Identification Scoring

MS mass coeff (m Da)	2.0
MS mass coeff (ppm)	5.6
MS/MS mass coeff (MDa)	5.0
MS/MS mass coeff (ppm)	7.5
MS isosope abundance	7.5
Retention time:	0.500
Isotope abundance score	60.00
Mass score	100.00
Isotope spacing score	50.00
Retention time score	0.00
MS/MS score weight	50.00

Figure A7. Generate formulas parameters.

Find Compounds

Find by Targeted MS/MS

MS/MS Integrator selection

Integrator Selection	Agile

MS/MS ChemStation Integration settings

Tangent skim mode:	Standard
Baseline correction mode:	Classical
Front skim height ratio:	0.00
Tail skim height ratio:	0.00
Skim valley ratio:	20.00
Peak-to-Valley ratio:	500.00
0: Slope Sensitivity	5
0: Peak Width	0.05
0: Area Reject	5
0: Height Reject	1
0: Shoulders Mode	OFF
0: Baseline Now	False

Targeted MS/MS processing settings

Maximum chromatogram peak width	0.25
Limit to the largest compounds:	False
Extract MS/MS chromatogram	True
Extract MS/MS spectrum	True
Extract MS spectrum	False
Extract separate MS/MS spectrum per collision energy	True
Generate library spectra	False

MS/MS Universal integrator settings

Shoulder detection	OFF
Threshold:	0.00
Area reject:	0.00
Peak width:	0.00
Use Data Scale Factor	False
0: Baseline Now	False

Targeted MS/MS chromatogram peak filter settings

Peak height (counts) >=	600

MS/MS Peak spectrum extraction settings

Average scans above (%):	10
TOF saturation limit (%):	40.0
Restrict saturation m/z range:	False
MS/MS background source:	None
Also evaluate with no background	False
Never return an empty spectrum	True
Tof saturation mz range option	In the m/z ranges used in the chromatogram

Find compounds results settings

Delete previous compounds	True
Highlight all compounds	False

Figure A8. Find by targeted MS/MS parameters.

APENDIX B. METABOLITE PROFILING METHOD DESCRIPTION

Data Processing Using Molecular Feature Extraction Algorithm

Result ".d" files from the Mass Hunter acquisition software were processed using Mass Hunter Qualitative (MH Qual) software. Within this software, the Molecular Feature Extraction (MFE) algorithm provided a naïve finder that is effective as a first way to scrutinize LC-QTOF/MS raw data. The algorithm was set accordingly for small molecules discovery.

Once in MFE algorithm, in the Extraction section, the option "target data type chosen" was "small molecules". For "restrict retention option time" was set between 0.5-29 min. This time was chosen to discard the void volume. In addition, after 29 min there was no visual evidence of peaks. The "use peaks with height of >= counts" was set to 600. This was set according to a signal to noise ratio of 3:1.

In the "ion species section" for "positive ions", the cations options +H and +Na were ticked. The reason for this was that only positive ionization mode was utilized. The sodium cation was considered being present in sufficient high amounts to be seen as potential for adduct formation. In the negative ions only –H ion was ticked.

In the Charge State section, the "peak spacing tolerance" was set to 0.0025 m/z, plus 7.0 ppm, with an "isotope model" of Common organic molecules. This was a default that works well for small molecules. The charge state was limited to a maximum of 2; which, according to the manufacturer, is to avoid too much of a restriction in exclusively finding a single ion.

In the compound filter section, the "absolute height" was ticked and also set to >=5000 counts. Since the search was for small molecules, the "charge state restriction" was ticked and set to 1 Z.

The “mass filters”, “mass defect” and peak filters (MS/MS)” sections within the MFE, were left with no selection. In the results section, the “delete previous compounds” was checked as well as “highlight first compound”. The idea of this was to avoid overloading the system.

At the advanced section, the “compound ion threshold” was set to “two or more ions” as recommended by the manufacturer. Selecting the correct actions for the software to run was performed by going to the “work list automation” category in the “method explorer” of the left panel. In “work list actions” the “find compounds by molecular feature” and “Export to CEF” options were selected in the “available actions” drop box. The options were set in that order. This action was saved.

Next in the “export” category, after selecting “CEF options”, a specific folder was created by clicking the option “at specified directory”. Once these options were set, they were saved as a method to use in all data processing experiments.

The MH Qual software has to be assisted by the DA reprocessor program by setting the total raw files to look for in the “Data file” column. Each “.d” file was loaded by highlighting the first row and selecting “add multiple samples” with the right mouse button. After that, it was necessary to load the method that was created in the MH Qual by clicking the first row within the “method” column. All the files need to be set with this method so the DA reprocessor can effectively process the files according to the method previously set.

After this, the file was saved clicking the “save work list” icon. This was used for recursion analysis in future steps. The data processing started by clicking the green “start” button on the upper left section of the main window. The processing time was dependent on the amount of data.

Mass and Retention Time Alignment

The output ".cef" files were aligned for time and mass using Mass Profile Professional (MPP) software. A "new project" or "new experiment" was selected in each case (NIL or Wheat varieties) setting the "experiment type" to "unidentified", and choosing the "workflow type" to "data import wizard". This means that the data processing will not be limited by any default workflow.

After selecting "OK" in the "Select Data Source" was left as "mass hunter Qual" and "organism" as "none" due to the data type and that no pathway analysis is to be perform with this data. After selecting "OK" in the "select data import" window, data selection was uploaded by clicking "select data files". This action opened the destination ".cef" files that were generated by the DA reprocessor-MH Qual software. After highlighting and clicking "OK" in the window, the selected files appeared in the original "select data to import" window. By clicking "OK" the files were validated and were shown in a new window named "sample reordering". There was no need to reorder the samples since they were coded. So the "next" button was clicked.

The following windows named "experiment grouping" and "filtering" window were left as default. There was no need to modify any parameter since only retention time (RT) alignment was to be performed.

After clicking "next", in the "alignment parameters" window, the "compound alignment" option was modified as to set a RT window of 0.15 minutes in the "min" slot for the NIL except NIL Block 3, where it was set to 0.37 minutes. The RT correction was set to 0.15 minutes for all wheat varieties. The retention time window was evaluated by comparing the sample chromatograms peaks within their blocks as follows:

Examination of raw data was performed in Mass Hunter Qualitative software. A set of files in interest were selected by going to the "file" menu and selecting "open file". The set of files were highlighted and in the window "option menu" the "use current method" was selected. By default, the sample files opened with a Total Ion Current (TIC) scan. After this, the "overlaid" icon was selected so to view all TICs from the sample files over each other.

Retention time drift was estimated by clicking the apex of the left-most peak of a zoomed in plot. Then looking at the text at the top of the spectrum where the retention time is listed. This time was recorded and subtracted to the right-most peak of another TIC. The result should be the RT window.

After clicking "next" a "result summary" window was viewed. A "compound frequency" plot is visualized. The plot displays "no. of compounds" vs. "frequency". After clicking "next" and with the alignment for RT and mass finished, the "filter by flags" option located in "Quality control" under the "workflow" panel was selected. The idea was to filter out some of the artifacts generated by the last processes.

The first window that opened was the "entity list and interpretation". After clicking next, in the "input parameters window" and inside "retain entities in which at least", there is a blank slot that continues with "out of x samples have acceptable values". The blank was filled with the 10% of the total samples that were to be analyzed. This was selected as a recommended number according to trials performed by the manufacturer.

After clicking "next" a display of the "output views" of filter by flags could be seen in a window. Then after finishing the sequence a total number of passed samples were seen on top of the graphic.

The “export for recursion” option was selected by going to the right “workflow” panel, under “result interpretation”. In the export window, the “output file” browse option was used by selecting the appropriate folder as a destination for the composite .cef file. This file had to be stored with a unique name.

Recursion Analysis

The recursion analysis was performed after completing the MFE run, mass and time alignment. Utilizing this approach reduces in great amount the false positive entities generated by the MFE. It uses three algorithms of “find by formula” which include: “find by formula – options”, “find by formula – chromatograms” and “find by formula – mass spectra”.

Find by Formula – Options Settings

In the section “formula source”, the option “compound exchange file (.cef)” was selected. Also, the appropriate “.cef” file was selected by browsing in the files generated by the retention and mass alignment procedure. The “maximum number of matches” was set to 1 and the “automatically increase for isomeric compounds” was checked. The “values to match” was set to “mass and retention time required”

In the section “formula matching, the “masses” were set to +/- 10 ppm and “retention times” were set to +/- 0.2 minutes. The “possible m/z” was set to symmetric (ppm) with +/- 20. The “limit EIC extraction range” was selected and the “expected retention time was set to +/- “1.5 minutes. In the section “positive ions”, the “charge carriers” were selected as +H and +Na, with a “charge state range” of 2 to match the setting on MFE. The “negative ions” sections were left as default. In the “scoring” section, the “contribution to overall score” were set as follow: “mass score” 100, “isotope abundance score” 60, “isotope spacing score” 50, “retention time score” 0. The “expected data variation” parameters were left as: “MS mass” 2, mDa + 5.6 ppm.

The “MS isotope abundance” was: “MS/MS” mass 5.0 mDA + 7.5 ppm. At “retention time” 0.5 min. was used.

In the “results” section, the “delete previous results” was checked as well as selecting the “highlight first compound” Everything else in that section was not selected. In the “result filter”, the “only generate compounds for matched formulas” was selected. The “warn if score is <” was set to 75. The “do not match if score is <” was set to 60. The “warn if the second ion’s expected abundance is >” was set to 50. The “do not match if the second ion’s expected abundance is >” was set to 300.

Find by Formula – Chromatograms

In the section “EIC smoothing”, “smoothing function” was set as Gaussian. The “function width” was set to 15 points and the “Gaussian width” was set to 5 points. In the “EIC integration” section, the “integrator selection” was Agile. In the “EIC peak filters”, the “filter on” was set to peak height. The “absolute height >=” was checked and set to 3000. The “limit (by height) to the largest” was set to 5.

Find by Formula – Mass Spectra

In the “peak spectrum” section, the “average scans >” were set to 10% of peak height. The “exclude if above” was checked and set to 10% of saturation. The option “In the m/z ranges used in the chromatogram” was selected, as well as “never return an empty spectrum. The “peak spectrum background MS” was set to none. In the “peak location” section, a “maximum spike width” was set to 2. The “required valley” was set to 0.7.

In the “charge state”, the “peak spacing tolerance” was set at 0.0025 m/z default value, but with a “plus” of 7 ppm. The “isotope model” option was set to “common organic molecules”. The “limit assigned charge states to a maximum of” was checked and set to 2.

In the MH Qual software, selecting the correct actions for the software to run was performed by going to the “work list automation” category in the “method explorer” of the left panel. In “work list actions” the “find compounds by formula” and “export to CEF” options were selected in the “available actions” drop box. The options were set in that order and saved.

Next in the “export” category, after selecting “CEF options”, a specific folder was created by clicking the option “at specified directory”. This was the same folder as the previous aligned file. Once these options were set, they were saved as a method to use in all data processing experiments.

The MH Qual software has to be assisted by the DA reprocessor program. After opening the software, the “open work list” was clicked and selected the saved “.wkl” file to load. This file was created previously and contains the raw files directory plus the current MH Qual method. After all was set, the green “start” button was selected and the run started. Depending on the number of files, it took a few hours or days to complete the run.

MPP Data Mining

Creating a New Experiment

After the recursion analysis, the output sample files were loaded to the MPP software. A “new project” or “new experiment” was selected in each case (NIL or Wheat varieties) setting the “experiment type” to “unidentified”, and choosing the “workflow type” to “data import wizard”. This means that the data processing will not be limited by a default workflow.

After clicking “OK”, the “Select Data Source” was left as “mass hunter Qual”. The “organism” option was set as “none” due to the data type and that no pathway analysis is to be performing with this data.

After selecting “OK” in the “select data import” window, data selection was uploaded by clicking “select data files” which opened the destination “.cef” files that were generated by the recursion workflow using the DA reprocessor-MH Qual software. After highlighting and clicking “OK” in the window, the selected files appeared in the original “select data to import” window. By clicking “OK” the files were validated and were shown in a new window named “sample reordering”. There was no need to reorder the samples since they were coded. So the “next” button was clicked.

The following window called “experiment grouping” was used to group the samples in parameters that were used later in the interpretations. The parameters used were: Block, numeric for block number; Genotype, numeric for allele in NIL: “4” is resistant and “6” is susceptible. Name was used for wheat varieties; Treatment, either “M” for mock or “I” for inoculated; Sample, biological sample as S1, S2, S3, S4, S5, S6; Collection time: 0, 6, 12, 24, 48 hours.

For the varieties, the code was as follows:

First letter for implied variety (G for Glenn, SND for Steele ND and R for reed); B1, B2 or B3 for block number; Sample, biological sample as S1, S2, S3, S4, S5, S6; Treatment, either “M” for mock or “I” for inoculated. Clicking next to the “filtering” window was left as default modifying the “minimum number of ions” to 1. It was necessary to modify the RT window to the one set before in the “alignment parameters” windows.

After clicking “next”, in the “alignment parameters” window, the “compound alignment” option were left as to follow the RT window slot previously determined for the NIL and wheat varieties. After clicking “next” a “result summary” window was viewed. A “compound frequency” plot is visualized. The plot displays “no. of compounds” vs. “frequency”.

Clicking next in the “normalization criteria” and “baselining options” windows, groups were processed without any normalization or baselining (to get the most entities). Still, the algorithm does log2 scaling as default. Clicking “next” completed the experiment generation. The data was ready for the statistical analyses in MPP.

Blank Subtraction

This operation was necessary to effectively subtract the entities (potential compounds) found in the blanks (extraction solvent) from the samples. There was need to create an interpretation of only the blank samples and also another of only the treatment samples. Then a “filtering by flags” was used before performing a Venn diagram to separate and save the entities unique to the experimental samples.

Creating an Interpretation

While on MPP software, in the “workflow” column and under the “experiment setup” a “create interpretation” was opened. A panel opened and only “block” and “blank” parameter were selected. For the experimental samples, the rest of the parameters were selected except “block” and blank”. After clicking “next” a “select profile plot display modes” window appeared. This was left as default (categorical), since for this software it only influences the outcome of the final graphic as dots connected or not.

The next window was “select conditions”. Under “unselect conditions to exclude”, the one corresponding to “blanks” was selected. For the experimental samples, it was enough to select “genotype” or “variety”. Under “average over replicates in conditions” the selection was “non-averaged”. The next window “save interpretation” was opened and a name of “blanks only” or “unique to samples” was typed. Other interpretations were created in this fashion but were specific to answer unique questions.

Filtering by Flags

Once the interpretations were created, it was necessary to apply a "filter by flags". Flags are attributes of quality. After setting a window, the filter will allow to find masses depending on data quality flags. Flags could be present (signal detected); marginal (signal saturated) or absent (no mass detected). For this purpose, only the first two flags were used. As recommended by the manufacturer, a 10% window (from a particular interpretation) was applied in this filter.

While on MPP software, in the "workflow" column and under the "quality control" a "filter by flags" was selected. A window titled "entity list and interpretation" was then opened. In the "entity list" option slot, the correct entity was selected by pressing "choose" button on the right. For this case, it was the "all entities" list. For the "interpretation" slot, either "blanks only" or "unique to samples" was selected.

After clicking "next", a window titled "input parameters" opens. Here the option "at least…out of x samples have acceptable values" was selected. A 10% out of the total samples displayed here was applied and clicked next.

The next window showed an "output views of filter by flags". It displayed how many samples pass the filter out of the total. The next window was "save entity list" a name displaying "blanks only" or "unique to samples" was typed for each case.

Selecting Sample Entities Using Venn Diagram

While in MPP software, an icon located on top of the display was selected. The icon shows a blue and red circle on top of each. This opened the "Venn diagram" window. Here, the "all entities" folder was opened to select both, the "blanks only" and "unique to samples" files. After clicking "ok" a Venn diagram is displayed. Selecting the "unique to samples" semi-circle and clicking to the paper and pencil icon on the upper-left of the display brought a new window.

By clicking “next” to the “choose columns to import”, a “save entity list” window appears. A name like “Blanked samples” was typed and the “finish” button was clicked. These entity lists were saved in another folder below the “My favorites” one.

Filter by Frequency

The resulting entity lists from the Venn diagram were again filtered using a frequency filter. This option is based on the number of occurrence of a particular entity across the sample.

The “filter by frequency” option was selected located in the “workflow column” under “quality control” section. This opened a window named “entity list and interpretation”. The entity list named “blanked samples” was chosen. In the interpretation slot, the appropriate interpretation was chosen. For the case of a NIL, the interpretation of “Block-Genotype-Treatment-Sample no.-collection time (non-averaged)” was selected. For the wheat varieties, a “Block-wheat type-treatment-sample no.” interpretation was chosen.

After clicking next, a new window “input parameters” opens up. The “filtering conditions” option was left as “retain entities that appear in at least 100% of samples in at least one condition”. This gave a final polish to the data, since at this level; it generally only took a few entities out of the total.

After clicking next, a final plot was visualized in a window “output views of filter by frequency”. The final window “save entity list” was named and clicked “finish”. These filtered entity lists were used on statistical testing.

Volcano Plot

This statistical test was very useful for visualizing differences between any two conditions. It consists of a scatter plot in which one axis corresponds to the p-value and the other to the fold change. Both axes are in log scale (log10 for P-value; log2 for fold change). This

arrangement allows distinguishing masses with a fold-change (magnitude of change) as a biological significance; and also statistical significance (takes both magnitude of change and variability into consideration). In this study it was used extensively to separate compound candidates that were unique to an induced resistant condition from the ones produced by the plant or pathogen. The results of the tests were saved as independent entity lists to work on in another stage of the data mining.

In the MPP software, a new test was opened by choosing “filter on volcano plot”, located under the “workflow” column and in the “analysis” section. A window named “input parameters” appears.

This window contains three options. In the “entity list” option, an appropriate entity list was chosen, one that has been blanked and filtered by frequency at 100%. Button “choose” was clicked and the entity list selected from the list.

In the “interpretation” option, an appropriate interpretation was selected. For the comparison of experimental conditions in the case of a NIL; the interpretation of “Block-Genotype-Treatment-Collection time (non-averaged)” was selected. This allowed having grouping without the level of separation from sample 1 to 6, thus considering a mixed pool at the level of sample for each category. For the wheat varieties, a “Block-wheat type-treatment.” interpretation was chosen.

The option “exclude missing values from calculation of fold change and p-value” was selected. This was important to avoid greater errors from missing values.

After clicking “next” a window named “select test” appears. There are three options to set: “condition 1”, “condition 2” and “select test”. The purpose of the first two options is to

select the experimental conditions (created when the parameters were added to the samples) and defined by the interpretation. The last option opens a selection of T-tests.

For the NIL, defined selections of comparisons were decided as: RM vs SM, RI vs RM, SI vs. SM, RI vs. SI; where "R" stands for resistant, "S" is susceptible, "M" is mock and "I" stands for inoculated. The entity separation would be classified accordingly if they are Pathogenesis related (PR) or resistance related (RR).

A PR could be found either in a resistant wheat genotype as in RI>RM (PRr), or as SI>SM (PRs) in a susceptible genotype. Any entity that had higher abundance in the resistant genotype than in a susceptible such as RI > SI or RI>RM was considered a RR induced (RRi). If this was based on Mock inoculation as RM>SM, then it was considered as RR constitutive (RRc).

These comparisons were made for each collection time and for each block. The "T-Test unpaired unequal variance" was chosen for T-test, since the experimental conditions were not tested within each individual (unpaired comparisons). It may also correct for differences between variances. In addition, it was noticed that compared to a Moderated T-Test option (aids to avoid false discovery rate), the unpaired unequal variance option yielded same entity masses, plus a few more. This would be verified in a visual inspection of the spectra.

By clicking "next" the "p-value computation" window appears. This option is necessary to correct for multiple T-testing. If no corrections are made, the number of compounds that appear by chance increases. The p-value options were left as default. The options were "p-value computation asymptotic"; which did not make a difference when compared with "permutative" for 10000 combinations. The "multiple testing correction Benjamini-Hochberg FDR" was

selected as provided a balance between the restrictive “Storey with bootstrapping” and “no correction”.

After selecting “next”, the “results” window appears. At this window it was possible to select the compounds that are statistically significant (above a horizontal green line) and biologically important (> or = to a fold change of 2, vertical green lines). These compounds were represented in red for each quadrant of the volcano plot. If the comparison is A vs. B, the interesting compounds in A (higher in A than B) will be visualized on the right quadrant. The reverse is true for B. Multiple entity lists from all combinations described previously were created in this way.

At this same window, they are three important options to set: “corrected p-value cut off”, was set at “0.05” as it was the default value and a good overall level of error. The “fold change cut-off” was set at “2.0”. A twofold change in magnitude represents biological relevance literature and is equal to the absolute ratio between the normalized average intensities of condition 1/condition 2. The “abund diff (raw, abs) cut-off” is set to lower the number of false positives originated by the process. It was necessary to verify the raw intensity and spectra by opening a promising compound out of the resulting list. A value of 500 was enough to eliminate meaningless fold change differences.

After clicking the volcano plot window, a corrected list with fewer compounds replaces the old list. The compounds in which the “FC” is blue, corresponds to a “down regulated” (left quadrant) or lower in frequency in a particular comparison. The compounds in which the “FC” is red, corresponds to an “up-regulated” (right quadrant) or higher frequency for a particular comparison.

Before selecting the custom sub-list from the main result list, the each entity was visually verified by double clicking the entity at the list or at the volcano lot area. Doing that opened a new window in which is possible to verify the "profile plot" and "spectra". The first option was used to visually testify if the "raw intensity" of the candidate entity really is more/less double of that in the comparing group. The second option is used to verify if the composite spectrum of a given entity is really consistent with a minimum of 3 and a minimum of 2 ion peaks. If one of the two options was not satisfactory, the entity was not taken into account for the sub-list.

After selecting the blue or red compounds, it was possible to save a custom list of each group for each of the comparisons being made by clicking "Save custom list".

By clicking "next", the window "save entity list" can be seen. The default optional name of the analysis can be left since it shows the specific comparison. This was useful since they were many comparisons to make. After clicking "finish" The new entity lists could be seen under the by the filtering by frequency list, and inside the "significance analysis custom selection"

Visual Inspection of Spectra

To reduce the number of false negatives in the entity lists that could have been generated at the level of volcano plots, it was necessary to visually compare the EIC (extracted ion chromatogram) form each original acquisition file. This was performed by using the m/z of each candidate compound in Mass Hunter Qualitative. The comparisons were made according to the pairs used in the volcano plot testing.

If for example, the "A vs B up-regulated" list was to be analyzed, the original biological samples for A and B were screened for a particular m/z contained in the "A vs B up-regulated" list. Once having the graphic plots of the EIC's count vs. acquisition time, it was possible to compare areas between A and B. If the "A" area did not have a 2 fold difference over the B

(expected to be upregulated over B), that would mean a false positive result. For a candidate compound to not be considered a false negative, at least 4 out of the 6 biological samples per comparison pair should have a 2 fold difference in area. The exclusion process is described as follows:

Exporting Significance Analysis Entity Lists

At the MPP software, under the "significance analysis custom selection" folder, a t-test comparison entity list was selected using the right mouse button. At the drop box, "export list" was selected.

A new window "export options" appeared. The default checked options were set to unselect and at the "selected items" box, the options "compound name", "mass, and "retention time" were selected by using the arrows to include the options in the box.

After selecting "OK" and typing the name of the new "TXT" file to be generated, the entity list will be generated in the destination folder that was specifically assigned for. The folder was not in the MPP but in the computer's memory.

Doing this process only gave the information of mass, retention time and name of the compound (which at this stage was "neutralmass@retentiontime" format). There was still need to obtain the m/z. To do so, while at the MPP software, the "export inclusion list" located under "results interpretations" in the "workflow" column was opened. The "entity list a file path chooser" window opened. In the browse option "output file", an appropriate location was chosen and the file was named.

After clicking "next" the window "filtering parameters for inclusion list" appeared. The parameter "retention time window" has to be adjusted with the minutes that the particular set of samples had for correction. The "limit number of precursor ions per compound to" option was

checked and set to 1. Under the “Exported m/z value”, the “export highest abundance m/z” option was selected. For “positive ions” the “+H” and “+Na” options were checked. In the “charge state preference” the “prefer highest abundance charge state (s)” was selected.

The idea to do the above selection was to limit the m/z value to only 1, which would be the highest isotope with the most abundance in its own spectra. The MPP software already has arranged all the potential isotopes that correspond to the same spectrum in only a few when the time and mass alignment was performed. The “finish” completed the task and a new “CSV” file is generated at the same location were the first TXT file was.

After generating both “TXT” and “CSV” file for a particular entity list comparison, there was need to include the compound name of each entity found in the “TXT” file into the CSV file. The purpose was for ease of use, since the “CSV” file was used further as a visualization quality score sheet.

Visual Verification of Candidate Compounds

A visual inspection of the potential entities that passed the volcano plot (as “up” or “down regulated”) was performed. At the Mass Hunter Qualitative program, the method was set using the “method” option located at the top menu. The method chosen was the same one used for the initial data screening (MFE) named “Metabolomics ggg mpp.m”.

After the method was set, the original acquisition files were opened according to each T-test comparison. This was performed by going to “file”, “open data file”. A window appeared and the correct files having “.d” as extension were selected. The “option” used in this window was always set to “use current method” and “open” was selected. The procedure was repeated twelve times (one for each biological sample per comparison per block). This generated TIC (total ion chromatogram) graphics which are plotted in Counts vs Acquisition time (minutes).

The TIC's were extracted to EIC's by selecting the list of files and clicking the "chromatogram" button at the top menu. A drop-box opened and "extract chromatograms" was selected.

At this level, a new window opened showing a pre-selection of the loaded files. At the "MS chromatogram" subsection, the option "type" was set to "EIC". The "integrate when extracted" option was checked. The option "m/z value(s)" was changed according to the compound being investigated. At the advanced subsection, the "single m/z expansion for this chromatogram" was set to "symmetric (ppm)" with +/- of 10. The rest of the options were left as default. By clicking "OK", the EIC graphics appeared showing the specific area and retention time for the compound in question.

The comparison process was numerical and visual for each compound in each entity list (as described before). Additional T-tests (areas as dependent variable and a Confidence level of 95%) were performed only when visually there was a draw (3 out of 3). Once a decision was made, the "CSV" file containing the m/z of the candidate compound was modified to include the quality grade and a score. This was useful later to select the main final compounds.

The selected passed entities were compiled into a single excel file. Each spreadsheet contained a comparison. The spreadsheets were then divided to include the up and down-regulated entities, and also to be organized by collection time. In this way, it was very practical to localize the appearance of a specific entity in the time course.

If an entity was found the same in one of the other comparisons (e.g. resistant vs. susceptible line), the particular entity would then be analyzed and compared using a T-test/Venn diagram strategy to distinguish what entities in that comparison have the higher fold change.

Compound Annotation

Accurate mass identification

The resulting entity lists were then annotated using the "ID browser software". This software is integrated into the MPP main software. This software uses four different reference data internet sites as well as a unique Agilent one.

Once in the MPP software, ID browser is located on the right menu column under "results interpretations". Once opened, an option window named "choose the entity list to be identified" appears. This allowed choose from all approved entity lists.

After clicking next, a new window "compound identification wizard" appears. Here the "identify all compounds" was selected. Also, the "database search (CSV, PCD/METLIN)" and the "molecular formula generator (MFG)" were selected. In this last option, the "generate formulas only for unidentified compounds" was included. This because of the database search algorithm that includes isotope abundance matching, therefore, it is typically only necessary to generate formulas for unidentified compounds.

The next window named "compound identification wizard", has a general option named "identify compounds". Under this category, there are the "search database" and the "general formulas" menus. The "search database" menu has a set of 8 sections. Each one of them was set accordingly as follows. In the "search criteria" section, the "mass" was chosen as a "value to match". A number of 5 ppm was set as "match tolerance". In the "Database section" the Database path selected was for the "Metlin_AMRT_PCDL.cdb" database.

In the section "peak limits", the "maximum number of peaks to search when peaks are not specified graphically" was set to 5, since this was enough number of hits to compare the theoretical isotope ratios.

For the “positive ions” section, the Charge carriers were set as before, being +H and +Na ticked, with a “charge state range” of 1. The “negative ions” section was left as default.

The “scoring” section, the settings were left mostly as default as they were adequate: “mass score” 100; “isotope abundances score” 60; Isotope spacing score 50. There was no score associated with “retention time score” since this parameter was not considered for the final number.

In the “expected data variation” the parameters were left as the manufacturer recommended, with an “MS mass” of 2 and “mDa +” of 5.6 ppm. For the “MS isotope abundance” subsection, the “MS/MS mass” was left at 5.0 and “mDa +” 7.5 ppm. The “retention time” subsection was not used.

The “search mode” section, for the “ion search mode” when searching masses for single ions, the option chosen was left for “cation or anion entries” For the “search results” section, the “limit to the best” was ticked and set at 10 hits. The “generate formulas” menu has 4 sections. The settings here affect the type of empirical formulas that are generated. For the “allowed species” section, “charge carrier to be assumed if not known” was “H” for both positive and negative ions. However, this did not take effect since the features were determined by the “Molecular feature algorithm” and by the “Find by formula” (at the Mass Hunter Qual level) do not use the charge carrier specified here. The “MS ion electron state” selection was “even electron” to filter out formulas containing odd number of nitrogen atoms. The “elements and limits” were set to: C; H; O; N; S and Cl. The “minimum” atoms for C was 3, all the other elements had no minimum. The maximum were: 60; 120; 30; 30; 5 and 3 respectively. An alternative way was set to the first 4 elements and excluding the rest.

For the “limits” section, the “maximum neutral mass for which formulas should be calculated” was set to 950. This was set according to the 4GHZ dynamic range for the setting of the QTOF section to cover all the maximum neutral mass detected as to avoid unsuccessful formula generation. The “limits on results” was ticked to a minimum overall score of 50. Most reasonable formula generation scores would be 80 or higher.

The “charge state” section was left with a “peak spacing tolerance” for matching of 0.0025 m/z, plus 7 ppm. This would be the m/z amount to use in deciding how closely the spacing of measured peaks must come to the theoretical spacing to be considered a match. The “isotope model” was set to “common organic molecules”. In “charge state” the “limit assigned charge states to a maximum of” 1, which it is to be expected in small molecules.

The “scoring” section was set up in the same way as in the one located in the “search database” menu. The results of the potential identifications were collected in an Office Excel spreadsheet to serve as starting point and as a reference start point for the Tandem MS confirmation.

Tandem MS identification

The use of MS/MS was chosen to aid in the identification of the candidate compounds. This technique was employed using the same LC-MS QTOF equipment. After stablishing the best settings for the tandem MS/MS, a set of samples from the previous experiments were analyzed to obtain a fragmentation spectrum of each of the candidate compounds. These spectra used as fragmentation ions and abundances, were compared to the ones found in online libraries and literature. The tandem MS analysis was perform in two ways: as a Targeted MS/MS, were the candidate compounds were strictly used as targets on a list to be found. The advantage in this

modality was that the mass accuracy and retention time are more precise since the software has a guide to look for.

The other mode was the Auto MS/MS. The ion selection is based on the abundance of the fragments mostly. It was also possible to use with a target list to give it a preference over the rest of the ions. It is less accurate in terms of mass and retention time, but can perform a wider scan of masses. The final settings for the acquisition MS/MS at the QTOF level were chosen to yield the highest number of found targets.

The general settings for the MS/MS section at the acquisition level were mostly the same for the MS1 method previously described. However, the particular MS/MS settings were as follow: Targeted MS/MS method. Absolute threshold was set to 5 and relative threshold % was set to 0.01. The acquisition was set to targeted MS/MS option; acquisition rate/time for the MS section was set at 8 spectra/s; acquisition rate for the MS/MS section was set to 4 spectra/s. Time between MS1 spectra was set to 5s.

Collision energies (CE) were fixed to three. These were: 10, 20 and 35 or 40 Volts. The use of one or another energy profile depended on the fragmentation patterns.

The targeted list was selected depending on the particular list that resulted from previous analysis. In all cases the delta retention time was set to 0.2 minutes.

Auto MS/MS settings were similar to the targeted MS/MS method, with some differences: the absolute threshold was set to 600 counts with a relative threshold% of 0.01. The acquisition was set to Auto MS/MS option; Acquisition rate/time for the MS section was set at 4 spectra/s; acquisition rate for the MS/MS section was set to 2 spectra/s. The isolation width was set to medium (4m/z).

The “sort precursor by abundance only” was selected. The “isotope model” was set to common organic molecules. The “scan speed based on precursor abundance option” was selected. The acquired data files were analyzed in the MH Qual Software. Importing the files was performed as the same form as previously described. At the left column or “Data navigator” under “Find by compounds”, the option “find by auto MS/MS” or “find by targeted MS/MS” were used depending on the type of file to be analyzed.

Settings for “Find by Auto MS/MS were as follows: at the “processing” tab, “retention time window” was set at 0.25 min. “Positive MS/MS TIC threshold” set was 600. The rest of options were left as default. At the “Excluded masses” tab, the option for “exclude masses (or m/z ranges) from all new chromatograms” was selected and the values “121.0504, 922.0097” were typed (internal mass standards). The “single m/z expansion for this chromatogram” was set to the minimum of +/-10 ppm. At the “Results” tab was kept as default except for selecting the “Extract EIC”, “Extract MS”, “Extract MS/MS” and “extract separate MS/MS spectrum for all collision energy”.

The settings for the “find by Targeted MS/MS option were: at the “integrator” tab, the “integrator selection” was set to Agilent. The “processing” tab was set by unchecking the “limit to the largest compounds”, this meant that there was no limit for the targets to be found. For the “cpd TIC peak filters”, the “peak height” filter was selected. The “absolute height” was set at 600 counts. The rest of the options for that tab were unselected. At the “peak spectrum” tab, the “average scans” were set to 10% of peak height. The “TOF spectra” category was selected to “in the m/z ranges used in the chromatogram”, as well as “never return an empty spectrum”. The rest of the options were left as default. For the “Results” tab, the “Extract separate MS/MS spectrum per collision energy” was selected. The rest of the options were left as default.

After pressing the Run button for the "find compounds by auto MS/MS" or "find compounds by targeted MS/MS" to obtain the compounds from the selected files, it was necessary to highlight the compound results column and click the right mouse button. This will bring the "generate formulas from compound" option. By selecting this option it was possible to obtain the original spectrum and related fragmentation spectra of any particular compound. By clicking the right mouse button again, the option "search database for compounds" was selected. At this instance, a potential candidate name for the compound was sometimes available only if the Agilent Database had it.

Using online tools for metabolite identification

The fragments that compose each of the compounds spectra, consisting of m/z and abundances, were used as raw data input for online in silico identification. Results were then collected and documented in the same excel file. The process was as follows:

As described in the previous section, after obtaining the spectra of a particular mass at the MH Qualitative software, its product ion list was selected by choosing one spectrum at the compound MS spectrum results window. The option to activate the window was located underneath the bar menu. The CE spectrum selection (1 out of 4 CE), was the one that had a lower MS/MS precursor ion abundance percentage compared to the original MS precursor ion. Abundance below 20 but more than 5% was preferred, however this was not always possible to obtain. Therefore, the next criterion was to select the CE that had product ions that could not be encountered in the original acquisition spectrum but repeated the pattern in the rest of the CE spectra. This paired with a good abundance of the product ions determined the best choice to use for a particular compound.

After deciding the appropriate spectrum to look at, it was necessary to activate the "MS spectrum peak list 1" option located under the general top menu bar. To look at the pre-selected spectrum product ions m/z and abundances it was necessary to de-select the rest of the CE spectral options. This was achieved by going to the "Data navigator" column at the left of the screen and un-checking the ones not interested in. After that action, the product ion list refreshed updating it automatically. Product ions m/z and abundances were selected in each case avoiding the inclusion of ions above the base peak m/z for a particular compound.

The list of product ions was formatted for columns using an excel spreadsheet. The formatting depended on the destination data base search engine. A number of three *in silico* fragmentation computer assisted identification libraries were used. These were: Metfrag; Metlin MS/MS spectrum match and Mass Bank metabolite prediction. They were selected because they have the option to compare the query to its database resulting in a score and number of matching peaks. They also have links to sites like Pubchem, Chemspider and KEGG, which are all well-known compound databases.The parameters to be adjusted in each are as follow:

Metfrag: Parent ion was used according to the m/z of result as [M+H]+; precursor tolerance ppm was set at 5; the molecular formula used same as Targeted MS/MS output; biological compounds option was used; number of structures in the output was limited to 100. The rest was left to default. The results were collected as a score, number of matching spectrum peaks, potential structure and name of compound.

Metlin: A maximum of 30 product ion peaks out of the total could be selected. The selection was based on abundance but included the base peak for the compound in question. Positive mode was always selected; collision energy was set accordingly to the spectrum that was selected; tolerance precursor (ppm) was set to 5. Everything else was left as default.

The results were collected as a score, number of matching spectrum peaks, potential structure and name of compound.

Massbank: Precursor m/z was set; positive mode selected always, Cutoff set at 0; tolerance at 0.005. The results were collected as a number of matching spectrum peaks, potential structure and name of compound.

APENDIX C. FRAGMENTATION RESULTS

Mass	m/z	Ret. Time'	CE volts
226.1679	*227.17354*	*3.0548627*	*10*

m/z	Abund	m/z	Abund	m/z	Abund	m/z	Abund
72.0803	139.43	226.1031	14	141.5224	4.81	209.1082	2.33
70.0655	122.25	227.0735	13.57	86.2628	4.78	70.0885	2.31
116.0704	110.55	211.1508	13.54	55.0685	4.51	70.1018	2.28
93.069	100.58	193.1581	12.75	163.0055	4.31	86.3029	2.28
226.096	83.34	70.0762	12.16	152.1027	4.3	68.075	2.27
113.0343	58.52	210.158	11.3	127.0443	4.01	108.0841	2.25
86.0972	54.13	100.3385	11.15	212.1835	3.92	152.1145	2.06
210.1467	51.13	72.0981	11.06	100.0959	3.76	93.1133	2.01
100.0765	48.29	116.0909	10.67	57.0332	3.69	107.0651	2.01
111.0821	42.47	70.083	10.53	72.1065	3.56	100.3465	2
107.0497	40.73	86.2963	10.03	74.561	3.5	70.1086	1.83
68.0506	40.28	145.0643	9.85	114.1209	3.5	94.4282	1.79
227.1737	39.86	139.5592	9.75	163.1343	3.45	145.0867	1.77
152.0789	37.13	152.0897	9.64	86.1149	3.27	93.1265	1.76
193.141	36.49	93.0864	9.53	192.5156	3.27	113.0655	1.76
95.0846	34.23	127.0346	9.28	58.0706	3.25	226.9757	1.69
209.0757	33.94	129.0517	8.83	145.0785	3.25	140.09	1.56
72.0866	31.13	226.1256	8.39	227.2025	3.02	86.6487	1.53
116.0801	28.65	86.1051	8.25	70.1148	3.01	108.101	1.53
212.1649	26.36	95.0962	8.25	100.1031	3.01	145.7109	1.52
140.0678	26.01	79.0243	8.17	108.0763	3.01	93.1038	1.51
108.0512	25.31	103.0609	8.17	97.0798	3	163.0227	1.51
163.1139	24.86	212.1754	8.13	139.5728	3	227.2112	1.51
103.0548	23.39	227.156	7.99	68.0678	2.76	193.1859	1.5
227.1047	21.48	210.1734	6.82	70.0945	2.75	113.0979	1.41
114.101	21.35	227.1825	6.06	86.2695	2.56	163.1576	1.31
156.8858	19.5	193.1685	6.03	226.2972	2.56	210.1925	1.28
55.0564	19.34	200.0568	5.55	66.9746	2.54	116.098	1.27
97.0632	19.2	111.1026	4.97	100.1177	2.47		
113.0435	16	93.0955	4.88	227.522	2.36		

Figure C1. Fragmentation of mass 226.1679 Da.

Mass	m/z	Ret. Time'	CE volts				
234.1367	235.1436	2.467515	10				
m/z	Abun	m/z	Abund	m/z	Abund	m/z	Abund
147.0438	13743.11	91.054	90.56	89.0984	32.05	115.1062	18.17
235.1438	6269.56	219.1332	87.75	127.0551	30.18	145.0745	18.01
89.1075	3292.77	189.0549	79.13	237.1508	29.78	73.0941	17.89
218.1173	2692.85	58.9607	72.81	235.4064	28.4	89.1637	17.53
72.0812	1723.72	89.1349	70.26	89.1422	28.22	147.2014	17.46
147.0547	1582.37	148.0714	69.4	236.1026	27.3	147.7271	17.44
148.0473	1138.39	195.9125	67.99	90.1039	26.91	235.4492	17.01
236.1471	809.95	73.0852	67.86	87.0974	26.44	147.1037	16.9
147.0671	677.67	147.1137	67.64	193.9477	26.4	147.0332	16.81
219.1208	444.01	236.1753	58.48	98.0694	26.39	90.1298	16.37
119.0491	427.9	119.0588	53.59	147.3801	25.88	147.4311	16.33
235.1578	392.87	120.0556	53.38	147.2115	24.24	218.8992	15.87
235.1725	363.1	235.2115	52.14	80.7667	23.88	91.0602	15.84
115.0858	359.92	133.0658	51.54	115.054	23.81	163.0398	15.75
89.1159	327.08	145.0649	48.57	147.4136	23.44	147.3531	15.71
218.1301	285.52	65.0379	46.69	235.2324	22.64	194.9327	15.66
89.1254	221.86	236.1275	45.61	234.1157	21.06	205.1036	15.57
72.0883	191.4	218.1584	45.2	119.0712	21.02	148.1038	15.56
90.1109	178.52	84.9589	44.94	192.9396	21.02	235.6363	15.34
147.0782	173.3	115.0965	42.91	147.4853	21.01	147.5182	15.3
148.0588	170.33	90.1199	41.48	91.1089	20.68	118.9813	15.28
235.1255	155.13	152.948	41.21	149.0477	20.6	318.4717	15.16
99.9868	144.94	116.0907	39.48	235.8728	19.82	235.1112	15.14
218.1454	143.88	70.0647	38.79	236.1943	19.09	219.1477	15.12
98.0594	130	120.0463	37.14	164.0711	18.91	72.118	15.07
72.0977	108.93	218.1022	36.87	193.9857	18.91	89.0601	14.96
193.9727	101.62	161.0599	34.4	122.0597	18.79	236.2952	14.89
147.096	99.6	114.0922	33.31	147.1879	18.59	104.0631	14.82
236.1582	95.9	104.0544	32.92	88.0774	18.57	147.5363	14.74
235.1884	93.13	72.1075	32.61	158.5244	18.56	218.1838	14.69

Figure C2. Fragmentation of mass 234.1367 Da.

Mass	m/z	Ret. Time	CE volts
234.1363	*235.1422*	*3.127965*	*10*

m/z	Abund	m/z	Abund	m/z	Abund	m/z	Abund
147.0441	80911.44	219.1334	209.39	147.5291	57.88	147.4245	40.16
235.1441	35468.86	149.0493	208.93	72.1317	57.05	203.9894	39.61
89.1077	20669.46	218.099	196.42	147.3916	54.43	148.002	39.4
218.1175	13877.7	99.9879	187.22	147.4149	54.32	147.4739	39.35
72.0812	11073.06	120.0512	154.49	147.5474	53.2	149.0639	38.86
147.0551	6362.17	152.9461	147.78	147.443	52.27	147.5171	38.55
148.0474	6290.9	218.159	147.43	89.0949	51.71	140.1013	38.52
147.0673	4026.88	119.0703	143.67	219.1012	51.41	147.5008	38.47
119.0495	2430.45	91.0633	129.97	147.8558	51.13	58.9616	38.13
115.0865	1995.19	89.1494	126.76	147.6933	50.77	117.9352	38.05
89.1161	1968.81	115.1069	124.1	147.0209	50.75	98.0795	37.98
219.1211	1871.49	89.1636	120.11	115.1164	50.57	147.872	37.7
89.1258	1364.82	176.1069	118.33	218.2043	49.15	218.6464	37.69
72.089	1322.26	147.4581	114.16	147.5615	47.11	90.1274	37.31
91.0545	984.13	116.0891	105.76	164.0873	46.4	226.1171	36.62
90.1108	819.64	98.0692	96.74	218.7933	46.05	220.1247	36.21
218.1452	776.4	72.1178	96.25	147.3283	45.46	193.9719	34.7
72.0976	703.02	219.149	95.12	151.9221	44.64	147.5781	34.35
98.0603	579.36	218.1835	93.94	147.7931	43.76	148.1672	33.9
218.1315	480.63	235.0999	84.36	147.6596	43.71	235.0371	33.82
89.1342	431.3	195.9129	83.2	119.0798	43.52	147.7775	33.79
148.0707	430.46	90.1208	80.59	148.2504	43.31	102.9497	32.8
73.0847	380.82	70.0662	76.02	147.5953	43.15	114.0827	32.56
164.0711	364.13	147.3652	74.17	147.4905	42.92	147.3476	32.56
119.0593	331.95	55.0555	72.25	147.6083	42.68	147.7658	32.46
148.0592	320.79	148.0824	71.89	146.6953	42.39	89.2877	32.38
115.0954	310.56	147.4831	71.09	147.4022	41.28	89.3825	32.33
114.0924	265.8	149.0403	70.59	175.6348	41.26	114.1015	32.15
65.0387	257.38	91.0726	69.09	147.3126	40.94	148.508	32.07
72.1054	219	235.1133	67.69	193.9833	40.74	148.0175	31.56

Figure C3. Fragmentation of mass 234.1363 Da.

Mass	m/z	Ret. Time'	CE volts				
248.1521	*249.1587*	*4.01088*	*20*				
m/z	Abund	m/z	Abund	m/z	Abund	m/z	Abund
147.044	25082.92	141.0332	59.56	148.0819	35.2	103.476	24.04
119.0492	3369.46	147.0973	59.18	91.0721	34.15	129.0502	23.34
86.0969	2506.8	130.1077	56.38	147.3127	34.13	68.0468	23.33
147.0546	2299.95	70.0712	55.68	147.8051	33.4	91.4716	23.04
148.0474	1993.04	91.0251	55.3	148.3105	33.29	147.3987	23.04
147.0673	1593.54	148.0364	53.8	146.9902	33.1	148.0207	22.75
103.1233	1184.54	147.0016	53.33	103.0536	33.03	147.4819	22.72
91.0548	912.42	147.3021	51.91	147.2434	32.8	92.0577	22.67
147.0785	474.44	147.3466	50.73	191.0808	32.13	73.9358	22.12
120.0527	238.77	84.0822	50.39	61.0108	32.11	148.1	22.12
119.0613	237.14	69.0333	48.04	174.0518	30.48	147.3605	22.03
86.115	186.77	219.0747	47.07	86.1382	29.55	69.0389	21.37
119.0703	172.24	104.1269	46.12	91.0367	29.32	71.0564	21.26
70.0653	156.29	122.0602	45.76	115.9555	29.25	119.088	20.74
148.0585	144.82	147.4679	45.73	147.4077	29.11	147.5666	20.58
147.1155	130.2	146.8385	45.3	128.9479	28.48	207.1473	20.35
69.0696	126.21	120.0645	45.13	232.133	27.8	147.7801	20.33
148.0704	109.4	71.05	44.46	119.0805	27.68	147.5807	20.3
103.1352	105.35	150.0796	44.01	149.0509	27.46	147.8664	20.21
88.0762	104.26	147.2215	43.92	147.2353	27.4	119.0977	20.19
86.1064	92.62	69.0769	43.8	220.0808	27	147.2718	20.13
91.065	89.77	65.0387	43.79	147.3301	26.46	233.1355	20.06
87.0992	84.91	147.6569	43.52	147.4137	26.24	147.7148	19.74
118.0427	79	230.1294	42.04	65.0449	26.12	160.9652	19.67
98.9727	77.92	147.3691	41.56	149.5807	25.86	147.128	19.64
249.1578	74.51	147.5364	39.11	91.6087	25.56	115.9637	19.6
147.0252	66.4	147.2556	38.95	237.0922	25.02	232.1469	19.13
112.0755	64.4	129.1029	38.39	119.3567	24.89	148.1888	19.05
103.1438	62.89	86.1257	38.08	147.0107	24.57	247.0724	19.01
75.0233	62.2	147.6196	35.31	145.0261	24.19	147.15	18.5

Figure C4. Fragmentation of mass 248.1521 Da.

Mass	m/z	Ret. Time'	CE volts				
250.1314	*251.1401*	*1.847577*	*10*				
m/z	Abund	m/z	Abund	m/z	Abund	m/z	Abund
147.0442	14681.5	149.0493	103.94	147.2688	27.09	147.1937	18.11
251.1393	5766.38	235.1177	102.86	88.1016	26.66	115.0554	17.93
105.1026	4834.73	147.114	97.55	147.5316	26.56	147.3204	17.61
233.1287	3344.27	164.0707	86.71	242.0979	25.72	147.4706	17.56
88.0762	2008.47	148.0715	86.58	88.061	24.79	111.1119	17.52
147.0546	1724.92	105.1308	78.17	58.0652	24.75	205.0651	17.43
148.0477	1494.29	119.0602	76.74	121.0653	23.33	147.6717	17.42
204.1016	1253.78	216.1023	73.07	107.1069	22.5	105.1383	17.38
70.0657	1015.64	234.149	67.54	147.4573	22.44	91.0732	16.01
147.0674	826.03	204.1332	66.39	204.0541	22.36	147.7099	15.91
105.1119	626.91	129.102	63.31	147.4288	22.21	88.1311	15.61
234.1126	597.19	70.0822	63.2	250.0924	21.66	147.3723	15.59
234.1329	560.77	114.0544	60.11	193.0859	21.38	147.549	15.45
119.049	425.78	233.1009	59.36	147.789	21.26	147.3283	15.37
105.1223	323.27	147.0273	57.37	210.0071	21.22	136.9309	15.25
233.1427	284.66	251.1121	54.6	233.1809	21.12	148.0378	15.12
87.092	275.81	89.0801	45.69	70.0892	21.11	147.4441	14.95
91.0548	228.19	233.1704	43.38	147.3127	20.96	217.0952	14.92
204.1148	193.85	147.0159	41.67	233.2015	20.63	233.4555	14.8
106.1055	190.07	148.0841	40.92	147.3044	20.6	73.031	14.69
147.0782	171.64	91.0624	39.67	148.1004	20.36	149.0629	14.67
205.107	154.65	105.147	34.84	121.0285	19.84	87.0988	14.17
88.0864	139.62	234.1633	31.74	129.3649	19.83	109.0648	13.89
233.1575	135.67	106.1149	31.24	105.9324	18.99	105.3918	13.63
131.082	133.88	147.5837	30.72	163.0387	18.88	164.0832	13.54
148.0598	131.49	119.0711	30.71	147.3401	18.4	234.0838	13.54
88.094	126.45	147.4912	30.36	174.0871	18.29	87.111	13.45
147.0971	108.64	71.0624	30.29	233.0526	18.2	120.0539	13.39
65.039	105.59	87.1032	29.14	131.0949	18.18	147.4026	13.37
70.0735	105.04	235.1067	27.99	105.0933	18.17	106.1242	13.17

Figure C5. Fragmentation of mass 250.1314 Da.

Mass	m/z	Ret. Time'	CE volts				
251.1393	*250.1317*	*1.889441*	*10*				
m/z	Abund	m/z	Abund	m/z	Abund	m/z	Abund
147.0438	2812.65	205.0937	19.56	164.0731	8.46	148.159	5.56
251.139	1109.91	129.1023	19.31	234.159	8.45	148.0814	5.42
105.1022	988.43	85.0282	19.24	59.0689	8.35	189.0529	5.36
233.1284	517.68	251.1088	18.35	74.9347	8.33	233.175	5.32
88.0758	314.67	145.0028	17.63	147.0321	8.29	105.1459	5.27
147.0547	307.39	119.0587	17.51	174.0948	8.27	84.9598	5.25
204.1015	305.83	105.1315	17.34	89.024	7.89	193.9746	5.25
70.0654	215.17	204.1152	17.31	206.119	7.86	211.3258	5.22
148.047	200.51	187.0238	16.77	119.0695	7.84	205.4176	5.18
105.1116	134.17	204.1276	16.03	105.5989	7.77	233.8675	4.99
234.1291	131.23	147.0986	15.68	151.0802	7.56	215.0212	4.92
147.067	130.75	148.0724	15.38	130.0862	7.14	131.0797	4.91
119.0489	92.62	219.4884	15.08	98.059	7.13	208.9396	4.89
234.1127	82.47	88.0948	15.02	204.1446	6.99	105.1537	4.83
205.1039	64.79	169.9749	14.17	97.991	6.85	147.8684	4.81
105.1222	60.33	147.7517	14.03	190.9327	6.6	251.094	4.79
88.0852	56.4	216.1029	13.91	147.0894	6.55	147.6556	4.68
233.1429	42.1	201.0616	13.78	235.1176	6.47	92.0561	4.62
157.0074	35.06	215.0087	12.41	147.2671	6.38	105.4515	4.6
148.0573	34.38	235.1302	12.13	210.9533	6.26	205.123	4.49
147.0787	33.42	70.0822	11.88	105.3262	6.21	140.0164	4.48
70.0721	33.16	164.0636	11.56	147.9436	6.17	72.0803	4.46
87.0918	30.89	155.0315	11.06	148.1831	6.15	129.1109	4.44
234.1429	29.79	91.0551	10.39	250.1778	6.15	216.9404	4.3
106.1053	29.72	251.1202	10.31	147.3481	6.05	89.0893	4.23
177.0591	28.11	233.8524	10.14	205.136	6.05	187.0392	4.15
233.1585	26.9	147.2588	10.1	147.3662	5.93	148.4837	4.13
89.0794	25.61	211.954	9.8	105.3173	5.84	105.1377	4.12
209.4199	24.34	147.1118	9.66	169.0069	5.75	216.1146	4.04
251.0869	20.37	87.1038	8.9	205.0147	5.63	114.0555	4.02

Figure C6. Fragmentation of mass 251.1393 Da.

Mass	m/z	Ret. Time'	CE volts				
250.1314	*251.1403*	*2.648122*	*10*				
m/z	Abund	m/z	Abund	m/z	Abund	m/z	Abund
147.0444	74267.05	89.0794	322.76	233.2177	77.51	147.6132	41.45
251.1395	27632.28	204.1293	315.49	147.3614	76.83	147.6008	41.18
105.1027	25591.12	119.0602	286.48	148.1014	67.03	132.0866	40.74
233.1288	16933.34	114.055	270.65	205.1187	66.85	205.1298	39.92
88.0763	10039.54	148.0717	265.1	131.0935	61.63	147.4558	39.79
147.0549	8128.72	216.1025	260.27	147.0244	60.42	148.1208	39.39
148.0478	5723.44	58.0659	223.56	164.0827	59.86	204.1678	38.36
204.1021	5276.18	88.1027	208.73	233.1075	59.39	147.589	37.87
70.0658	5239.59	87.1012	186.2	147.3375	58.56	147.6885	37.73
147.0676	5046.44	119.0705	186.17	92.0587	58.44	147.5212	37.57
105.1117	2816.51	149.0502	174.86	233.0803	57.53	112.0769	37.56
119.0497	2689.94	234.157	164.25	88.1317	56.98	204.0844	36.41
234.1125	2612.02	65.0396	146.38	147.6472	55.93	105.0886	36.38
234.1317	2271.51	204.1157	140.55	217.1039	54.28	147.3741	36.16
233.1426	1785.21	233.1965	138.69	147.3123	53.83	233.3776	35.48
105.1226	1735.5	235.1325	137.39	147.4101	53.52	147.706	35.36
87.0922	1474.18	120.0521	134.7	234.1803	53.2	233.3276	34.89
88.0845	1266.09	70.0895	117.11	234.0976	51.74	235.0926	34.6
106.1059	1083.28	106.1159	115.26	106.0982	51.33	131.1038	34.5
233.1572	910.01	233.1717	109.96	147.4223	48.91	234.202	34.43
88.0946	691.52	148.0836	106.67	147.3878	47.98	119.0801	34.42
91.0549	678.14	87.1104	105.13	147.0025	47.65	114.0655	33.86
131.0822	643.86	71.0687	104.19	233.4087	46.65	147.546	33.5
148.0587	589.75	105.1635	103.46	147.0111	46.16	233.4413	32.94
105.1313	535.86	204.1423	99.16	147.5115	45.72	251.0694	32.74
205.1057	522.68	251.1035	95.17	147.6623	45.31	147.4343	32.63
70.0727	499.77	105.1476	93.79	70.1025	43.47	120.0611	32.43
164.0706	413.93	91.0645	85.07	89.089	42.45	147.5685	31.94
235.1164	371	88.1175	81.31	129.1024	42.17	233.4255	31.91
70.0821	337.54	106.1263	79.4	91.0733	41.9	233.0947	31.74

Figure C7. Fragmentation of mass 250.1314 Da.

Mass	m/z	Ret. Time'	CE volts
264.147	*265.1556*	*3.870367*	*10*

m/z	Abund	m/z	Abund	m/z	Abund	m/z	Abund
177.0545	5128.43	89.0386	22.59	178.4892	13.22	91.061	9.16
265.155	1972.6	265.022	21.86	194.5044	12.43	90.1112	8.9
89.1078	566.61	217.1228	21.86	177.4286	12.26	177.7379	8.87
178.0576	420.1	177.6011	21.74	116.0988	12.17	178.112	8.85
145.0283	402.39	70.0646	21.29	120.0736	12.06	180.0831	8.47
248.1286	356.38	201.1282	20.85	150.0626	12.05	117.0558	8.46
72.0815	309.47	151.0858	20.51	177.3509	12.04	147.1242	8.43
177.0798	289.33	224.9949	19.81	174.9429	11.81	245.0291	8.15
177.0677	247.14	114.0935	19.38	115.107	11.54	145.631	8.13
115.0872	179.35	178.0447	19.05	189.0553	11.07	177.2594	8.09
89.1163	99.22	177.4399	18.87	265.0394	11.04	177.6109	8.06
177.093	84.12	229.1216	18.58	178.4251	10.95	177.5652	8.06
145.0401	70.88	177.322	18.55	177.4925	10.92	145.1025	8
265.1356	70.56	264.0925	17.86	255.1324	10.76	187.1166	7.97
120.0816	67.33	177.0308	17.85	175.0845	10.75	117.0445	7.81
249.1324	60.73	145.0523	17.63	177.3885	10.5	265.1065	7.75
117.0335	60.65	175.072	17.61	145.0634	10.29	177.6752	7.75
177.0421	53.59	95.0849	17.47	60.0458	10.27	55.0162	7.62
248.1439	46.7	177.405	16.54	177.3768	10.17	174.7334	7.58
178.0704	45.52	248.1584	16.02	72.0982	10.09	161.0625	7.57
89.1267	41.95	177.3649	15.63	146.0314	10.03	177.6845	7.49
72.0919	36.86	115.0999	15.6	177.2396	9.87	177.9758	7.48
116.0915	33.58	248.1128	15.39	177.6373	9.86	177.8121	7.45
178.0829	33.13	115.0601	15.12	249.1455	9.67	248.4186	7.31
177.1106	31.36	177.2889	14.87	153.0529	9.63	188.1104	7.31
177.1259	30.02	172.0886	14.65	217.1327	9.61	248.3011	7.22
98.0614	28.76	115.0934	14.59	177.6616	9.59	172.1017	7.17
149.059	25.63	158.9993	14.3	72.2155	9.25	178.816	6.94
63.0242	24.6	134.0373	14.23	177.7609	9.22	177.2525	6.72
91.0539	23.78	122.0739	13.54	175.3584	9.22	135.9504	6.48

Figure C8. Fragmentation of mass 264.147 Da.

Mass	m/z	Ret. Time'	CE volts				
272.1276	*273.1335*	*3.531639*	*Ave*				
m/z	Abund	m/z	Abund	m/z	Abund	m/z	Abund
273.1348	1421.95	69.058	40	127.2324	16.19	105.0705	9.1
127.0981	1261.09	255.1417	39.56	148.0565	15.41	110.3317	8.86
147.0445	1112.72	153.0567	39.16	273.0919	15.35	214.1287	8.75
255.1248	550.23	98.0688	37.65	91.0741	14.92	272.1145	8.7
91.0549	337.5	256.109	37.63	148.0689	14.81	207.9797	8.58
119.0494	315.2	214.0863	36.8	147.5294	14.5	69.1429	8.07
213.1031	283.68	85.0722	34.36	121.0397	14.49	191.3148	7.94
69.0451	196.09	78.0412	33.91	56.0498	14.06	127.2657	7.7
147.0571	174.46	85.0759	32.52	194.1569	14.03	134.0466	7.7
110.0716	171.89	215.088	29.78	65.0382	13.13	68.0673	7.34
127.1083	159.28	72.0823	26.57	85.0825	13.07	93.0482	7.34
148.0471	158.28	125.0839	26.55	147.7122	12.96	111.0764	7.32
256.1279	126.94	110.0817	26.29	256.1565	12.89	112.0758	7.21
126.0906	103.31	138.9678	24.98	164.072	12.03	91.088	7
68.0503	81.52	126.1027	24.91	190.0097	12	255.5503	6.83
127.1198	79.44	111.0628	24.47	215.1006	11.75	60.3933	6.81
214.0998	69.94	256.1389	24.1	213.1493	11.67	110.0986	6.65
147.068	69.57	83.0657	23.53	98.0773	11.3	148.5339	6.64
119.0587	65.85	69.0345	23.41	139.2732	11.22	112.082	6.57
153.0769	64.75	127.1303	20.83	153.0884	11.02	147.1161	6.56
111.0552	59.63	161.0817	19.98	83.0725	10.79	126.1121	6.36
55.0187	58.92	153.0652	19.2	147.382	10.55	147.492	6.36
213.1183	58.34	119.0695	19.02	78.0508	10.47	194.1692	6.29
231.1098	57.99	128.1026	18.75	256.3921	10.35	119.2363	6.12
273.1162	52.27	273.0736	18.51	69.0525	9.92	126.2436	5.81
188.1062	47.64	120.0614	18.39	106.0507	9.63	147.0283	5.78
120.0524	47.08	147.0852	17.34	223.9443	9.53	255.1931	5.77
91.0642	45.53	60.1354	17.31	72.0907	9.41	147.6547	5.7
83.0602	42.11	213.1309	17.26	119.0855	9.4	110.0926	5.5
255.1564	40.98	136.0712	16.9	186.0948	9.35	111.0691	5.47

Figure C9. Fragmentation of mass 272.1276 Da.

mass	Prec. m/z	Ret. Time'	CE volts				
275.1517	*276.1571*	*6.006978*	*Ave*				
m/z	Abund	m/z	Abund	m/z	Abund	m/z	Abund
276.1582	937.56	179.0849	67.23	157.1189	34.27	159.0447	19.66
70.0654	786.96	171.0431	60.49	127.0978	33.72	126.0902	19.25
72.0808	587.26	98.0694	60.01	239.1283	33.38	218.0701	19.09
131.1288	569.1	219.0794	57.45	56.0575	32.73	97.0827	18.92
147.0438	456.48	191.0845	54.86	217.1328	31.51	257.1533	18.83
98.0602	398.47	70.0817	53.11	55.0292	31.29	235.0915	18.74
114.1028	388.87	114.1122	52.59	114.1227	31.16	172.0482	18.72
55.0544	349.55	55.0179	52.51	176.1066	30.25	220.0822	18.55
265.085	270.85	264.0746	51.76	263.086	29.59	206.0734	18.55
60.056	264.84	266.0889	49.73	120.0549	29.28	132.1249	17.92
157.1078	248.9	147.0558	49.5	115.0958	27.74	112.1079	17.87
112.0867	248.14	265.1015	48.06	115.1058	27.44	119.0582	17.47
263.0687	218.03	190.0769	46.15	152.9467	27.03	255.1465	17.36
235.075	159.8	55.0621	45.21	197.0995	25.36	181.0632	17.26
119.0491	155.58	211.0974	43.88	265.0705	25.35	60.0649	16.72
246.6345	107.85	115.0542	43.55	148.0475	25.26	219.0927	16.32
247.0746	102.46	143.0489	43.15	223.0753	23.75	165.0691	16.23
275.1502	101.3	267.6452	42.48	268.1482	23.57	158.111	15.94
115.0867	98.72	112.097	42.35	194.0725	23.35	166.0731	15.68
257.1385	97.88	91.0542	42.02	264.0975	22.55	73.0843	15.37
70.0734	97.71	201.069	41.35	131.1509	22.2	69.0332	15.34
131.0486	92.42	218.1168	40.48	121.0266	22.2	193.0653	14.84
131.1409	80.12	103.0545	39.11	144.0551	22.03	235.1441	14.59
72.0886	79.88	98.0789	38.75	208.0836	21.93	258.1406	14.42
189.069	79.31	193.9721	38.69	247.0898	21.76	87.0791	14.34
207.0807	78.29	71.0691	38.33	260.1381	21.72	268.6505	14.32
97.0756	76.43	72.0976	38	131.061	21.44	157.1329	14.26
58.9608	76.35	237.0896	36.97	107.0489	21.06	265.1168	14.17
99.9871	72.56	247.1355	35.4	55.0691	20.81	60.0713	13.97
178.077	69.76	147.0659	35.33	236.0789	19.77	275.1765	13.63

Figure C10. Fragmentation of mass 275.1517 Da.

mass	Prec. m/z	Ret. Time'	CE volts
276.158	*550.3016*	*6.039715*	*20*

m/z	Abund	m/z	Abund	m/z	Abund	m/z	Abund
131.129	382.62	263.0776	30.89	190.0754	15.09	110.07	8.89
114.1024	267.4	247.1319	29.22	247.0924	14.89	198.1081	8.8
265.0853	219.64	265.1077	28.99	72.0758	14.81	216.9347	8.6
55.0545	200.78	69.0331	28.71	269.7325	14.53	132.1376	8.49
157.1072	188.07	238.0979	28.59	219.0821	14.47	70.2563	8.43
70.0652	181.74	264.0721	26.4	179.0898	14.33	239.1251	8.3
98.0595	178.08	131.1519	24.65	70.0803	14.31	117.069	7.87
263.0696	131.41	157.1241	23.27	147.0574	13.28	132.0666	7.84
72.0817	89.16	88.0209	22.58	69.0392	13.26	146.9552	7.81
60.0564	86.85	246.63	21.27	98.0783	12.89	187.0366	7.67
171.0455	69.64	110.0618	21.21	100.0004	12.85	152.9592	7.65
119.0487	62.4	189.0675	20.79	119.0613	12.8	247.5848	7.6
147.045	58.48	264.1039	20.71	170.0615	12.67	177.8945	7.54
99.9865	58.09	266.083	19.7	276.1568	12.6	184.0782	7.06
131.1423	53.57	115.1047	18.7	72.0874	12.49	230.1571	6.8
247.075	53.56	247.0575	18.41	150.9707	12.43	194.9347	6.76
55.0615	53.07	215.1393	18.14	55.069	12.26	144.0926	6.68
137.0879	52.63	247.3066	18.06	156.0894	12.05	139.9569	6.66
58.9607	51.8	107.0501	18.02	88.0285	12.02	189.0835	6.63
237.0891	45.15	144.0831	17.01	86.9661	11.8	137.1119	6.61
235.078	43.13	197.0991	16.9	114.1237	11.34	58.9675	6.56
176.1061	41.91	158.1111	16.78	98.0684	10.89	237.1145	6.47
97.0752	39.18	236.9794	16.49	236.7653	10.61	170.0696	6.46
100.9927	38.25	230.1441	16.48	159.7253	10.17	247.3174	6.4
152.946	38.13	110.9775	16.16	131.1601	10.12	264.364	6.23
207.0792	36.92	183.1025	16.15	236.9891	9.89	219.0738	6.21
112.0852	33.62	176.1181	16.08	70.819	9.85	266.0927	6.2
240.1053	33.37	263.0937	15.5	194.0021	9.85	99.3382	6.18
114.114	32.96	56.0117	15.35	112.0933	9.64	266.1059	5.93
132.1248	32.11	127.0994	15.23	70.0725	9.54	117.4029	5.82

Figure C11. Fragmentation of mass 276.158 Da.

Mass	Prec. m/z	Ret. Time'	CE volts
276.1591	*277.1669*	*4.459288*	*Ave*

m/z	Abund	m/z	Abund	m/z	Abund	m/z	Abund
147.0441	123754.7	72.0975	844.01	120.0736	159.13	101.0393	71.76
277.1663	71168.28	219.1213	842.72	116.0906	155.79	277.0941	70.98
119.0493	37536.49	55.0548	824.35	132.132	154.82	147.4966	70.79
114.1028	20188.02	92.058	702.41	217.1616	153.99	147.0035	70.56
91.0545	15728.62	98.0605	652.84	115.1166	151.6	73.0781	70.33
72.0812	12027.11	157.1082	631.31	89.1154	150.03	55.0186	69.66
260.1395	9505.31	148.0707	513.06	148.082	135.12	277.116	69.51
148.0475	9086.55	260.1698	489.2	65.0547	125.75	146.0595	69.45
218.1175	5926.92	60.0627	463.82	98.0713	115.92	131.161	69.15
147.0676	5839.6	55.0294	453.56	219.1351	111.45	157.1202	68.95
60.056	4251.76	148.0575	443.44	164.0706	107.48	63.0235	68.72
115.0868	4009.09	73.0843	437.08	236.1473	106.1	107.051	68.58
119.0584	3953.11	131.1392	419.1	97.0948	104.88	206.0919	68.36
217.1338	3922.52	121.0652	408.4	147.43	103.35	147.6918	67.73
131.1292	3755.57	115.0978	389.64	121.0742	94.28	89.1258	66.33
120.0525	2517.31	73.0401	375.53	259.1541	92.91	115.128	64.83
114.1122	2436.76	260.1548	360.27	114.1664	91.55	72.0554	64.29
147.0552	2269.83	114.1323	326.49	118.0643	89.34	147.7086	63.96
97.0762	2177.11	120.0624	325.31	98.0798	81.81	148.0997	63.88
65.039	1805.69	60.071	319.7	147.3962	81.64	55.0368	63.58
119.0704	1741.93	217.1473	315.99	147.4156	81.47	147.7202	63.19
261.1433	1337.37	72.1051	250.24	218.1467	81.12	147.4561	62.07
218.1348	1261.3	131.1508	241.54	58.9608	79.22	56.0573	61.45
114.1232	1242.74	235.1577	239.54	147.6293	78.53	148.2525	61.24
235.1443	1149.6	91.081	229.38	72.1185	76.64	147.6566	60.65
91.063	1093.78	65.0469	218.15	72.1312	76.37	148.0291	59.9
115.1059	1076.55	70.0655	212.83	60.0774	75.59	147.5484	59.68
91.0728	1056.25	97.0861	203.91	93.0705	72.64	147.5389	59.64
72.0888	978.85	261.1571	174.03	147.5232	72.59	119.0802	58.91
89.1075	969.59	77.0394	159.39	147.018	72.43	75.022	57.8

Figure C12. Fragmentation of mass 276.1591 Da.

Mass	Prec. m/z	Ret. Time'	CE volts
290.1742	*291.1807*	*5.019515*	*20*

m/z	Abund	m/z	Abund	m/z	Abund	m/z	Abund
147.0439	3312.34	127.0993	80.18	218.1059	37.59	219.2064	22.69
128.1179	1074.8	88.0744	78.89	65.0452	36	115.0978	22.15
218.1178	800.64	147.1333	77.21	275.1579	35.65	111.0892	21.73
291.1809	631.23	111.0554	76.14	260.1514	34.61	174.1017	21.39
72.0816	390.58	70.0726	70.9	89.1134	34.58	264.0755	21.34
217.1334	338.75	74.067	69.36	265.0956	33.86	91.0628	20.95
291.0648	314.82	128.1397	67.38	218.0877	33.12	291.0855	20.75
115.0864	281.86	218.146	62.38	72.0976	32.49	127.1093	20.67
235.1441	257.22	235.0739	60.88	126.0893	31.48	195.1095	20.49
147.0553	241	263.0718	60.73	204.098	30.86	73.064	20.34
129.1139	235.12	194.126	52.82	218.3538	30.26	147.8914	20.22
148.047	229.47	219.1202	52.36	145.0614	29.89	160.0867	20.06
114.1023	202.52	173.1009	51.21	129.1243	29.25	274.1278	19.68
128.1284	200.13	130.0963	50.35	111.0643	29.22	128.1508	19.65
129.102	195.53	217.1506	48.52	60.0546	28.68	291.0987	19.03
147.0676	189.59	119.061	46.75	193.0627	27.96	119.4572	19.01
89.1074	183.21	247.0704	45.72	112.0881	27.65	207.0825	19
70.0654	179.97	69.0454	44.69	96.0441	26.8	217.8745	18.78
218.1345	164.25	217.1242	44.56	115.1125	26.25	236.1457	18.76
119.0474	158.23	93.0698	44.24	147.0829	25.93	70.08	18.52
147.1246	158.04	57.0335	44.01	57.0445	25.71	69.0525	18.36
160.0755	146.23	236.1548	44.01	129.1348	25.7	237.0933	17.71
145.1435	137.06	147.0287	43.23	145.026	24.88	275.1731	17.71
265.0825	108.98	105.0996	43.08	57.0492	24.68	219.6615	17.67
65.0376	108.86	110.0745	42.87	148.0711	24.63	235.1754	17.56
274.157	99.91	147.0759	42.78	274.1739	24.17	145.167	17.54
91.0543	94.03	153.0531	40.71	57.0382	23.47	174.0525	17.36
72.089	93.02	178.0889	40.34	147.3077	23.22	217.1621	17.3
260.1392	91.4	178.9152	40.34	235.1648	23.01	115.1065	17.08
291.1646	82.03	205.1007	39.56	165.0718	22.92	156.0768	16.93

Figure C13. Fragmentation of mass 290.1742 Da.

Mass	Prec. m/z	Ret. Time'	CE volts				
291.1447	*290.1381*	*2.973196*	*10*				
m/z	Abund	m/z	Abund	m/z	Abund	m/z	Abund
273.1353	1560.11	172.076	15.35	71.0603	8.37	250.0811	4.95
255.1233	254.65	273.8661	14.44	291.0337	8.32	60.0612	4.94
147.0437	229.68	224.5084	14.28	266.925	8.18	290.0796	4.93
274.1366	218.19	148.0446	14.27	290.1253	8.17	227.9639	4.86
127.0977	168.53	233.1062	13.93	157.0807	8.03	159.0751	4.72
291.1466	86.63	235.6358	12.81	91.0537	8.01	273.8856	4.63
273.1629	78.52	204.1	12.27	139.0665	7.89	198.0418	4.57
273.1173	58.78	273.1803	12.08	128.1019	7.78	273.944	4.57
256.1289	50.28	247.0307	11.78	273.3934	7.69	273.6393	4.46
274.1637	46.9	143.1188	11.58	140.066	7.57	127.1284	4.36
60.0559	40.45	147.1263	11	273.4797	7.5	273.4983	4.35
110.0721	36.06	214.18	11	248.9285	7.4	260.5035	4.3
235.6253	30.21	273.2133	10.39	273.5675	7.14	273.2987	4.3
147.0569	27.41	120.0659	10.01	273.0674	7.01	255.5913	4.18
130.0972	27.14	147.0701	9.75	143.3475	7	273.688	4.15
175.0619	24.88	120.0796	9.57	256.1505	6.89	235.653	4.13
260.0636	24.6	178.0484	9.57	127.328	6.31	150.0558	4.03
248.9133	24.46	291.0853	9.48	224.5177	6.31	273.2534	4.02
127.11	24.34	127.0702	9.44	273.5489	6.12	255.1397	4.01
214.0851	23.15	127.1197	9.31	232.0946	5.86	247.0475	3.9
153.076	19.47	228.1594	9.2	273.6115	5.74	147.1718	3.86
227.9467	19.46	116.0537	9.15	291.1106	5.73	273.3644	3.83
275.1781	19.31	119.0502	9.06	273.7145	5.71	274.7806	3.74
213.1042	19.05	173.1257	9.02	214.1963	5.48	273.3721	3.72
255.1546	18.09	291.0601	9.02	185.8922	5.31	256.3058	3.68
291.1291	16.54	221.126	8.97	273.731	5.17	228.5963	3.58
151.0377	15.87	290.0413	8.86	173.1368	5.14	273.7939	3.55
116.0905	15.51	126.0925	8.66	189.1273	5.14	226.1194	3.45
173.0427	15.45	274.1163	8.48	147.2841	5.13	228.1761	3.45
256.1099	15.39	172.0846	8.45	255.5605	4.98	237.2192	3.29

Figure C14. Fragmentation of mass 291.1447 Da.

Mass	Prec. m/z	Ret. Time'	CE volts
291.1941	*292.2029*	*1.333834*	*20*

m/z	Abund	m/z	Abund	m/z	Abund	m/z	Abund
204.1018	716.21	85.0292	22.8	101.027	10.2	204.627	5.56
72.0811	642.52	155.1164	22.14	119.0593	9.66	73.0975	5.43
147.0439	548.48	130.9915	22.06	118.1036	9.31	205.5064	5.2
204.1159	122.31	148.0581	21.09	204.5792	9.29	146.1855	5.07
275.1748	108.98	229.1234	21.01	72.341	9.13	110.0743	5.01
205.1109	106.22	292.2017	20.89	83.0137	8.61	72.2628	4.96
147.055	101.89	275.1926	20.8	129.152	8.51	137.0715	4.8
118.0845	76.71	130.0497	20.78	204.9676	8.5	188.0113	4.51
148.0465	72.98	140.0486	20.61	91.0648	8.11	147.295	4.41
112.1116	72.75	146.0618	20.17	220.2034	8.08	101.0355	4.4
129.1396	63.33	175.1213	19.51	204.1638	8.04	152.0443	4.4
130.1411	46.49	102.09	17.75	113.9404	7.93	204.739	4.38
73.0842	45.29	83.0079	17.28	275.1588	7.91	147.4728	4.36
119.0494	45.1	165.057	16.81	152.0353	7.82	73.0912	4.24
221.1304	44.85	206.8985	15.84	174.1239	7.45	131.0602	4.2
203.1186	44.33	203.0206	15.37	204.1906	7.45	129.7187	4.16
72.0875	43.3	116.0697	15.26	129.0382	7.21	147.1111	4.07
72.0914	42.68	87.9614	14.98	276.035	7.01	203.1469	4.03
276.1768	41.95	131.0487	14.67	204.3989	6.91	275.2092	3.98
155.031	40.05	75.0909	14.28	206.9155	6.41	276.2994	3.85
205.1004	39.73	188.0009	13.63	203.1773	6.26	112.1572	3.83
147.0678	37.61	137.0595	13.49	165.066	6.01	206.1094	3.81
118.069	35.47	152.9037	13.43	130.0704	5.89	174.1336	3.8
72.0977	35.31	221.1422	13.43	120.1712	5.83	72.1197	3.67
204.1315	33.89	98.0607	12.47	220.2121	5.82	112.1364	3.66
146.1649	29.96	276.1588	12.4	130.1612	5.8	276.4376	3.64
91.054	27.42	71.0862	12.33	205.1336	5.79	113.0725	3.45
72.1045	24.29	291.0968	11.41	131.0053	5.69	72.3482	3.41
118.092	24.09	147.0797	10.75	204.2193	5.68	202.7148	3.4
111.0181	23.06	203.0021	10.49	204.233	5.66	291.1115	3.4

Figure C15. Fragmentation of mass 291.1941 Da.

Mass	Prec. m/z	Ret. Time'	CE volts
292.1538	*293.1617*	*2.851297*	*20*

m/z	Abund	m/z	Abund	m/z	Abund	m/z	Abund
147.0441	24919.87	216.115	213.2	128.1016	100.28	147.1781	54.87
70.0655	3392.56	70.0818	208.49	146.0594	99.79	147.0052	53.5
293.1607	3218.98	257.1384	206.76	147.0966	96.48	90.0923	52.52
147.0555	3137.5	275.1717	202.54	129.1343	93.69	115.089	51.95
148.0474	2942.15	65.0384	191.13	260.1112	93.29	105.1144	50.14
129.1135	2814.11	234.1135	188.6	276.1354	89.65	147.3622	49.95
112.0871	1835.58	147.0773	187.61	100.0859	89.64	129.1472	49.76
275.1508	1824.82	148.071	181.03	216.1294	88.8	88.1023	48.93
147.1241	1615.93	127.0975	168.28	60.063	84.18	71.0562	48.88
147.0677	1499.92	112.0974	167.23	113.0795	83.54	126.0889	48.38
130.0976	1467.31	71.069	166.07	87.0925	80.87	72.0558	48.23
216.1023	1396.79	217.1054	164.25	275.13	80.65	275.5425	47.99
119.0493	1369.43	119.0609	156.53	119.0716	80.42	157.1076	47.48
88.076	1316.54	129.1257	155.14	61.0528	78.32	147.4993	46.49
113.0711	1091.13	88.0874	152.36	70.0886	73.58	164.0843	45.51
60.0558	1020.32	204.1156	151.47	155.0923	69.56	147.5268	45.4
204.1014	970.93	88.0944	149.29	214.0954	66.74	116.0837	43.52
259.1085	695.6	148.0381	146.32	234.1292	66.01	83.0713	43.25
91.0548	474.66	71.0504	141.93	127.1039	64.57	147.9229	42.56
148.0577	443.97	92.0583	141.23	118.0658	64.53	148.0876	42.13
105.103	400.23	131.0814	140.69	113.0912	63.74	147.4171	42.13
83.0608	387.04	173.104	136.27	120.0813	62.95	114.095	41.61
276.1501	348.7	256.1221	132.36	60.0709	62.16	149.1004	40.84
114.0745	295.69	258.1446	123.73	164.0602	61.22	215.1165	40
130.1134	288.88	128.0922	123.12	147.2911	61.06	259.1385	39.52
233.1283	284.78	205.104	117.65	89.0779	60.91	276.2767	38.47
164.0702	269.75	101.071	113.59	92.0646	57.98	148.1306	38.3
274.1367	237.08	112.1061	112.86	85.0781	57.19	131.0905	38.26
70.0727	225.11	256.134	103.1	120.0463	56.51	146.9928	38.06
147.1434	216.29	259.121	102.54	275.1998	56.36	147.3918	37.97

Figure C16. Fragmentation of mass 292.1538 Da.

Mass	Prec. m/z	Ret. Time'	CE volts
293.1604	*292.1538*	*2.868245*	*20*

m/z	Abund	m/z	Abund	m/z	Abund	m/z	Abund
147.0439	6424.62	70.0733	74.4	276.1691	30.74	275.1829	19.08
293.1611	798.45	275.1673	72.56	205.1047	30.34	277.1372	18.78
70.0653	647.39	164.0701	72.55	65.0392	30.26	217.0923	18.34
129.1138	639.24	147.1359	69.41	88.0953	29.3	69.0447	18.21
148.0474	558.64	234.1122	68.12	87.0446	28.78	106.1099	18.08
147.124	541.05	148.0587	67.96	119.0697	27.61	163.0509	17.05
147.0542	493.78	131.1285	66.12	147.1518	27.48	92.0613	16.44
119.0488	446.69	274.1383	62.53	130.1199	27.33	216.0916	16.44
275.1498	436.13	72.0803	51.43	120.0519	26.82	145.0639	16.43
130.0975	403.26	119.0602	51.43	258.1414	26.75	217.127	16.4
147.0666	363.24	173.1045	50.7	114.0679	26.67	147.0126	16.05
113.0704	363.08	87.0914	50.48	84.0541	26.56	235.1138	15.95
88.0761	270.36	260.1054	48	112.1068	26.08	127.1095	15.75
112.0868	260.12	147.0982	47.5	259.123	25.05	160.5406	15.66
216.1021	226.2	88.0851	43.45	204.1153	24.95	101.0694	15.18
204.1017	192.47	128.1005	42.71	86.0588	24	180.0686	15.17
60.0555	175.86	293.1385	42.44	72.0549	23.1	258.1208	14.98
259.1064	164.09	113.0917	42.38	274.1581	22.34	147.2685	14.97
91.0546	140.26	276.134	41.86	126.0924	22.27	128.0936	14.91
163.0387	118.08	274.1255	39.52	132.1319	21.72	158.0924	14.59
276.1522	106.56	113.0824	39.51	114.0997	21.69	86.0714	14.39
127.0975	98.81	71.0694	39.22	147.1825	21.53	156.0768	14.34
130.1084	96.68	129.136	37.8	60.0651	21.36	256.1215	14.19
257.1377	91.64	112.0991	36.33	92.0559	21.14	56.05	13.94
233.129	89.08	84.9529	36.26	145.9572	20.72	110.0725	13.75
129.125	83.84	256.1346	35.2	257.1577	20.28	192.0653	13.66
147.0785	83.07	148.0702	35.02	147.1136	20.04	111.0737	13.29
105.1029	80.56	94.0648	34.89	216.1286	19.53	98.0603	13.16
217.1069	80.05	275.1312	31.97	147.5863	19.3	147.7996	13.03
83.0606	76.26	70.082	31.79	147.4309	19.26	214.1104	13.01

Figure C17. Fragmentation of mass 293.1604 Da.

Mass	Prec. m/z	Ret. Time'	CE volts
306.1692	*307.1762*	*4.005104*	*Ave*

m/z	Abund	m/z	Abund	m/z	Abund	m/z	Abund
147.0438	4820.71	161.1397	69.62	86.0711	25.89	86.0971	14.63
307.1764	2320.4	260.1392	67.02	146.0598	25.23	70.0893	14.51
119.0491	1568.69	249.1592	65.68	72.081	24.86	126.1134	14.42
70.0655	746.24	147.0784	63.25	147.0969	24.66	217.1192	14.28
91.0544	601.07	74.0715	59.69	92.0573	23.96	105.1214	14.1
147.0546	496.88	70.0725	56.47	177.0548	23.69	71.0609	14.06
88.0759	411.33	114.1013	53.95	120.0617	23.37	119.0974	13.95
148.0472	301.22	290.1697	51.94	143.1408	23.08	147.105	13.87
147.067	270.54	148.0566	48.97	119.0809	22.01	89.0788	13.33
289.1663	251.6	234.1117	48.28	260.1083	22.01	277.1387	13.18
233.1285	196.59	70.0816	47.67	217.1043	21.39	120.0803	13.13
119.0591	192.37	91.0726	45.78	127.0958	21.12	65.0479	12.85
216.1015	182.94	87.0915	43.24	205.1037	20.7	85.076	12.79
105.1024	172.75	290.1501	42.96	278.1714	20.29	57.0545	12.75
60.0558	170.12	171.0986	42.84	218.1181	19.46	60.0503	12.4
204.1012	168.93	234.1314	39	259.1248	19.29	88.0396	12.32
57.0454	161.68	276.1331	38.95	103.1232	19.25	216.1178	12.1
143.129	137.7	88.0934	37.98	147.1151	19.16	251.1552	11.92
144.1126	106.16	148.0647	33.49	70.0286	19.11	289.2004	11.91
120.0524	105.97	130.0975	33.27	105.1112	18.61	84.0424	11.76
277.1661	99.34	289.1832	33.17	145.0293	18.42	60.0712	11.72
119.0703	98.03	88.084	32.95	60.0637	18.22	148.0402	11.64
259.1082	95.65	71.0687	29.38	57.0504	18.18	113.0809	11.24
127.0859	90.65	147.0253	29.28	307.1427	17.69	220.8803	11.18
65.039	86.56	233.1408	29.1	77.0393	16.85	260.1616	11.15
306.1598	84.93	144.1338	28.8	131.0826	16.79	307.0394	11.04
126.1024	83.11	204.116	28.79	277.1788	16.39	204.1292	10.99
251.1388	78.62	97.0762	28.11	58.0659	16.19	101.0707	10.92
91.0633	70.81	71.0494	27.7	233.1537	15.55	95.0609	10.83
113.0712	70.41	144.1238	26.59	307.1272	14.95	147.295	10.49

Figure C18. Fragmentation of mass 306.1692 Da.

Mass	Prec. m/z	Ret. Time'	CE volts
322.1637	*323.1718*	*4.133874*	*20*

m/z	Abund	m/z	Abund	m/z	Abund	m/z	Abund
177.0542	9469.63	145.0508	90.86	305.1963	32.44	177.1001	20.73
323.1711	2221.84	112.0965	83.83	306.1102	31.49	145.0645	20.2
145.0278	1703.74	178.0687	82.39	147.1594	31.14	117.0545	19.96
147.124	1195.36	173.1024	79.96	112.1064	30.57	306.0083	19.8
129.1132	1138.58	70.074	77.22	162.0295	30.32	177.5332	19.72
177.066	893.58	289.1166	74.42	246.1259	30.19	136.0589	19.61
305.1611	730.81	129.1355	68.5	91.0548	29.89	291.1178	19.3
178.0578	692.89	264.1382	66.06	178.0809	28.33	131.0829	19.24
70.0651	602	87.0908	64.62	305.1132	28.02	214.4591	18.91
177.0796	546.77	56.0496	63.58	68.0496	27.85	146.044	18.85
112.087	489.78	235.1145	63.14	78.0462	27.5	177.608	18.81
113.0709	393.13	130.1083	62.89	177.2614	27.22	177.4021	18.8
130.0961	371.26	130.1178	60.41	152.061	26.82	289.1306	18.61
117.0336	312.87	306.1638	60.32	177.6621	26.64	305.136	18.35
145.0386	293.46	113.0821	59.88	149.0748	26.26	234.1366	18.31
246.1121	253.43	177.1126	57.05	177.2158	25.61	151.0744	17.74
60.0557	232.69	288.1513	54.1	101.0915	25.16	130.0487	17.26
234.1118	226.54	117.0424	53.55	131.0498	24.68	60.071	17.02
149.0589	180.13	305.1799	53.41	323.1194	24.27	177.2463	16.79
88.0758	173.34	148.1272	51.73	60.0616	24.26	177.5587	16.67
129.1238	163.78	113.0917	48.71	173.1148	24.24	177.6381	16.59
306.145	161.07	308.1445	46.32	194.0905	23.39	177.7748	16.15
147.1355	138.93	83.0572	45.75	265.127	23.2	306.1883	16.1
177.0919	130.52	72.056	45.38	178.0943	22.23	323.15	15.78
89.0386	116.93	155.0935	43.21	101.0339	21.81	177.4694	15.51
146.0316	110.87	112.076	43.06	130.1284	21.78	177.33	15.48
105.1012	105.93	287.1501	39.44	88.087	21.32	56.014	15.39
263.1385	104.96	70.0816	37.3	290.1377	21.32	129.1449	15.34
264.1221	91.24	194.079	34.47	145.0138	21.25	147.1154	15.01
147.1468	91.04	177.134	33.89	235.1288	20.91	130.0403	14.92

Figure C19. Fragmentation of mass 322.1637 Da.

Mass	Prec. m/z	Ret. Time'	CE volts
336.1796	337.1875	5.462968	20

m/z	Abund	m/z	Abund	m/z	Abund	m/z	Abund
207.0645	2021.15	251.0222	29.92	278.1486	17.35	175.0803	9.58
337.1859	732.06	120.0823	28.71	176.0629	17.26	95.094	9.05
175.0391	457.66	207.5492	28.62	114.1206	16.19	114.3375	9.04
114.1017	262.63	105.0705	28.04	337.0063	16.08	115.1814	9
131.1281	249.59	181.0853	27.68	60.0706	16.04	279.144	8.73
60.0549	149.07	119.0609	26.2	335.2903	15.89	114.7594	8.71
115.0879	139.55	114.4263	25.19	157.1072	15.87	120.0915	8.67
278.1364	115.33	336.1325	24.82	322.0987	15.38	207.2293	8.64
119.0499	114.6	278.1151	24.34	205.0502	15.11	279.8527	8.59
278.1643	84.23	207.1033	24.1	199.1065	15.04	175.5093	8.41
320.1599	78.97	107.0505	23.93	207.2595	14.56	239.6007	8.35
208.0687	78.71	114.3304	23.68	115.1131	14.44	72.09	8.08
207.0794	74.39	265.5777	23.43	290.8752	14.34	207.9822	8.08
98.0597	70.36	160.0977	22.84	206.0779	13.67	163.038	8.05
207.0913	56.57	148.0467	21.9	208.0798	13.57	117.1125	7.84
176.0475	55.56	320.1751	21.38	175.7324	13.33	175.4446	7.73
91.0544	51.01	113.026	20.75	207.5646	12.92	207.3764	7.67
72.0821	48.86	95.0872	20.52	207.1137	12.51	289.1051	7.48
175.0553	46.36	145.9742	19.84	206.5632	12.42	147.0655	7.43
147.0455	44.26	337.0999	19.72	337.1411	12.04	208.4265	7.42
73.0645	43.42	177.3108	19.68	159.0848	11.76	248.8201	7.41
337.1196	41.5	114.113	19.4	174.5733	11.49	248.08	7.19
277.1547	41.07	115.0949	19.33	206.0669	11.23	207.1439	7.12
115.1054	40.56	336.1793	19.02	131.1469	11.08	207.1315	7.06
176.0406	39.92	176.5753	18.68	97.075	10.89	208.0525	7.06
337.1629	38.03	233.08	18.67	119.559	10.74	113.0196	6.96
248.0618	37.51	183.0478	18.43	73.0833	10.68	207.6292	6.75
206.0561	37.3	91.0655	17.97	85.5187	9.83	60.0758	6.56
289.086	33.31	175.0681	17.74	178.9108	9.76	153.2295	6.4
65.0402	30.35	131.1562	17.59	295.1634	9.7	233.0949	6.31

Figure C20. Fragmentation of mass 336.1796 Da.

Mass	Prec. m/z	Ret. Time'	CE volts
375.0924	*376.0977*	*4.552373*	*10*

m/z	Abund	m/z	Abund	m/z	Abund	m/z	Abund
214.0481	132.16	69.072	5.14	127.0535	2.64	374.8734	1.44
376.0998	115.17	308.0943	5.13	213.1352	2.64	77.8181	1.38
375.1269	82.33	195.102	4.98	205.1477	2.55	174.0571	1.38
375.1584	32.84	110.069	4.97	277.0415	2.52	177.0709	1.33
213.1108	20.79	260.0533	4.53	214.9428	2.47	214.3882	1.27
375.251	17.69	187.1423	4.49	195.1117	2.45	127.0647	1.25
214.0615	15.18	286.1032	4.39	120.0955	2.32	214.9206	1.25
375.1953	14.36	97.0273	4.38	294.8609	2.27	217.1743	1.24
137.0593	13.41	374.1885	4.34	260.0663	2.26	298.1174	1.22
283.5611	12.47	337.1244	4.16	84.6272	2.25	91.0591	1.21
87.1008	10.88	375.9241	3.92	216.0797	2.25	85.0752	1.19
253.108	10.53	331.1075	3.88	89.8079	2.2	283.5928	1.19
197.0825	10.31	375.068	3.83	333.517	2.05	375.09	1.17
120.0809	10.27	118.1228	3.78	112.9879	1.91	197.1109	1.16
214.0759	10.01	177.0576	3.69	254.1493	1.91	137.0684	1.13
179.0708	9.73	243.0194	3.58	214.2954	1.84	137.0846	1.13
70.0668	8.97	114.1028	3.57	145.288	1.82	199.0938	1.13
294.836	8.84	145.0577	3.44	198.9966	1.82	217.1063	1.07
145.048	8.81	214.0913	3.29	254.8899	1.79	106.0775	1.06
81.0342	7.51	253.1275	3.19	157.8936	1.71	310.0894	1.02
375.1801	6.79	119.0147	2.98	372.273	1.68	142.9918	1.01
119.0082	6.68	261.0563	2.94	118.1294	1.66	89.817	0.98
131	6.15	85.0658	2.9	117.2638	1.65	213.1946	0.95
191.0249	6.07	91.0537	2.88	308.1119	1.63	87.1189	0.94
217.1538	6.03	191.0852	2.78	253.1391	1.57	281.5984	0.94
357.2062	6.01	191.035	2.75	375.2264	1.57	357.6324	0.94
112.0832	5.83	268.0298	2.75	114.1123	1.5	316.9827	0.93
106.0645	5.44	97.0341	2.66	158.9649	1.45	185.8203	0.91
198.9841	5.44	217.095	2.65	274.5229	1.44	213.1491	0.9
213.1212	5.34	298.1048	2.65	277.0526	1.44	269.156	0.9

Figure C21. Fragmentation of mass 375.0924 Da.

Mass	Prec. m/z	Ret. Time'	CE volts
378.2883	*379.2962*	*11.53511*	*20*

m/z	Abund	m/z	Abund	m/z	Abund	m/z	Abund
361.2849	2497.81	345.2629	118.58	204.139	69.76	171.1182	46.45
72.0813	1479.97	69.0707	112.27	246.1938	68.7	163.0884	46.42
344.2589	1309.68	149.0598	110.73	274.1878	67.82	361.3191	45.83
379.2944	569.37	290.2264	102.47	145.1006	66.42	163.1076	45.47
273.1851	515.79	217.1229	101.16	81.0782	63.96	105.0704	45.39
361.3025	507.73	177.0932	100.39	191.1028	63.27	177.1267	44.05
245.1886	441.84	161.1313	100.12	79.0549	62.97	160.1215	43.95
290.2108	440.39	157.1019	100	361.2579	61.76	204.1015	43.64
81.0704	439.01	245.2036	97.66	262.2177	60.9	151.1078	42.42
67.0549	297.1	189.1326	95.56	229.1948	57.65	111.0804	42.35
175.1132	274.81	211.1438	95	71.0858	57.51	218.1651	41.91
175.0754	269	194.1169	93.35	302.2125	56.97	247.1905	41.74
151.075	263.07	218.1529	90.33	194.1884	56.05	154.0859	41.26
147.0814	234.63	55.0547	85.97	137.129	55.3	170.1075	41.25
95.0856	220.76	133.1012	83.03	149.1006	54.57	163.0638	40.02
123.1167	218.07	206.1182	82.93	220.1342	54.02	379.2497	39.09
255.1747	203.41	275.1987	82.76	100.0742	52.44	89.1168	38.43
109.103	201.93	135.0811	82.46	344.2962	52.36	173.1303	38.01
343.2739	201.39	273.2	82.37	219.1348	52.27	218.1203	37.93
163.0765	195.87	107.087	81.07	121.1057	52.26	379.2377	37.61
72.0887	181.53	72.0979	77.11	159.1154	52.17	213.1263	37.57
89.1066	171.39	255.1901	76.49	185.1335	51.6	117.0714	37.11
129.0692	165.6	119.0849	76.28	379.2055	51.23	217.1618	37.1
189.0918	165.03	272.2015	76.21	362.3069	50.74	203.133	36.83
203.1067	140.25	165.0922	76.14	70.0665	49.09	107.0503	36.77
93.0701	137.19	164.0711	75.97	150.0927	48.66	178.1243	36.7
362.2886	133.48	326.2482	75.02	263.2014	48.21	207.1378	36.53
227.1815	125.33	201.1284	74.93	344.2234	48.04	77.039	36.24
58.0651	123.58	185.0971	72.42	175.0887	47.98	215.1446	35.81
147.1165	120.93	223.1434	71.63	199.1125	47.18	232.1364	35.72

Figure C22. Fragmentation of mass 378.2883 Da.

Mass	Prec. m/z	Ret. Time'	CE volts				
380.3037	*381.3117*	*12.2023*	*10*				
m/z	Abund						
363.302	1542.11	381.2166	38.24	95.087	23.07	110.097	15.7
346.2748	778.41	304.2259	37.55	119.0848	23	210.2257	15.61
72.081	515.29	363.3378	35.92	151.0871	22.9	147.0814	15.55
292.2273	420.96	259.2042	35.88	363.6429	22.26	125.0574	15.44
275.2007	287.19	109.1006	35.83	165.1034	21.96	204.1397	15.31
163.0748	226.28	345.3051	35.09	362.2814	21.96	328.2644	15.03
69.0697	204.18	187.1128	34.22	292.2568	21.95	86.0613	15
381.3099	163.05	72.097	32.81	191.1048	21.27	69.0859	14.86
151.0754	141.95	364.2832	32.8	69.0783	20.77	97.0945	14.36
346.2971	141.12	73.0637	32.25	164.109	20.58	161.0981	14.31
363.273	126.64	196.2069	32.01	135.1164	20.18	363.3561	14.22
247.2058	113.55	274.2148	29.99	73.0845	19.85	364.2416	14.14
165.0911	102.65	381.2666	29.63	55.0543	19.77	347.2944	14.03
70.065	101.62	205.1222	28.91	111.1182	19.74	107.0486	14.02
364.3076	96.87	67.0544	28.86	206.1193	19.74	72.1066	14.01
345.2892	95.55	121.1007	28.7	247.2247	19.51	217.1945	14
347.2778	84.35	163.089	28.49	125.0956	19.05	84.0889	13.93
135.0791	77.56	105.0659	27.92	159.0778	19.02	116.0529	13.89
292.2409	75.51	380.2655	27.39	135.0906	18.53	266.2173	13.43
257.1914	74.02	258.1957	27.25	122.0616	18.32	163.1004	13.41
175.1111	72.62	185.1331	27.14	275.2332	18.16	380.2233	13.26
89.1072	70.27	163.1134	27.06	93.0707	17.47	89.1143	13.02
72.0889	47.1	145.1014	26.87	131.0864	17.37	101.0968	12.52
316.2644	44.68	126.09	26.67	97.0999	16.77	83.0853	12.4
201.1261	44.1	178.0868	26.5	113.098	16.77	147.1243	12.25
275.2161	44.08	346.2477	26.05	164.0698	16.49	104.0619	12.18
147.1159	41.36	79.0536	24.63	318.28	16.31	346.6441	12.18
149.096	40.05	105.1029	23.36	195.1168	16.16	133.0983	12.14
276.2026	39.51	70.0728	23.09	127.1124	16.01	239.1784	12.02
58.0647	38.49	177.0917	23.09	269.1754	16	346.9169	11.98

Figure C23. Fragmentation of mass 380.3037 Da.

Mass	Prec. m/z	Ret. Time'	CE volts		
360.1054	*383.094*	*3.512235*	*10*		
m/z	Abund	m/z	Abund	m/z	Abund
383.0938	234.86	132.0167	7.34	98.0497	2.42
185.0419	93.33	382.1481	7	109.0505	2.33
86.0962	70.05	382.652	6.89	143.0758	2.33
315.144	69.81	221.1744	6.86	174.1818	2.03
223.0282	60.58	165.0781	6.75	224.7112	1.88
221.0412	58.58	323.1234	6.69	382.6684	1.68
108.996	54.69	381.3039	6	165.0926	1.67
165.0522	47.61	221.1844	5.78	345.9914	1.67
181.0498	45.39	365.017	5.37		
223.0624	45.06	345.9808	5.15		
295.1872	33.3	109.0142	5		
221.0496	29.7	221.0742	4.75		
364.9928	28.96	353.119	4.73		
98.0312	24.14	382.3235	4.52		
345.0748	21.04	381.2188	4.49		
382.2113	20.38	186.0282	4.38		
268.1672	19	382.3384	4.34		
132.0093	17.22	323.111	4.16		
185.062	17.08	145.5656	4.08		
166.0853	16.7	345.097	4.05		
223.0465	16.7	223.09	3.71		
237.0786	15.93	277.164	3.69		
340.8646	15.56	382.2325	3.68		
382.3034	14.23	86.1235	3.38		
145.5518	13.9	181.0749	3.01		
337.8312	13.52	109.0222	2.83		
142.3029	9.92	181.0868	2.72		
340.8755	9.82	295.21	2.69		
143.1191	9.37	223.628	2.67		
166.096	7.36	268.1984	2.67		

Figure C24. Fragmentation of mass 360.1054 Da.

Mass	Prec. m/z	Ret. Time'	CE volts
382.1234	*383.1296*	*3.542645*	*Ave*

m/z	Abund	m/z	Abund	m/z	Abund	m/z	Abund
383.1293	215.97	145.033	11.64	166.076	4.27	381.1762	1.59
223.0242	100.94	382.0387	11.41	155.0872	4.06	217.1516	1.51
383.0915	79.86	217.0945	11.29	221.0597	4.04	241.976	1.5
188.9976	39.06	243.9485	10.5	145.0463	3.78	382.2554	1.41
381.1146	38.24	213.1207	10	322.0503	3.76	99.0838	1.34
193.9659	37.95	382.0482	9.88	382.322	3.76	381.5188	1.31
55.0171	34.5	166.0653	9.76	315.1413	3.44	363.2046	1.27
217.0815	31.28	325.0247	9.25	213.1299	3.23	195.1065	1.25
159.0916	30.07	185.0336	9.01	336.1019	3.17	382.0703	1.25
363.1686	28.59	322.0368	8.06	382.7497	3		
195.0791	23.25	159.1042	8.02	297.0877	2.79		
241.9264	23.02	118.0863	7.92	381.1536	2.76		
221.0456	22.82	297.0713	7.61	309.8973	2.61		
355.0289	22.09	383.1143	7.59	156.9041	2.56		
325.01	20.28	185.1246	7.56	147.0278	2.51		
341.0953	19.8	221.0307	6.76	107.3415	2.5		
365.1182	18.1	89.0769	6.39	192.2467	2.5		
177.0566	17.3	156.8933	6.08	314.1718	2.5		
221.0127	17.01	195.0947	6.02	315.5006	2.5		
147.005	16.54	147.0153	6	336.0888	2.42		
382.1797	16.37	189.0221	5.67	185.2828	2.39		
223.0447	15.81	217.1089	5.22	194.0114	2.25		
155.0788	15.41	211.9508	5	185.0549	2.22		
336.0645	15.26	99.0758	4.77	159.1264	2.03		
334.1565	15	337.0219	4.75	164.5844	2.03		
185.1157	14.75	221.6686	4.67	177.0714	2.03		
99.0638	14.27	341.1169	4.52	243.9784	2		
382.3018	13.32	147.7381	4.5	155.096	1.81		
192.9935	13.2	193.0062	4.5	176.0854	1.76		
185.0434	12.15	193.9937	4.36	223.0598	1.75		

Figure C25. Fragmentation of mass 382.1234 Da.

Mass	Prec. m/z	Ret. Time'	CE volts
392.2677	*393.2743*	*10.65348*	*20*

m/z	Abund
70.0654	3143.36
87.0918	1268.51
357.2535	869.92
375.2643	758.18
328.2247	471.48
243.1744	470.76
393.2732	441.68
70.0731	421.03
88.0753	406.23
121.1003	346.99
271.1687	336.4
358.2388	315.6
93.0695	255.79
70.0818	209.5
87.0995	196.89
225.162	189.23
58.0652	170.61
67.0542	162.02
109.1002	155.96
147.0801	146.58
253.157	145.95
133.1017	138.82
72.0813	135.27
245.1891	132.82
81.0699	131.84
183.1188	130.73
107.086	125.14
79.0548	123.68
201.0922	112.19

Mass	Prec. m/z	Ret. Time'	CE volts
394.2832	*395.2897*	*11.3066*	*20*

m/z	Abund
58.065	218.65
67.0543	139.17
70.0648	2064.63
70.0728	245.73
70.0814	154.05
81.0696	193.04
87.0915	1842.73
87.1104	126.3
88.0755	650.99
88.0842	103.17
123.1164	192.13
147.0789	243.86
151.0747	374.22
175.1107	141.37
180.1022	117.85
192.1006	118.56
229.1938	165.63
245.1896	351.59
255.1747	164.08
273.1852	265.12
330.2423	750.69
330.264	147.51
359.2689	1033.48
360.259	262.5
377.2789	1282.77
377.298	181.11
395.2596	141.16
395.2902	346.04

Figure C26. Fragmentation of mass 392.2677 Da.

Mass	Prec. m/z	Ret. Time'	CE volts				
398.1347	399.142	7.86875	Ave				
m/z	Abund	m/z	Abund	m/z	Abund	m/z	Abund
399.1413	7252.58	98.9747	15.62	295.1123	9.49	353.189	6.81
202.0595	445.79	397.3085	15.17	184.0494	9.4	202.1021	6.78
399.1049	121.93	187.0368	14.64	240.1089	9.16	397.6893	6.77
398.1812	111.12	85.1019	14.26	247.0785	9.01	337.1478	6.7
98.0601	86.55	361.2791	13.84	288.2004	8.93	398.5943	6.67
115.0866	84.29	398.2524	13.4	354.1904	8.86	381.1286	6.62
398.2152	61.18	397.2712	13	305.0355	8.81	143.1168	6.59
202.0736	61.1	201.0528	12.73	260.0764	8.74	159.05	6.44
278.0907	56.22	337.1286	12.49	203.0797	8.65	98.0716	6.24
175.0378	44.19	220.0753	12.35	219.082	8.59	268.065	5.93
116.0899	40.27	159.0417	12.33	248.0795	8.56	77.0396	5.87
86.0978	37.23	144.0425	11.92	73.0846	8.55	232.0729	5.82
203.0671	36.11	397.2519	11.8	108.053	8.53	220.0313	5.73
55.0546	34.39	171.0487	11.54	297.101	8.25	180.1019	5.66
72.0806	31.66	384.1196	11.48	98.0796	8.18	207.0928	5.63
202.0861	30.46	397.3742	11.25	203.1778	8.14	363.1539	5.59
107.0496	29.93	144.0801	11.24	85.0303	8.1	366.0667	5.58
295.0931	25.96	92.0552	11.22	317.0677	8.05	116.082	5.55
397.179	25.14	172.0461	11.19	249.0893	8.02	399.0514	5.53
277.0887	25.06	397.2211	10.97	114.1015	8.01	107.0571	5.45
266.0889	24.64	398.2676	10.83	296.1013	7.93	278.12	5.45
171.0388	22.49	189.1647	10.73	160.0487	7.85	89.1064	5.4
265.0876	21.97	70.0655	10.52	163.1113	7.85	397.3345	5.39
219.0653	20.21	398.2338	10.51	326.1838	7.83	72.0873	5.33
241.0851	19.3	380.1395	10.45	369.1305	7.78	278.1075	5.32
399.0761	18.86	380.1696	10.43	397.3463	7.72	309.0726	5.32
221.0963	18.39	201.0647	10.1	363.3006	7.69	205.0717	5.31
99.0636	17.85	397.1951	10.01	380.2129	7.61	355.1901	5.21
202.04	16.67	229.1538	9.69	265.1034	7.43	397.9197	5.16
115.097	15.89	101.0718	9.68	267.0824	6.82	185.0604	5.09

Figure C27. Fragmentation of mass 398.1347 Da.

Mass	Prec. m/z	Ret. Time'	CE volts
378.2883	*401.2774*	*11.57072*	*Ave*

m/z	Abund	m/z	Abund	m/z	Abund	m/z	Abund
401.275	241.68	88.407	10.62	184.6829	4.34	288.1496	2.23
70.0655	161.91	88.0755	10.29	72.1792	4.28	71.0316	2.22
67.0552	105.94	111.0964	10.09	81.0972	4.2	173.0386	2.2
55.0546	58.81	223.0984	10	193.1066	4.09	181.0731	2.2
81.0711	52.1	72.0865	9.29	247.2039	4	90.9948	2.15
116.0714	35.88	133.1048	9.27	335.084	4	55.0785	2.07
71.069	26.63	209.178	9.25	223.1107	3.96	401.2055	2.03
193.0902	25.5	401.1743	9.13	169.1704	3.88	154.1414	1.85
90.9771	22.52	154.1244	8.8	181.0643	3.83	111.1104	1.83
95.0861	22.07	284.1536	8.8	81.1104	3.54	399.0468	1.8
72.0802	21.85	137.3278	8.4	95.4377	3.44	81.1043	1.75
383.2638	21.77	109.1005	8.33	117.0809	3.38	85.057	1.67
365.2846	20.2	55.0624	8.31	85.0472	3.26	71.0862	1.63
169.1428	19.58	256.3649	8.2	67.0729	3.25	266.9837	1.55
173.0131	19.46	81.0882	7.87	116.0916	3.2	383.7896	1.45
71.0134	17.01	181.0533	7.85	133.1147	3.2	50.9225	1.43
70.0751	16.71	365.3066	7.84	209.1925	3.16	133.1306	1.41
58.0671	16.21	81.0356	7.61	81.0435	3.14	383.8034	1.41
123.0823	16.18	266.9538	7.2	121.0988	3.06	383.2864	1.4
111.0894	15.87	150.092	6.88	137.3376	3.03	91.067	1.21
395.0801	15.43	395.0931	6.31	401.1296	3	81.1219	1.2
184.665	13.77	73.0668	6.27	256.378	2.85	323.8292	1.2
67.0604	13.6	55.0698	6.23	284.171	2.85	103.2112	1.13
116.0533	12.78	70.0825	6.13	365.3198	2.83	67.089	1.02
90.9836	12.63	71.0783	6.07	247.2208	2.73	94.0781	1.02
117.0685	11.8	401.0437	6.04	73.0289	2.71	137.346	1.02
247.1906	11.29	67.0669	5.65	123.1045	2.67	116.1251	1
91.0554	11	70.0701	5.64	95.0594	2.42	401.0619	1
95.0485	10.71	173.0282	5.6	109.1122	2.4		
95.0944	10.64	67.0787	4.45	72.0969	2.29		

Figure C28. Fragmentation of mass 378.2883 Da.

Mass	Prec. m/z	Ret. Time'	CE volts
412.2072	*413.2142*	*9.257571*	*35*

m/z	Abund	m/z	Abund	m/z	Abund	m/z	Abund
413.2144	185.09	58.0656	13.48	187.1173	9.12	159.0253	5.86
70.066	82.02	254.1745	13.12	411.0169	8.65	121.1108	5.82
72.0809	56.45	117.0678	12.95	74.0588	8.56	319.1072	5.82
79.0548	55.53	140.1437	12.87	329.0701	8.52	259.0755	5.81
81.0687	41.32	98.1043	12.86	72.0738	8.46	317.2639	5.74
109.1025	36.1	230.0732	12.8	56.0508	8.34	128.0765	5.7
67.0547	28.93	216.1395	12.72	413.1876	8.34	206.1205	5.67
123.1159	28.43	85.0268	12.57	110.0957	8.12	70.083	5.62
123.0806	27.16	131.0497	12.56	83.0631	8.03	109.1134	5.57
233.1553	26.57	249.1466	12.42	88.0956	7.93	86.2496	5.56
55.0184	25.91	277.8484	12.24	215.1347	7.82	159.0803	5.46
121.1001	23.39	412.2435	12.2	355.997	7.69	135.0871	5.41
173.0962	22.61	155.0874	12.16	175.0924	7.53	72.0978	5.32
251.167	22.07	202.0942	11.91	146.0709	7.47	179.1774	5.32
133.101	21.19	225.159	11.52	133.1116	7.38	216.1501	5.32
201.0904	20.86	232.1335	11.51	95.0844	7.25	99.0805	5.31
93.0683	19.57	271.1719	11.51	183.0814	7.19	67.0599	5.3
69.0341	18.63	84.0439	11.15	157.0647	6.9	72.0867	5.23
93.0732	18.36	70.0753	11.1	214.9211	6.9	269.8523	5.11
140.1089	18.26	173.9978	11.1	123.1273	6.75	127.0366	5.1
187.1075	16.56	187.1472	10.94	176.0827	6.64	161.0611	5.08
192.0043	16.11	259.1634	10.01	189.0906	6.58	234.1428	5.01
107.0784	15.7	213.1226	9.62	412.2013	6.33	146.0786	5
251.1564	15.61	206.1112	9.4	225.1707	6.28	149.1349	4.94
119.0493	15.32	159.0166	9.38	221.1417	6.13	195.1028	4.93
175.0757	15.31	195.1157	9.32	190.0983	6.09	69.0695	4.83
135.0797	15.11	222.0562	9.32	201.0515	6.09	81.0869	4.82
246.1936	14.93	162.9896	9.31	233.1773	6.03	99.7394	4.73
73.0844	13.75	133.0648	9.25	188.081	5.92	183.1119	4.66
183.097	13.63	256.1605	9.23	293.0795	5.91	141.0963	4.4

Figure C29. Fragmentation of mass 412.2072 Da.

Mass	Prec. m/z	Ret. Time'	CE volts		
392.2677	*415.257*	*10.6991*	*40*		
m/z	Abund	m/z	Abund	m/z	Abund
157.1335	55.54	80.953	8.81	83.1019	3.8
70.0649	53.28	72.0907	8.36	80.9599	3.78
415.2565	46.47	57.0745	8.33	244.2213	3.59
156.1215	42.21	60.4109	8.26	145.1092	3.56
60.0462	36.35	79.0842	8.25	68.0582	3.5
121.102	36.12	117.0715	8.09	55.4578	3.28
72.0809	35.25	68.0489	7.91	86.3106	3.27
100.0472	32.81	93.0783	7.76	70.275	3.26
57.0667	32.61	196.1473	7.59	143.4227	3.06
88.0757	27.24	139.7352	7.57	132.0004	3.03
131.9784	26	60.0642	7.25	72.1031	3.02
93.0706	25.95	254.1491	7.03	85.1143	3.01
60.0556	25.85	156.1442	6.95	123.0553	3
80.9476	21.94	59.993	6.29	196.1624	3
70.0702	21.57	83.0955	6.04	55.2669	2.64
83.0864	21.26	70.0819	6.03	156.1549	2.56
161.0975	21.04	100.0587	6.03	60.4187	2.51
196.135	19.61	91.3402	5.81	273.2192	2.34
55.0546	17.78	121.1146	5.79	93.0895	2.31
172.0906	17.4	208.7458	5.75	60.0013	2.28
273.1875	16.77	81.0764	5.58	68.5204	2.25
157.1481	16.7	262.2213	5.56	254.1634	2.25
69.0705	16.29	57.081	5.31	97.1009	2.05
81.0697	15.29	70.0758	5.31	121.128	1.53
149.1004	14	195.6229	5.31	55.0777	1.38
156.1326	12.75	131.992	4.77	57.0886	1.34
123.0432	12.13	78.1877	4.75	86.3169	1.27
88.083	11.98	88.0936	4.61	149.1195	1.27
192.8931	11.95	161.1101	4.3	160.8769	1.27
85.101	11.55	172.1072	3.81	161.1216	1.26

Figure C30. Fragmentation of mass 392.2677 Da.

Mass	Prec. m/z	Ret. Time'	CE volts
424.2106	425.2187	7.958773	35

m/z	Abund	m/z	Abund	m/z	Abund	m/z	Abund
277.0867	2257.48	55.0175	118.89	132.0779	52.78	235.0602	35.17
265.0854	1427.48	259.0905	116.4	147.0435	52.52	277.1339	34.54
107.0491	1140.94	249.1057	113.87	159.0424	51.85	119.0491	34.26
231.0801	914.65	366.1702	113.47	103.0609	51.08	120.0576	33.91
249.0904	871.17	233.0951	110.69	235.0951	50.22	223.1164	33.59
131.1289	734.17	131.0588	92.53	237.0713	50.08	223.0391	33.47
259.0752	658.33	232.0883	88.7	124.0746	49.38	180.1169	32.75
157.1084	653.61	425.2172	86.98	218.07	49.16	210.0667	32.26
221.0958	600.02	295.1138	85.58	335.1743	49.15	131.1517	32.26
132.0558	549.9	55.0548	83.92	221.1135	48.79	226.124	31.41
114.1023	536.83	145.063	83.24	157.1325	46.82	158.1107	30.88
131.0493	502.83	265.1164	79.05	181.0618	46.36	115.0975	28.76
295.0965	452.16	277.1169	74.93	133.0648	43.99	140.0832	28.59
235.0761	427.9	107.0687	72.97	86.0357	42.6	237.1059	28.45
171.0441	385.13	171.0552	70.92	103.047	42.59	347.1699	28.26
72.0805	367.47	231.1012	70.87	262.062	41.96	265.0642	28.22
247.0748	316.94	209.0962	65.13	121.0295	41.65	90.9754	27.9
60.0557	316.37	97.0767	64.57	191.0856	40.63	165.0672	27.73
98.0605	277.01	206.0723	63.31	129.0696	40.39	295.1293	26.93
219.0805	226.7	143.0473	62.15	223.083	39.84	201.0684	26.86
203.0841	213.33	219.0977	60.77	71.0475	39.79	276.0778	26.59
157.0647	180.13	189.0693	60.1	247.0913	39.76	127.0303	26.54
251.1067	160.45	114.1124	59.79	98.0726	39.03	140.1066	26.25
115.0864	159.69	234.0675	58.41	202.0795	38.2	132.0629	26.07
237.0903	144.29	248.0958	57.38	131.0704	38.12	251.0956	26.06
183.0437	134.75	60.0626	56.75	221.126	37.95	201.0474	26.02
157.119	132.46	72.0911	54.82	249.122	37.72	277.0624	25.77
107.0586	125.25	93.0342	53.94	112.0869	37.62	236.0828	25.43
265.1007	124.79	103.0535	53.9	205.1013	36.09	204.0878	24.76
207.0793	119.09	131.1408	52.84	249.0704	35.27	56.9655	24.44

Figure C31. Fragmentation of mass 424.2106 Da.

Mass	Prec. m/z	Ret. Time'	CE volts
437.231	*438.2392*	*7.537101*	*35*

m/z	Abund	m/z	Abund	m/z	Abund	m/z	Abund
147.0437	9310.55	204.1433	42.39	290.0831	21.04	204.5256	15.16
204.1013	3732.74	275.2003	41.69	204.058	21	266.0906	15.08
72.0809	1007.11	146.1785	39.62	151.0409	20.71	249.0979	14.82
119.0489	846.96	119.0697	37.61	109.0752	20.41	147.3855	14.62
292.2021	747.05	147.1155	36.86	147.2496	20.13	277.0832	14.51
147.0548	741.63	292.2356	35.7	127.1236	20.02	204.7101	14.47
218.1166	621.97	420.2291	33.7	98.061	19.89	204.3974	14.43
147.067	548.1	84.0818	33.57	75.0234	19.5	204.186	14.34
275.1755	444.08	112.1231	33.18	438.2406	19.45	275.2167	14.32
204.1153	368.72	437.2379	31.35	119.081	19.34	437.2596	14.22
146.1642	316.53	292.1883	30.32	147.35	19.02	75.1079	14.2
129.1387	232.15	129.1493	28.49	247.0712	19.02	204.4493	13.97
204.1285	195.08	147.2255	28.16	240.0881	18.01	147.5221	13.83
91.0545	193.64	421.2139	27.91	57.0698	17.85	91.0656	13.78
112.1122	193.15	146.1879	27.56	147.1649	17.85	189.0899	13.7
119.0592	117.95	218.1453	26.76	204.1655	17.22	147.2946	13.68
75.0917	117.54	155.1298	25.89	147.5341	17.21	204.3514	13.42
72.0891	107.52	204.0745	25.79	101.1066	16.79	123.1139	13.25
218.1308	99.53	70.0657	25.62	350.1327	16.57	204.4658	13.24
147.0785	92.06	437.2993	25.35	72.105	16.46	147.1826	13.1
155.118	88.9	115.0853	25.11	147.2637	16.37	204.5456	13.1
292.219	88.07	292.1717	25.05	204.4289	16.32	165.0689	13.09
221.1279	84.05	221.1417	24.64	340.6333	16.31	148.0494	12.91
203.1176	79.03	120.0797	24.08	171.0428	16.18	129.1612	12.9
235.1428	78.76	89.1077	23.57	147.4157	16.09	95.0601	12.77
72.0972	74.51	156.122	23.36	292.2553	16.08	161.1349	12.56
147.0979	57.52	65.0379	22.78	203.1305	16.02	135.1146	12.54
274.1959	52.14	164.1086	21.53	98.0973	15.62	204.3347	12.46
291.0617	47.67	147.4933	21.29	203.9504	15.54	176.1014	12.19
172.1441	44.15	292.0653	21.07	86.0969	15.42	113.0707	12.13

Figure C32. Fragmentation of mass 437.231 Da.

Mass	Prec. m/z	Ret. Time'	CE volts		
440.1664	*441.1747*	*4.9166*	*40*		
m/z	Abund	m/z	Abund	m/z	Abund
95.0116	180.49	233.0083	15.35	149.0192	4.34
204.0755	88.66	263.0715	14.44	223.0862	4.33
91.0551	72.22	88.0808	14.13	70.0407	4.12
84.0178	72.05	141.0145	12.76	124.7539	3.69
185.0451	61.79	126.9714	12.69	147.0579	3.67
161.0984	51.73	70.0347	12.52	263.0874	3.54
223.0571	51.54	155.114	11.94	207.1082	3.38
202.0461	42.18	172.091	11.38	84.0352	3.36
98.0595	35.69	98.0685	11	141.0252	3.33
148.9943	33.38	202.0596	10.97	148.0899	3.03
157.0486	31.44	91.0754	10.05	188.2106	2.78
172.0772	30.74	264.358	9.76	126.0513	2.75
126.0294	29.48	189.0568	9.01	167.0541	2.69
167.0292	28.49	157.0634	8	210.1014	2.35
98.0892	28.32	205.0969	7.69	98.0793	2.25
70.03	28.24	83.0181	7.44	227.142	2.17
88.075	24.3	210.0849	6.78	126.9863	2.08
207.0799	23.98	95.0383	6.68	91.0863	2.05
210.0698	23.79	167.0423	6.48	126.0613	2.03
205.0844	23.77	247.0988	6.48	126.9951	2
81.0331	22.99	342.9161	6.43	265.09	2
441.1741	21.67	98.1023	6.35	88.0926	1.69
204.0907	20.06	188.2218	5.97	95.054	1.69
227.12	19.38	142.0024	5.67	247.1141	1.69
98.0951	18.45	379.2789	5.54	88.0988	1.68
95.0306	18.37	211.3843	5.44	91.1045	1.67
147.0447	17.22	81.0436	5.34	189.072	1.67
161.1074	16.67	161.1245	5.3		
141.9925	16.37	84.0428	5.05		
379.2566	16.01	342.9286	5		

Figure C33. Fragmentation of mass 440.1664 Da.

Mass	Prec. m/z	Ret. Time'	CE volts				
448.1607	*449.1693*	*8.874018*	*35*				
m/z	Abund	m/z	Abund	m/z	Abund	m/z	Abund
449.1691	245.44	212.0593	11	57.4378	5.92	186.147	4.15
273.1206	70.28	70.0737	10.84	193.0826	5.89	211.8716	4.05
434.1459	29.09	131.0838	10.8	273.1808	5.85	449.1443	4.04
74.0963	28.34	211.8615	10.66	173.1383	5.76	133.1014	4.03
199.036	24.06	186.1333	10.25	107.0878	5.75	357.2035	4.02
431.253	22.97	255.0293	9.79	278.1164	5.75	433.0698	3.88
184.99	22.77	210.971	9.27	385.6922	5.66	147.0448	3.78
431.1615	22.16	447.2503	9.27	447.1591	5.66	57.0418	3.77
169.0305	19.04	95.0486	9.18	291.1913	5.64	448.2474	3.54
120.0433	18.54	269.1872	9.13	434.1629	5.64	211.1451	3.52
113.0001	18.3	60.0451	8.81	365.1751	5.63	232.1441	3.52
184.0141	18.11	69.0353	8.79	120.056	5.42	71.0962	3.5
143.0007	17.74	121.0668	8.72	209.091	5.34	269.1132	3.42
109.065	17.17	147.1173	8.5	121.0603	5.29	167.0833	3.4
331.1473	16.46	431.1966	8.47	58.0719	5.27	365.1896	3.38
62.0607	15	267.0939	8.37	68.0498	5.25	70.0638	3.24
267.127	14.22	163.1099	7.55	98.9748	5.2	185.017	3.19
262.9946	13.95	185.0707	7.38	263.0071	5.13	184.0356	3.17
71.0873	13.73	159.0798	7.37	205.0495	5.04	121.0748	3.15
273.1354	13.34	181.121	7.07	431.2761	4.91	181.1336	3.13
285.1157	12.81	433.1358	7.07	143.0131	4.79	431.219	3.07
58.0663	12.25	214.0161	6.83	74.1107	4.78	147.7986	2.78
95.0851	12.15	109.1043	6.64	298.1208	4.63	329.0667	2.76
173.1288	12.02	145.1034	6.62	329.0551	4.62	410.2205	2.75
363.1905	11.98	303.137	6.53	255.117	4.55	145.1123	2.68
447.1474	11.8	169.9986	6.51	294.1367	4.52	433.9282	2.66
448.2267	11.66	185.1255	6.41	199.0525	4.43	69.1591	2.64
57.0328	11.63	287.6607	6.38	389.1546	4.38	357.192	2.64
410.2029	11.5	197.0652	6.27	449.1246	4.32	434.9288	2.53
72.0814	11.05	317.8816	5.96	95.0933	4.17	95.058	2.51

Figure C34. Fragmentation of mass 448.1607 Da.

Mass	Prec. m/z	Ret. Time'	CE volts
467.2404	*468.2497*	*7.796289*	*20*

m/z	Abund	m/z	Abund	m/z	Abund	m/z	Abund
468.2497	192.47	201.1631	20	219.1835	8.51	292.2289	5.33
467.2728	144.7	248.1306	19.91	99.3958	8.31	227.3298	5.27
467.1505	116.66	255.1371	19.33	432.1876	8.07	451.2351	5.27
467.1771	66.22	468.1547	19.04	70.0656	8.01	385.0662	5.09
204.0997	59.23	249.1881	18.83	415.3022	8	177.0808	5.01
467.2232	57.9	121.1016	18.45	177.0705	7.94	438.2467	5.01
177.0534	52.53	111.0905	18.3	433.894	7.87	239.1416	5
292.1999	51.87	185.1837	16.71	267.1516	7.69	269.1672	4.78
239.1117	50.78	315.0567	16.51	86.1061	7.35	271.7468	4.66
467.2497	48.66	339.1885	15.86	249.2066	7.31	191.074	4.59
322.2132	39.04	72.0818	15.26	267.7157	7.25	451.1032	4.51
275.1768	37.42	183.062	15.2	379.2918	7.02	142.9792	4.5
466.2665	36.85	218.12	15.05	277.0914	6.88	269.1552	4.42
395.14	34.85	279.0641	14.44	405.6313	6.84	468.2162	4.31
234.1154	31.61	275.1936	12.77	466.8847	6.82	467.4025	4.26
86.0984	30.83	249.1584	12.5	248.6889	6.78	249.1694	4.25
84.9596	29.25	423.1558	12.32	315.0682	6.59	176.2192	4.03
450.255	28.74	381.1592	11.91	402.5727	6.56	383.2158	4.01
130.0433	28.25	243.7949	11.78	467.3557	6.53	467.9411	3.94
466.2088	27.66	251.1416	11.76	451.0029	6.28	84.979	3.75
200.0243	27.35	200.0348	11.53	404.2152	6.26	234.1305	3.67
219.1739	25.71	404.1904	11.25	468.1746	6.14	415.3162	3.51
405.6051	24.97	84.9676	11.03	111.0974	6.11	249.0177	3.39
425.2083	24.09	254.0965	11.01	179.3181	6.08	423.173	3.28
467.2975	22.65	439.4751	10.41	435.297	6.06	267.1647	3.27
424.1678	22.32	235.852	10.28	218.1329	5.76	245.8083	3.25
267.1334	22.26	172.1461	10.25	467.3226	5.74	130.0655	3.17
204.1119	21.43	269.145	9.74	204.128	5.67	313.2755	3.06
142.9605	20.5	72.089	8.78	121.065	5.54	121.1259	3.01
449.2581	20.29	449.2334	8.59	201.0421	5.52	200.054	3.01

Figure C35. Fragmentation of mass 467.24044 Da.

Mass	Prec. m/z	Ret. Time'	CE volts				
472.2286	*473.2381*	*9.669422*	*40*				
m/z	Abund	m/z	Abund	m/z	Abund	m/z	Abund
86.0968	38.04	86.1144	4.26	472.1313	1.97	78.7162	0.81
161.0973	23.41	232.1362	4.2	443.2298	1.94	157.139	0.8
70.0655	14.08	260.1048	4	59.059	1.86	122.0058	0.72
124.0424	12.76	183.1626	3.95	124.0637	1.8	115.2941	0.71
209.0607	12.12	305.1455	3.71	86.1241	1.77	309.222	0.71
299.0693	11.28	245.1133	3.7	237.0506	1.76	333.1817	0.71
56.0493	10.71	105.0687	3.61	255.0221	1.76	358.0974	0.71
116.0516	10.38	358.0673	3.54	134.0824	1.71	472.1555	0.71
59.0499	10.29	336.1088	3.43	105.0774	1.7	123.1081	0.7
177.0534	9.72	131.0508	3.3	336.1205	1.7	160.5299	0.7
123.08	9.48	291.8057	3.22	455.2687	1.62	177.7881	0.7
222.082	9.47	124.0768	3.07	442.0354	1.51	245.13	0.7
357.9491	9.25	289.8074	3	154.0235	1.5	400.7358	0.66
88.0234	8.65	211.4196	2.91	161.1102	1.46	232.1629	0.62
183.15	8.21	274.1112	2.91	177.0713	1.46	227.7168	0.61
473.2379	8.07	189.0198	2.77	161.1237	1.44	167.8203	0.6
245.102	7.61	168.9563	2.62	222.1096	1.34	131.0625	0.52
121.9812	7.01	115.5102	2.52	371.1647	1.33	181.0889	0.51
154.0085	6.9	299.09	2.5	272.3301	1.31	274.1292	0.51
318.9056	5.51	88.0337	2.41	134.5918	1.24	336.133	0.51
86.1068	5.4	177.5775	2.4	211.431	1.23	209.0899	0.5
124.054	5.11	295.0963	2.3	56.0645	1.2	310.5921	0.5
209.0718	5.04	358.0839	2.24	371.1465	1.17		
237.0823	5.01	237.0948	2.21	179.5271	1.12		
244.0254	4.98	309.2034	2.21	299.1048	1.1		
69.0337	4.91	123.092	2.16	455.7469	1		
255.0071	4.83	152.0826	2.15	145.0373	0.96		
145.0231	4.81	343.1385	2.14	210.5167	0.91		
189.0333	4.7	70.0781	2.11	165.6911	0.86		
343.1199	4.34	232.1509	2.08	305.1596	0.86		

Figure C36. Fragmentation of mass 427.2286 Da.

Mass	Prec. m/z	Ret. Time'	CE volts
484.2322	*485.2387*	*8.059485*	*35*

m/z	Abund	m/z	Abund	m/z	Abund	m/z	Abund
337.107	428.92	305.0978	38.53	157.1275	19.9	201.0813	12.83
305.0801	380.93	60.044	34.84	175.0381	19.63	483.3429	12.53
201.0544	354.32	114.1111	32.18	128.0726	19.53	98.974	12.15
137.0589	353.73	205.0653	31.72	337.1458	19.4	97.0782	12.14
325.1061	167.14	234.0677	31.35	251.1101	19.22	214.0787	11.86
307.0946	158.15	325.0863	30.81	161.1321	18.89	109.0665	11.67
277.0855	157.25	295.1077	30.79	220.0255	18.87	161.1407	11.62
131.1293	123.38	161.0588	30.68	324.1216	18.25	277.1146	11.61
114.1017	120.06	291.0652	30.33	131.1402	18.05	309.1039	11.54
157.1083	111.09	137.0801	28.91	85.0287	18	246.0693	11.34
290.059	93.64	245.0611	28.87	430.3388	17.87	304.0731	11.3
337.1251	92.67	287.0623	28.86	60.0615	17.75	309.1142	11.18
213.055	90.08	322.1701	27.65	315.4212	17.44	98.0595	11.14
293.0819	89.91	123.1107	27.57	110.0302	17.43	145.1365	11.14
485.2391	80.76	59.0499	27.44	162.0673	17.22	137.0916	10.87
295.0978	77.83	434.1713	27.26	451.1417	17.16	322.1043	10.8
72.0807	71.31	237.0011	25.95	57.0346	16.73	214.0638	10.54
137.0699	69.29	325.1346	25.7	205.0744	16.64	290.0791	10.53
294.0871	58.27	113.1066	25.46	165.1027	16	180.0771	10.43
319.0977	53.33	290.0419	25.31	321.1634	15.99	274.0603	10.17
322.0842	49.52	227.1052	23.43	125.0569	15.46	270.9421	10.15
291.1025	49.4	305.1161	23.26	343.2676	15.44	321.1901	10.14
273.0546	48.81	291.1234	23.21	83.0481	14.39	385.2693	10.14
265.0854	47.69	307.1213	23.13	157.9024	14.33	299.1285	10.09
277.0988	46.28	233.0577	23.01	203.0482	14.29	410.1377	9.8
115.0873	46.2	309.0768	22.68	395.1881	14.29	262.0639	9.78
60.0556	45.87	261.054	21.72	321.0788	13.96	213.0723	9.68
249.0891	41.71	282.1203	20.53	127.0396	13.84	297.0752	9.62
70.0654	41.47	306.0891	20.43	105.0721	13.37	337.0889	9.59
201.0681	39.27	219.0678	20.34	165.1606	13.17	265.1051	9.38

Figure C37. Fragmentation of mass 484.2322 Da.

Mass	Prec. m/z	Ret. Time'	CE volts
494.2892	*495.2927*	*5.144057*	*10*

m/z	Abund	m/z	Abund	m/z	Abund	m/z	Abund
275.1749	677.25	494.2312	21.41	349.2705	8.22	186.9934	4.29
495.296	377.06	129.1405	20.6	204.6242	8.05	140.434	4.15
204.1019	335.05	477.0559	20.05	151.1565	7.78	350.1382	4.12
495.1437	134.38	493.2249	19.63	333.0231	7.7	251.1064	4.04
275.1908	125.13	477.2894	19.33	147.32	7.27	182.1103	4.01
204.1181	68.08	147.0446	18.92	186.114	7.19	426.1682	4.01
494.1613	57.29	182.0917	18.67	493.1365	7	129.1531	4
494.3539	55.18	494.1108	18.34	307.0647	6.75	275.5473	4
151.0415	54.15	251.0877	17.95	140.4216	6.52	376.5207	3.89
495.2634	54.14	314.8624	17.14	323.0647	6.48	204.1668	3.74
182.0818	48.36	333.0084	16.51	296.0391	6.33	494.6298	3.6
186.0878	45.5	494.3383	16.51	314.873	6.23	296.0618	3.52
494.2589	42.12	155.1156	16.14	493.2993	6.22	477.1016	3.43
186.9669	36.9	393.1058	16.01	393.1259	6.08	81.0533	3.33
495.1662	35.94	275.2097	15.39	204.131	6.01	349.2944	3.33
261.0416	34.31	297.4402	15.33	419.2144	6.01	275.6977	3.03
296.0138	33.24	349.2384	14.85	494.3836	5.89	419.23	2.82
275.1495	32.78	112.1013	14.67	261.0659	5.85	393.1452	2.69
376.4703	30.58	244.093	12.95	112.1087	5.67	146.2939	2.68
232.0605	30.37	426.1409	12.39	449.1013	5.67	494.2085	2.44
493.2834	28.27	81.0449	12.35	338.1131	5.52	400.696	2.42
81.0355	28.07	151.5008	12.23	275.6186	5.48	232.105	2.39
449.074	27.82	85.0285	12.06	151.6196	5.44	85.0345	2.38
494.3671	25.71	307.05	11.22	231.1004	5.34	182.122	2.36
323.0455	24.8	155.1081	10.72	131.134	5.12	307.0791	2.33
419.1949	24.3	131.1274	10.45	359.1408	5.06	186.1466	2.25
495.1966	22.75	275.5159	10.37	275.5306	5.03	493.2562	2.13
494.1376	22.72	477.0715	10	183.143	5.01	155.1354	2.04
349.2571	22.34	488.8462	9.43	182.1003	4.74	151.17	2.02
494.2905	21.68	275.2258	9.04	278.3139	4.46	493.1733	2

Figure C38. Fragmentation of mass 494.2892 Da.

Mass	Prec. m/z	Ret. Time'	CE volts
508.2798	*509.2877*	*5.202153*	*10*

m/z	Abund	m/z	Abund	m/z	Abund	m/z	Abund
265.0855	941.76	265.1174	24.91	351.9568	13.96	263.0874	8.56
291.0657	491.05	114.1226	24.85	265.1362	13.95	223.1023	8.53
247.0761	253.75	421.1865	24.23	265.6817	13.94	494.3113	8.46
72.0816	248.86	387.1302	23.79	225.0829	13.68	201.0922	8.42
114.102	244	336.1539	22.99	310.286	13.45	325.1528	8.4
157.1085	213.06	361.0929	22.86	55.0548	13.42	116.0989	8.05
509.285	197.3	225.0488	22.56	467.266	13.02	509.1829	8.01
263.0689	147.01	237.1118	22.53	291.5495	12.85	286.1697	7.84
237.0908	110.76	420.2042	22.21	300.1338	12.2	317.1602	7.65
265.1016	104.29	72.0979	20.88	72.0865	11.13	361.1622	7.62
219.0787	80.88	353.1887	20.6	184.0538	10.98	317.0425	7.48
98.0608	66.47	291.0418	20.2	387.1409	10.98	267.1185	7.43
404.1599	59.91	291.1005	19.8	219.0663	10.89	247.118	7.25
291.0856	56.62	60.0532	18.99	391.8613	10.78	185.059	7.18
240.0997	50.32	235.0755	18.09	263.1016	10.65	114.4109	7.16
223.0765	49.41	170.9969	17.88	257.1233	10.49	291.3736	7.05
171.0458	48.31	158.0941	16.87	115.0961	10.43	438.1912	7.03
282.1174	48.13	263.14	16.66	404.1764	10.32	240.1303	7
114.112	47.4	362.1394	16.55	336.1655	10.31	290.1864	6.96
264.102	44.28	400.0492	16.46	120.0451	10.23	206.0749	6.83
89.1089	43.16	217.063	16.2	379.1879	9.74	120.0517	6.63
492.2597	42.21	140.0802	15.82	138.0555	9.46	265.3886	6.48
201.072	42.09	157.1256	15.77	135.7612	9.34	89.1155	6.43
265.0704	40.62	211.1559	15.46	265.7222	9.06	268.673	6.32
290.0814	39.76	72.0911	15.36	122.0597	8.86	380.3835	6.28
115.085	39.62	509.1695	15.34	225.0601	8.85	492.2855	6.23
247.0978	37.56	218.0697	15.25	127.0404	8.82	235.0919	6.2
475.2333	36.48	121.0513	15	450.2399	8.82	114.1376	6.18
379.1646	30.1	57.0335	14.06	163.4051	8.68	191.071	6.04
265.0571	29.05	55.0173	14	291.5761	8.68	206.9691	6.04

Figure C39. Fragmentation of mass 508.2798 Da.